

Flanders
State of
the Art

13_041_1
FHR reports

Baseline Zuidwestelijke Delta

Set-up and Calibration of model waqua-schelde_nevla-j07_5

DEPARTMENT
**MOBILITY &
PUBLIC
WORKS**

www.flandershydraulicsresearch.be

Baseline Zuidwestelijke Delta

Set-up and Calibration of model waqua-schelde_nevla-j07_5

Chu, K.; Vanlede, J.; Decrop, B.; Mostaert, F.

Legal notice

Flanders Hydraulics Research is of the opinion that the information and positions in this report are substantiated by the available data and knowledge at the time of writing.

The positions taken in this report are those of Flanders Hydraulics Research and do not reflect necessarily the opinion of the Government of Flanders or any of its institutions.

Flanders Hydraulics Research nor any person or company acting on behalf of Flanders Hydraulics Research is responsible for any loss or damage arising from the use of the information in this report.

Copyright and citation

© The Government of Flanders, Department of Mobility and Public Works, Flanders Hydraulics Research 2019
D/2019/3241/030

This publication should be cited as follows:

Chu, K.; Vanlede, J.; Decrop, B.; Mostaert, F. (2019). Baseline Zuidwestelijke Delta: Set-up and Calibration of model waqua-schelde_nevla-j07_5. Version 2.0. FHR Reports, 13_041_1. Flanders Hydraulics Research: Antwerp.
IMDC: I/RA/11502/18.003/KCH/




Reproduction of and reference to this publication is authorised provided the source is acknowledged correctly.

Document identification

Customer:	Rijkswaterstaat Zeeland	Ref.:	WL2019R13_041_1
Keywords (3-5):	Hydrodynamics; Automatic Calibration; Scheldt		
Text (p.):	73	Appendices (p.):	9
Confidentiality:	<input checked="" type="checkbox"/> No <input checked="" type="checkbox"/> Available online		

Author(s):	Chu, K.; Vanlede, J.
------------	----------------------

Control

	Name	Signature
Reviser(s):	Decrop, B.; Vanlede, J.	 
Project leader:	Vanlede, J.	

Approval

Head of Division:	Mostaert, F.	
-------------------	--------------	--



Abstract

The main objective of this study is to improve the predictive ability of the operational 2D NEVLA model for the River Scheldt. The geometry of the model is stored in an updated Baseline database. Baseline is set-up to automatically create inputs such as bathymetry and bottom roughness files for the hydrodynamic model. The model constructed out of Baseline is then calibrated automatically on bottom roughness with OpenDA, which consequently leads to a success with cost function reduced by 20%. The model validation shows that the model predictive abilities on water level, salinity and cross-sectional discharges are generally good.

Contents

Abstract	III
Contents	V
List of tables.....	VII
List of figures	VIII
1 Introduction.....	1
2 Abbreviations and Conventions	2
2.1 Abbreviations.....	2
2.2 Conventions.....	2
3 Inner workings of Baseline – OpenDA – WAQUA.....	3
3.1 Clustering Ecotopes	4
3.2 Creating roughness elements.....	5
3.2.1 Ruwheid_vlakken.....	6
3.2.2 Ruwheid_lijnen	6
3.2.3 Ruwheid_punten	6
3.3 Conversion to WAQUA (calculation of area_u and area_v file)	7
3.3.1 Ruwheid_vlakken.....	7
3.3.2 Ruwheid_lijnen	9
3.3.3 Ruwheid_punten	9
3.4 Roughness parametrisation in WAQUA (ROUGH_CHAR).....	10
3.5 WAQUA to OpenDA.....	12
4 Data	13
4.1 Water level	13
4.2 Salinity	14
4.3 Discharge	15
5 Baseline Tree	19
5.1 Description of j07_5-v4	19
5.2 Migration to j07_5-w4.....	19
5.2.1 Adding bathymetric information	19
5.2.2 Assimilation of measure	22
5.2.3 Adding KUNSTWERKNAAM at Mechelen.	22
5.2.4 Combining zomerbed roughness polygons	23

6	Model Update.....	26
6.1	Grid comparison	26
6.2	Grid adaptation around Tielrode.....	28
6.3	Shift of MN index of output points.....	30
6.4	Barrier at Mechelen.....	31
6.4.1	Physical Description.....	31
6.4.2	Implementation in the model.....	32
7	Calibration with OpenDA.....	33
7.1	Introduction.....	33
7.2	The input files of OpenDA	33
7.2.1	Main input file	33
7.2.2	Stochastic model factories	34
7.2.3	Stochastic observers.....	37
7.2.4	Algorithms	38
7.3	The Optimization Algorithm - DUD.....	39
7.4	Cost function	39
7.5	Stop Criterion.....	40
7.6	Initial guess of roughness	41
7.7	Results	43
8	Validation with VIMM.....	47
8.1	Water Level Timeseries	47
8.1.1	Validation.....	47
8.1.2	Benchmark against manually calibrated 2D hindcast model	56
8.1.3	Benchmark against manually calibrated 2D forecast model (VSSKS).....	59
8.1.4	Comparison to the sensitivity analysis of NEVLA3D	59
8.2	Harmonic Analysis of Water Levels	60
8.3	Salinity	63
8.4	Discharge	67
9	Conclusions and Recommendations.....	71
10	References.....	73
Appendix A	Introduction of DUD	A1
Appendix B	Definition of Statistics.....	A3
Appendix C	Sensitivity analysis of roughness	A4
Appendix D	Definition of Vector Difference	A9

List of tables

Table 1 – Used abbreviations	2
Table 2 – Glossary of terms	4
Table 3 – Description of the roughness code (R_CODE) used in WAQUA.....	10
Table 4 – Available water level measurements for the year 2007.....	13
Table 5 – Overview of stations with salinity measurements of 2007.	14
Table 6 – Description of the 42 ADCP measurements of discharge.....	15
Table 7 – Merging zomerbed roughness polygons.	25
Table 8 – Overview of different model grid and depth files used.....	28
Table 9 – Changes of MN-depended input files associated with the new grid grid-nevla_5-v3-adjust.grd...	30
Table 10 – Update of M and N index at output stations.	31
Table 11 – Combined roughness polygons with initial estimation of manning coefficients used by OPENDA. The combination of roughness polygons is described in §5.2.4	42
Table 12 – Changes of cost function and parameter (manning coefficient) during the OpenDA calibration stage I.	44
Table 13 – Changes of cost function and parameter (manning coefficient) during the OpenDA calibration stage II.	45
Table 14 – Comparison of manning coefficient before and after the automatic calibration with OpenDA...	46
Table 15 – Description of model runs involved in the model validation.....	47
Table 16 – Definition of colour code in terms of bias, RMSE and RMSE0.....	48
Table 17 – Comparison of Bias, RMSE and RMSE0 of the complete time series.	49
Table 18 – Comparison of Bias, RMSE and RMSE0 of high water levels.	50
Table 19 – Comparison of Bias, RMSE and RMSE0 of low water levels.	51
Table 20 – Comparison of Bias of high water and low water between Run003 and Maximova et al (2009b).	57
Table 21 – Comparison of Bias of high water and low water time between Run003 and Maximova et al (2009b).	58
Table 22 – Comparison of error statistics of water levels between Run003 and VSSKS.....	59
Table 23 – 11 runs of NEVLA2D model out of the automatic calibration with OpenDA.....	60
Table 24 – Harmonic components of M2, S2 and vector differences for the tributaries of Scheldt.	63
Table 25 – Statistic analysis of salinity between model and measurements.....	67
Table 26 – RMSE of the comparable tide analysis.....	68

List of figures

Figure 1 – Flow chart of inner workings of Baseline-OpenDA-WAQUA. The elements in yellow are explained further in the text.	3
Figure 2 – Snippet of the conversion key used to convert from ecotope to ecotope_ruwhheid.	5
Figure 3 – Snapshot of the GUI for creating roughness elements in Baseline.	5
Figure 4 – Example of zomerbed polygons used in Baseline.	6
Figure 5 – Demonstration of the area_u (left panel) and area_v (right panel) files.	7
Figure 6 – Example of area_u and area_v with associated roughness codes (background color) at grid cell (383,2).....	8
Figure 7 – Example of the conversion of ruwhheid_lijnen to WAQUA.	9
Figure 8 – Example of a user-defined ROUGH_CHAR file (file name: roughcombination-westerschelde-2015_5-v1) for the area of Western Scheldt, with values (A) of manning coefficients.	11
Figure 9 – Measurement locations of water level.....	14
Figure 10 – Available measurements of discharge in the Western Scheldt.....	16
Figure 11 – Available measurements of discharge in the Lower Sea Scheldt.	17
Figure 12 – Available measurements of discharge in the Upper Sea Scheldt and Rupel.....	18
Figure 13 – Example of TIN generated in Baseline j07_5-v4 in the upper part of Zenne river.	20
Figure 14 – Display of the winter bed data (in red) and summer bed data (in black) from Baseline tree j07_5-v4.	21
Figure 15 – Example of TIN generated in Baseline j07_5-w4 in the upper part of Zenne river.....	21
Figure 16 – Example of model bathymetric samples at the upper end of the river Dijle	22
Figure 17 – The KUNSTWERKNAAM of the hydraulic structure at Mechelen are added to the Baseline tree j07_5-w4.....	23
Figure 18 – zomerbed polygons defined in j07_5-w4 (left) and combined in j07_5-v4 (right). Top:BeZS; Middle: BoZS; Bottom: Rupel.....	24
Figure 19 – Comparison of model grid grid-nevla_5-v2.grd and NEVLAV07.grd.	26
Figure 20 – Comparison of model grid grid-nevla_5-v2.grd and NEVLAV07.grd	27
Figure 21 – Comparison of model grid grid-nevla_5-v2.grd and simG36_simona.grd.	28
Figure 22 – Left Up: Summerbed and winterbed data recorded in Baseline database j07_5_w4	29
Figure 23 – Grid property of N Smoothness: grid-nevla_5-v2.grd (left) and grid-nevla_5-v3-adjust.grd (right).	30
Figure 24 – Schematization of the barrier at Mechelen in the Dijle river.....	31
Figure 25 – Sketch of barrier element implemented in this study.....	32
Figure 26 – Map of water level stations involved in the OpenDA calibration.....	40
Figure 27 – Comparison of Manning coefficient used by existing 2D and 3D hydrodynamic models along the navigation channel of the River Scheldt.....	42

Figure 28 – Evolution of cost function during OpenDA calibration stage I (left panel) and II (right panel)....	45
Figure 29 – Bias of complete time series of water levels along the Scheldt.	52
Figure 30 – RMSE of complete time series of water levels along the Scheldt.	52
Figure 31 – RMSE0 of complete time series of water levels along the Scheldt.	53
Figure 32 – Bias of high water levels along the Scheldt.	53
Figure 33 – RMSE of high water levels along the Scheldt.	54
Figure 34 – RMSE0 of high water levels along the Scheldt.	54
Figure 35 – Bias of low water levels along the Scheldt.	55
Figure 36 – RMSE of low water levels along the Scheldt.	55
Figure 37 – RMSE0 of low water levels along the Scheldt.	56
Figure 38 – M2 amplitude along the River Scheldt.	61
Figure 39 – M2 phase along the River Scheldt.	61
Figure 40 - S2 amplitude along the River Scheldt.....	62
Figure 41 – S2 phase along the River Scheldt.....	62
Figure 42 – Vector differences along the River Scheldt.	63
Figure 43 – Comparison of salinity between measurement and model runs at Vlakte Van De Raan.	64
Figure 44 – Comparison of salinity between measurement and model runs at Hoofdplaat.	64
Figure 45 – Comparison of salinity between measurement and model runs at Baalhoek.	65
Figure 46 – Comparison of salinity between measurement and model runs at Prosperpolder.	65
Figure 47 – Comparison of salinity between measurement and model runs at Boei84.....	66
Figure 48 – Comparison of salinity between measurement and model runs at Oosterweel.	66
Figure 49 – Time series discharge comparison at R12 Wielingen 20020528.	69
Figure 50 – Bias of complete time series of discharges (model - measurement).	69
Figure 51 – RMSE of complete time series of discharges.....	70
Figure 52 – Relative RMSE of complete time series of discharges.....	70
Figure 53 – M2 and M4 amplitude along the Scheldt between reference run and run with Manning increased by 0.002 in Zone 450.	A4
Figure 54 – M2 and M4 amplitude along the Scheldt between reference run and run with Manning increased by 0.002 in Zone 455.	A4
Figure 55 – M2 and M4 amplitude along the Scheldt between reference run and run with Manning increased by 0.002 in Zone 457.	A5
Figure 56 – M2 and M4 amplitude along the Scheldt between reference run and run with Manning increased by 0.002 in Zone 459.	A5
Figure 57 – M2 and M4 amplitude along the Scheldt between reference run and run with Manning increased by 0.002 in Zone 461.	A6
Figure 58 – M2 and M4 amplitude along the Scheldt between reference run and run with Manning increased by 0.002 in Zone 462.	A6

Figure 59 – M2 and M4 amplitude along the Scheldt between reference run and run with Manning increased by 0.002 in Zone 463.	A7
Figure 60 – M2 and M4 amplitude along the Scheldt between reference run and run with Manning increased by 0.002 in Zone 464.	A7
Figure 61 – M2 and M4 amplitude along the Scheldt between reference run and run with Manning increased by 0.002 in Zone 465.	A8
Figure 62 – M2 and M4 amplitude along the Scheldt between reference run and run with Manning increased by 0.002 in Zone 467.	A8

1 Introduction

Project '13_041: Baseline Zeeuwse Delta' aims for a further calibration of the WAQUA-Schelde_NEVLA model for the entire year of 2007, focusing on the Flemish part. In the summer of 2016, Deltares has finished the calibration and validation of the new WAQUA-Schelde_Nevla model (**waqua-schelde_nevla-j07_5-v4**) for the Dutch part of the River Scheldt. The task of model calibration for the Flemish part is delivered to Waterbouwkundig Laboratorium (Flanders Hydraulics Research or FHR). The project was kicked off on 09/02/2017.

This study involves the update of the existing Baseline database from **j07_5-v4** to **j07_5-w4**. The missing bathymetric data in several parts of the River Scheldt are filled up with existing data of model bathymetry. The updated Baseline database creates inputs for setting up the NEVLA2D model, which is automatically calibrated with open-source software of OpenDA. The automatic calibration leads to a reduction of the cost function by 20%. The model validation shows that the predictions of water level, salinity and cross-sectional discharge are well reproduced. The preliminary model calibration with OpenDA can therefore be considered successful.

In this report, the internal communication between Baseline, OpenDA and WAQUA model is elaborated. The experience of using OpenDA to calibrate the hydrodynamic model is described. The insights gained from this study are considered to be useful and supportive for future OpenDA studies.

The report is structured as follows: the first chapter of this report contains the general project description. The second chapter describes the abbreviations and conventions used in this study. The inner workings of Baseline, OpenDA and WAQUA are detailed in the third chapter. Chapter 4 describes the data used, followed by description of the Baseline tree and its update in Chapter 5. The WAQUA model is updated in Chapter 6 while Chapter 7 describes the automatic model calibration with OpenDA. The model validation results can be found in Chapter 8. In the end, Chapter 9 gives the conclusions and recommendations of this study.

2 Abbreviations and Conventions

2.1 Abbreviations

Table 1 – Used abbreviations

ADCP	Acoustic Doppler Current Profiler
BeZS	Beneden-Zeeschelde (Lower Sea Scheldt)
BoZS	Boven-Zeeschelde (Upper Sea Scheldt)
FHR	Flanders Hydraulic Research
HIC	Hydrological Information Centre
HMCZ	Hydro Meteo Centrum Zeeland
MET	Middle European Time
NAP	Normaal Amsterdams Peil (Dutch vertical reference level)
NEVLA	Dutch-Flemish hydrodynamic model
NOOS	North West Shelf Operational Oceanographic System
OpenDA	Open Data Assimilation
RD	Rijksdriehoekscoördinaten
RMSE	Root Mean Square Error. See Annex 2 for mathematical description
SIMONA	Simulatie MOdellen NATte waterstaat
TAW	Tweede Algemene Waterpassing (Belgian vertical reference level)
VSSKS	Voorspellingssysteem voor Kust en Schelde
WES	Westerschelde (Western Scheldt)
ZUNO	Zuidelijke Noordzee Model (Southern North Sea model)

2.2 Conventions

The following conventions are followed by this report:

- Times are represented in MET.
- The coordinate reference system, used by the model and for presentation of the model output is RD Parijs, expressed in meters.
- The vertical reference level used by this project is NAP. NAP is 2.35 m above TAW level.
- SI units are used.

3 Inner workings of Baseline – OpenDA – WAQUA

Baseline generates a series of input files for WAQUA, among which the bottom roughness files are the most important and relevant ones from the model calibration point of view. In this chapter, we elaborate the inner connections between Baseline, OpenDA and WAQUA, to clarify how the roughness files are constructed for WAQUA from Baseline and how it is linked with OpenDA to proceed with automated calibration.

Figure 1 demonstrates the inner workings of Baseline, OpenDA and WAQUA. The elements in yellow are briefly elaborated in the following sections. The glossary of terms used by this study are listed in Table 2.

Figure 1 – Flow chart of inner workings of Baseline-OpenDA-WAQUA. The elements in yellow are explained further in the text.

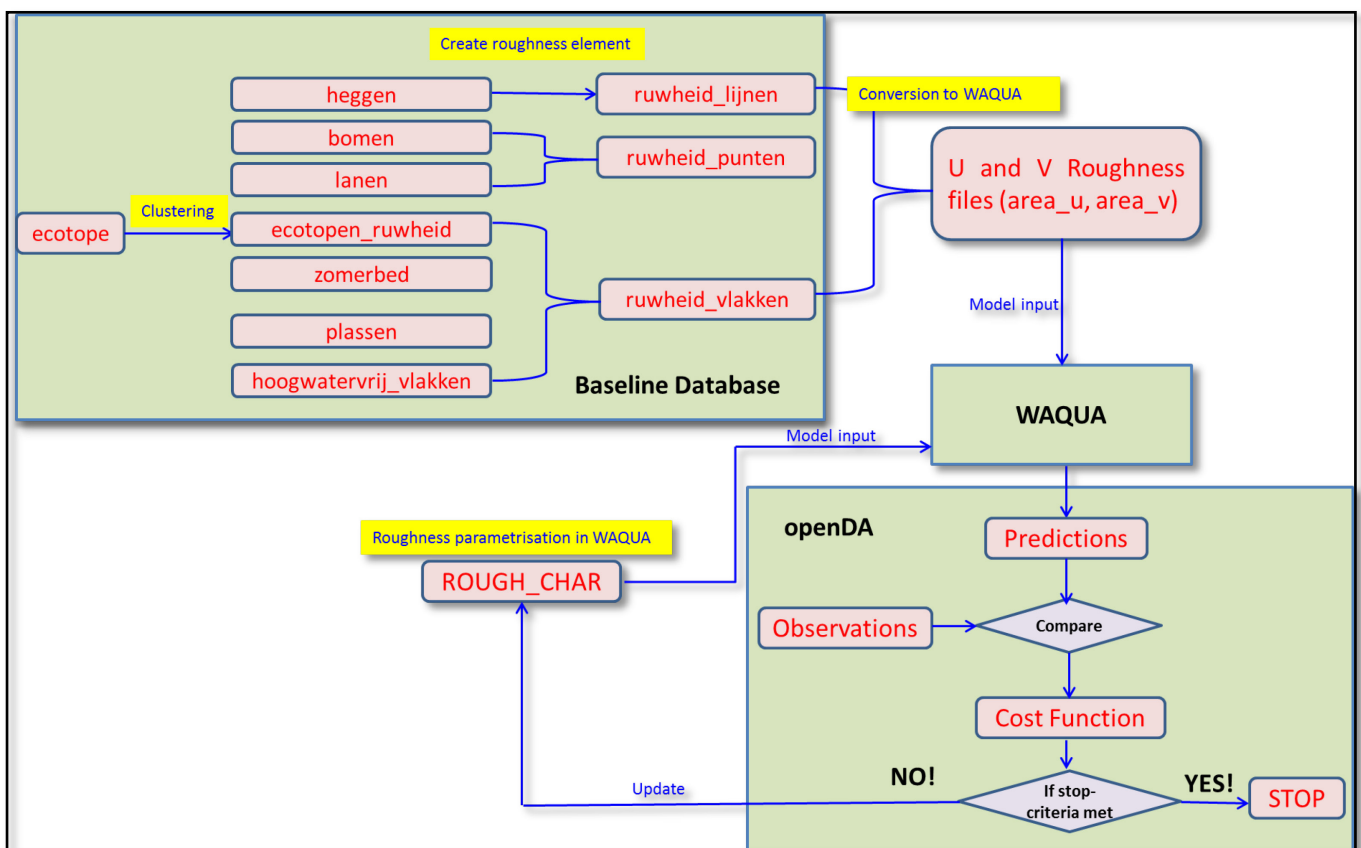


Table 2 – Glossary of terms

Term	Definition
Baseline	Baseline is a combination of an ArcGIS extension and a geographic database intended for the storage, viewing, editing and presentation of river data used to perform calculations with hydraulic models.
Feature Datasets Feature Classes tables	The Baseline files are stored in a Geodatabase File, a database structure specially developed for the processing of geographic data with ArcGIS. In a File Geodatabase, 'Feature Datasets' (comparable to ArcInfo Workspaces), 'Feature Classes' (comparable to ArcInfo Coverages) and tables (comparable to ArcInfo Info-tables) are distinguished.
active variant	An active variant is similar to a working environment/platform. All the functions that are called from the Tools menu in Baseline are executed in the active variant.
WAQUA	WAQUA is the 2D module of modelling software SIMONA, which simulates water movement and transportation of substances dissolved in water.

3.1 Clustering Ecotopes

With the function '**Clustering Ecotopen**' the Feature Class **ecotope** is translated to the **ecotope_ruwheid**. The **ecotopen_ruwheid** contains polygons with associated roughness codes.

In order to carry out the conversion, a conversion key is required (**sleutel.asc**, stored in the installation folder of Baseline: <installdir> / Deltares / Baseline 5 / Template / sleutel.asc). This is a table in which the ecotope codes in the **ecotope** are linked to roughness codes in the **ecotope_ruwheid** (see example in Figure 2). Be aware that if a code from the **ecotope** does not appear in the key, it will not be included in the **ecotopes_ruwheid**, the relevant polygon is ignored when it is converted. The key can easily be updated by the user by overwriting the aforementioned .asc file to a new version.

There are 6 types of ecotopes systems that are recognised in Baseline, among which the RES system is related to the present study.

RES: Rivers Ecotope System

MES: Lakes Ecotope System

BES: Lower tributary area Ecotope System

ZES: Salt waters Ecotope System

LGN4: National Land Use File Netherlands, fourth edition

Atkis: Amtliches Topographic Kartographic Information System, land use map for Germany.

Figure 2 – Snippet of the conversion key used to convert from **ecotope** to **ecotope_ruwheid**.
The full description is described in the Data Protocol Baseline 5 (Appendix C).

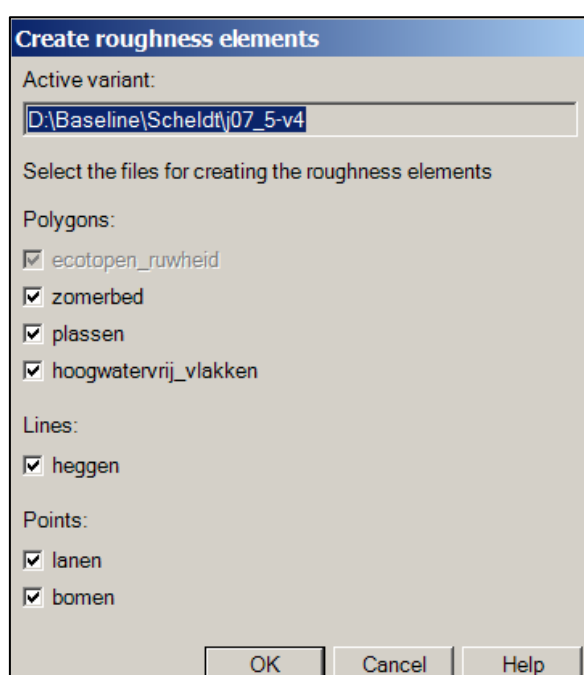
Codering RES (Rivieren) ecotopenstelsel:			
Ecotoop- code	Beschrijving ecotoop-code	Ruwheidscode	Beschrijving van de ruwheidscode
RZd-1	Diepe bedding	102	Diepe bedding
RZo-1	Ondiepe grindbedding	111	Kribvakstrand / Zandbank / Grindbank
RZo-2	Ondiepe zandbedding	111	Kribvakstrand / Zandbank / Grindbank
RZo-3	Ondiepe getijdebedding	111	Kribvakstrand / Zandbank / Grindbank
RZs-1	Grindbank	111	Kribvakstrand / Zandbank / Grindbank
RZs-2	Zandplaat/zandstrand	111	Kribvakstrand / Zandbank / Grindbank
RZs-3	Slikplaten/slikkige oever	106	Plas / Haven / Slikkige oever
RZs-4	Biezenoever	1805	Biezen
RZs-5	Afslagoever/steiloever	112	Ruwe oever

Be aware that the **ecotopen_ruwheid** mainly focuses on winter bed which is not within the scope of model calibration for this study. Instead, we focus on polygons with associated roughness codes on the summer bed which is given by **zomerbed** in Baseline (see §3.2).

3.2 Creating roughness elements

The **ecotopen_ruwheid**, **zomerbed** and other inputs (see Figure 3) are used to create roughness elements (**ruwheid_vlakken**, **ruwheid_lijnen** and **ruwheid_punten**). The results are stored under the Feature Dataset **ruwheid** of the active variant. The details of the creation and conversion of the roughness files in Baseline is described in Deltares (2016).

Figure 3 – Snapshot of the GUI for creating roughness elements in Baseline.

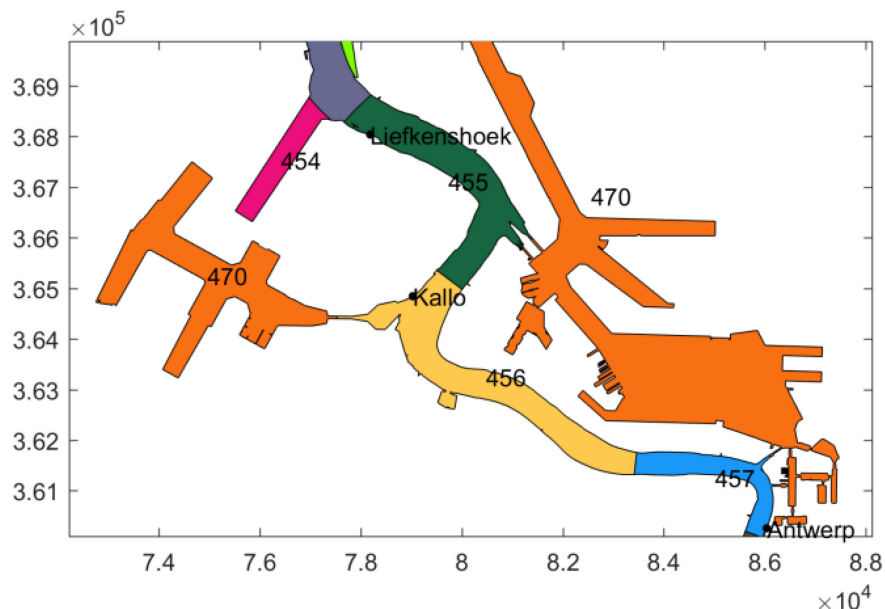


3.2.1 Ruwheid_vlakken

When creating **ruwheid_vlakken**, polygons with the same roughness code are combined.

- The **ecotope_ruwheid** is created by Baseline function '**Clustering Ecotopen**' as described in §3.1 and it mainly focuses on the winter bed.
- The polygons **zomerbed** are subsections of the summer bed (see example in Figure 4). The polygon limits are often determined by the location of water level measuring stations. This makes it possible to calibrate the hydraulic model by assigning different roughness to the different sections. This subdivision is user-defined. Note that in this study, some of the **zomerbed** polygons are merged for the purpose of more efficient automatic calibration with OpenDA.
- **plassen** defines the boundaries of open surface water (e.g. ponds) in the winter bed.
- The **hoogwatervrij_vlakken** are permanently dry points, which must be excluded in the calculations with flow models (e.g. bridge piers and buildings).

Figure 4 – Example of **zomerbed** polygons used in Baseline.



3.2.2 Ruwheid_lijnen

Heggen or hedges are continuous lines representing hedges in the winter bed. It contains roughness line element used to construct **ruwheid_lijnen**.

3.2.3 Ruwheid_punten

Lanen are continuous lines to indicate, for example, tree avenues in the winter bed. When processing to **ruwheid_punten**, the **lanen** are converted to points (individual trees). In the Feature Class **lanen**, the points (representing an individual tree) are placed depending on the value specified in the **AFSTAND** field. The result, together with the Feature Class **bomen**, is stored in **ruwheid_punten**. It is therefore important that when setting up the Feature Class **lanen**, a value is placed at the field **AFSTAND**, because otherwise an infinite number of trees will be placed.

3.3 Conversion to WAQUA (calculation of area_u and area_v file)

3.3.1 Ruwheid_vlakken

The above-mentioned roughness elements are used to create input for WAQUA through a function 'Conversion WAQUA'.

area_u and **area_v** represent U and V roughness codes for each grid cell. This data is stored in two ASCII files that are automatically generated from Baseline. Figure 5 illustrates the data format. Each file contains 4 columns: **N-grid index**, **M-grid index**, **roughness code** and **fraction**.

What the fractions is concerned: each cell can have more than one roughness code. The fraction is the ratio of the surface area within the cell that has a certain roughness code to the total surface area of the cell. Fractions within one cell sum up to 1. This is exemplified in Figure 6.

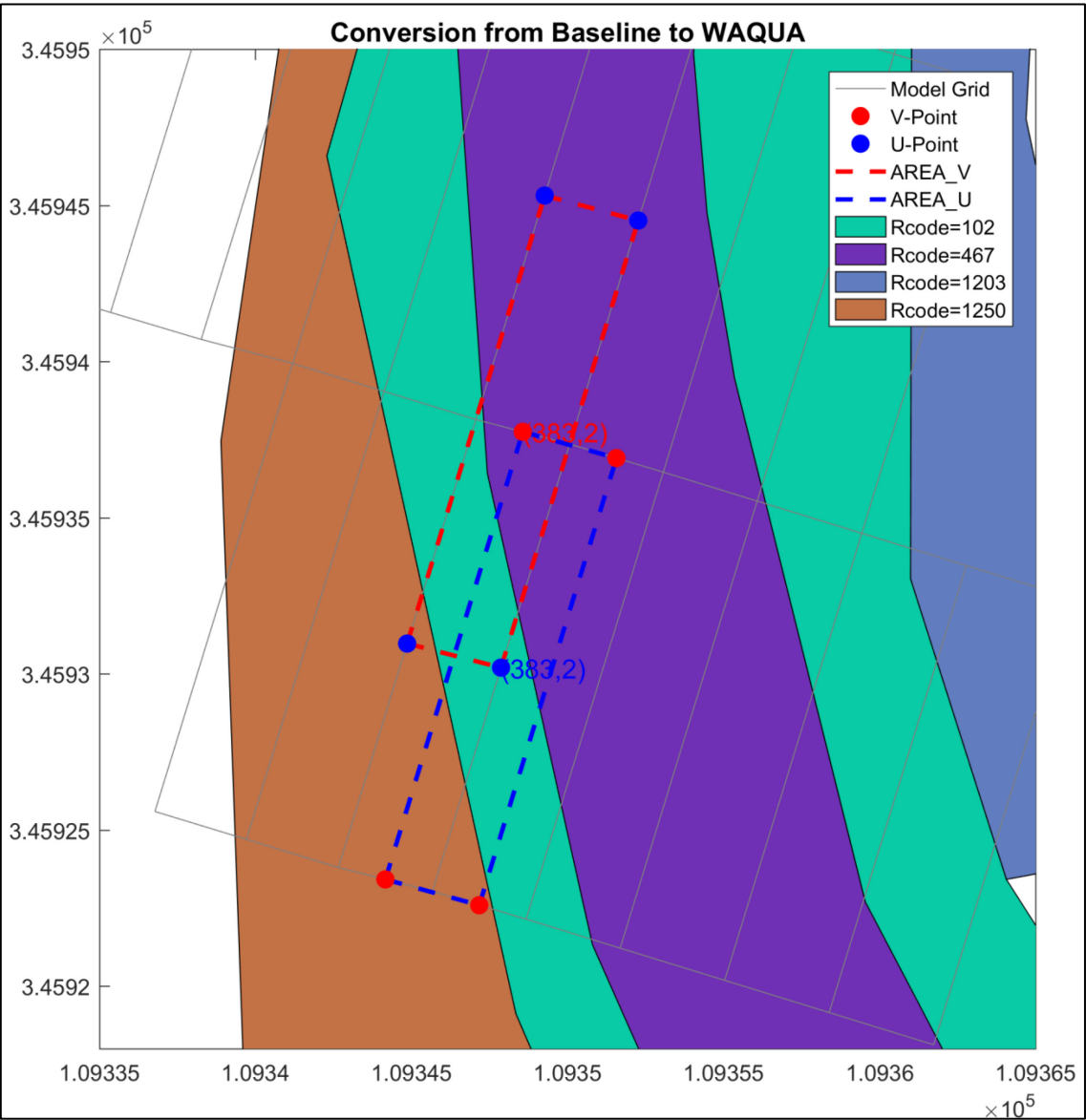
Staggered grid is important here: the cell around the U point is used to determine the U roughness, using V points as corner points. The cell around the V point is used to determine the V roughness, using the U points as corner points.

Figure 5 – Demonstration of the **area_u** (left panel) and **area_v** (right panel) files.
The blacked rows are corresponding to the visualization in Figure 6.

N-grid index	M-grid index	roughness code	fraction
2	381	102	0.057480
2	381	1250	0.900902
2	382	102	0.344668
2	382	467	0.043396
2	382	1250	0.611944
2	383	102	0.385559
2	383	467	0.373750
2	383	1250	0.240690
2	384	102	0.251799
2	384	467	0.744316
2	384	1250	0.003876
2	385	102	0.041989
2	385	467	0.958015
2	386	102	0.355406
2	386	467	0.644186
2	386	1203	0.000404
2	387	102	0.512162
2	387	467	0.274053
2	387	1203	0.213785
3	379	1250	0.515044
3	380	102	0.565818
3	380	467	0.010233
3	380	1250	0.423937
3	381	102	0.543275
3	381	467	0.422352

N-grid index	M-grid index	roughness code	fraction
2	381	102	0.342372
2	381	1250	0.657430
2	382	102	0.509974
2	382	467	0.193822
2	382	1250	0.296215
2	383	102	0.300788
2	383	467	0.681578
2	383	1250	0.017629
2	384	102	0.030688
2	384	467	0.969307
2	385	102	0.287255
2	385	467	0.712743
2	386	102	0.648856
2	386	467	0.338183
2	386	1203	0.012971
3	379	1250	0.394751
3	380	102	0.347130
3	380	467	0.014381
3	380	1250	0.638489
3	381	102	0.403878
3	381	467	0.596121
3	382	102	0.005680
3	382	467	0.994323
3	383	102	0.157899
3	383	467	0.842106

Figure 6 – Example of area_u and area_v with associated roughness codes (background color) at grid cell (383,2).

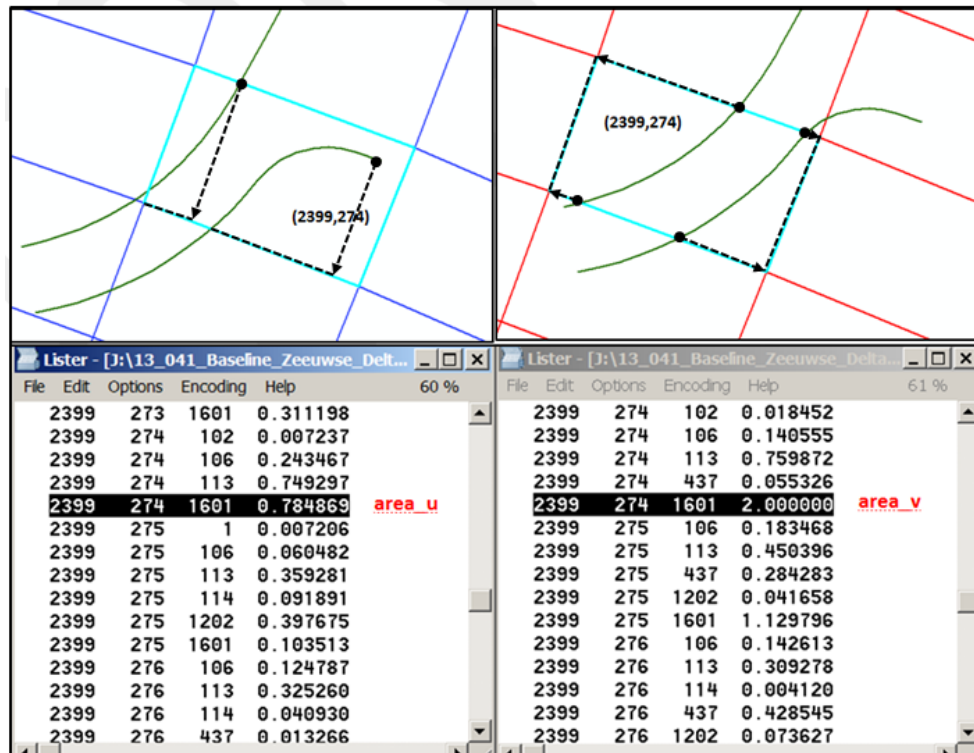


3.3.2 Ruwheid_lijnen

When starting from **ruwheid_lijnen** (hedges), for each U and V grid cell, the projected **length** of the hedge on the cell side is determined. The hedges are divided into categories based on the height. A hedge height of 1.5 meters comes in the category 1.5 to 2.5 meters and gets a standardized height of 2.0 meters. The length of hedges of the same category are added up. The total (relative) length can be more than 100%. This is illustrated by an example near Hansweert in Figure 7. The relative length is used to determine the resistance friction of each cell due to the hedges. The details of the mathematical calculations are referred to Velzen et. al., (2003a, 2003b).

Figure 7 – Example of the conversion of **ruwheid_lijnen** to WAQUA.

Top left: Blue line represents the area_u, cyan square shows an example of U grid (2399, 274), green line represent the **ruwheid_lijnen** (hedge) with roughness code of 1601 and hedge height of 1 meter. The black dash line shows the projection of hedge length on the cell side. **Top right:** Red line represents the area_v, cyan square shows an example of V grid (2399, 274), green line represent the same **ruwheid_lijnen** (hedge) with roughness code of 1601 and hedge height of 1 meter. The black dash line shows the projection of hedge length on the cell side. Bottom: **area_u** (left panel) and **area_v** (right panel) files.



3.3.3 Ruwheid_punten

During the conversion, **ruwheid_punten** (trees) are divided into 10 categories based on their **height**, varying from 0.5 meters to 10.5 meters with interval of 1 meter. For instance, a tree with a height of 2.5 m comes in the category of 2.5 to 3.5 m and then gets a standardized height of 3.0 m. The **diameter** of the tree is expressed in the density which is computed by adding up the diameters of all trees within the same category and dividing them by the cell area, both for the U and V-grid cells. The density cannot be greater than 1.

3.4 Roughness parametrisation in WAQUA (**ROUGH_CHAR**)

WAQUA uses the **ROUGHCOMBINATION** method to calculate bottom roughness for each cell. Following Rijkswaterstaat (2015), with this method it is possible to combine several roughness codes at fractions per grid cell. The input for these fractions per grid cell and the roughness codes is given in the **area_u** and **area_v** files which are automatically generated out of Baseline as described above.

Table 3 presents the possible roughness codes (1-1999) used in WAQUA. The area files essentially define which roughness method(s) shall be applied on each grid cell.

Table 3 – Description of the roughness code (R_CODE) used in WAQUA

R_CODE	Meaning
1-50	code for buildings and water free surface
51-100	not defined
101-300	code for roughness with a static k-Nikuradse value used in the White-Colebrook formula
301-500	code for roughness with a static n-Manning value used in the Manning formula
501-600	code for roughness with a static Chezy value
601-900	code for roughness for the main channel
901-1200	not defined
1201-1400	code for vegetation structure types (areas, like grass)
1401-1500	not defined
1501-1600	code for vegetation structure types (points, like trees)
1601-1700	code for vegetation structure types (lines, like hedges)
1701-1800	not defined
1801-1999	code for combinations of roughness areas

The actual roughness values are then given by **ROUGH_CHAR** which contains the conversion between an r_code and the actual roughness value that is used in the simulation. Figure 8 presents an example of a **ROUGH_CHAR** file (**roughcombination-westerschelde-2015_5-v1**) for the area of Western Scheldt. It can be seen that in the Western Scheldt, the roughness codes between 310 and 471 are applied which correspond to the Manning coefficient values (defined by the 'A' values in Figure 8) used by the Manning formula.

Figure 8 – Example of a user-defined **ROUGH_CHAR** file (file name: roughcombination-westerschelde-2015_5-v1) for the area of Western Scheldt, with values (A) of manning coefficients.

```

List - [D:\Gebruikersgegevens\saaaa520\Desktop\roughcombination-westerschelde-2015_5-v1]
File Edit Options Encoding Help 51 %

#-----
#
# Roughcombination : Rough karakteristieken voor de ROUGHCOMBINATION method in Waqua
# Der_code verwijst naar der_code in de area-u en area-v files
#
# De vegetatie waarden zijn afkomstig van het Handboek
# Stromingsweerstand vegetatie in uiterwaarden Deel 1 en 2
# Riza rapport 2003.028 en Riza rapport 2003.029
#
# De handboek ruwheden kunnen vrijuit gebruikt worden. Het betreft de codes:
# 101-122, 1201-1250, 1501-1510, 1601-1618, 1801-1807
#
# De overige codes zijn :
# - gecalibreerde waarden voor specifieke gebieden
# - coderingen gebruikt in WBR vergunningen
# - specifieke ruwheden voor projecten
# Deze ruwheden zijn niet vrijuit in andere projecten te gebruiken.
#
#-----
# Versie 2015_5-v1 (12-05-2015): - gebaseerd op Versie 0.85 van 'roughcombination.karak_5_vast'
# - opschonen code: alle gekalibreerde waarden voor specifieke
# gebieden worden in aparte files opgenomen
# - overgang naar nieuwe naam volgens naamgevingsconventie
#
#*****
# zomerbedruwheden Westerschelde, 5e generatie,
#
#*****
#-----
#
# CODE 433-473 : Ruwheids formulering volgens de formule van Manning
#r_code : de ruwheids code
# a : Manning (normaal of eb) (0.001 - 0.0263 - 100.)
# b : Manning (vloed) (0.001 - 0.0263 - 100.)
# c : geen betekenis
# d : geen betekenis
#
r_code = 310 A = 0.021677 # NOORDZEE - ZWD-SCHEMATISATIE - MONDING WESTERSCHELDE
r_code = 311 A = 0.021339 # NOORDZEE - ZWD-SCHEMATISATIE - KUNSTZONE ULAANDEREN
r_code = 433 A = 0.019776 # WESTERSCHELDE
r_code = 435 A = 0.022 # WESTERSCHELDE
r_code = 436 A = 0.030364 # WESTERSCHELDE
r_code = 437 A = 0.024862 # WESTERSCHELDE
r_code = 438 A = 0.022 # WESTERSCHELDE
r_code = 439 A = 0.022 # WESTERSCHELDE
r_code = 440 A = 0.026147 # WESTERSCHELDE
r_code = 441 A = 0.014706 # WESTERSCHELDE
r_code = 443 A = 0.022 # WESTERSCHELDE
r_code = 450 A = 0.026 # WESTERSCHELDE
r_code = 451 A = 0.028 # WESTERSCHELDE
r_code = 452 A = 0.034 # WESTERSCHELDE
r_code = 453 A = 0.026 # WESTERSCHELDE
r_code = 454 A = 0.030 # WESTERSCHELDE
r_code = 455 A = 0.024 # WESTERSCHELDE
r_code = 456 A = 0.023 # WESTERSCHELDE
r_code = 457 A = 0.022 # WESTERSCHELDE
r_code = 458 A = 0.023 # WESTERSCHELDE
r_code = 459 A = 0.024 # WESTERSCHELDE
r_code = 460 A = 0.020 # WESTERSCHELDE
r_code = 461 A = 0.018 # WESTERSCHELDE
r_code = 462 A = 0.020 # WESTERSCHELDE
r_code = 463 A = 0.023 # WESTERSCHELDE
r_code = 464 A = 0.025 # WESTERSCHELDE
r_code = 465 A = 0.024 # WESTERSCHELDE
r_code = 466 A = 0.026 # WESTERSCHELDE
r_code = 467 A = 0.020 # WESTERSCHELDE
r_code = 468 A = 0.018 # WESTERSCHELDE
r_code = 470 A = 0.022 # Antwerpse Havens/Dokken en Deurganckdok
r_code = 471 A = 0.022 # Kanaal Gent Terneuzen
#
#-----
#
# Einde roughcombination
#
#-----

```

3.5 WAQUA to OpenDA

The **ROUGH_CHAR** file is updated during the automatic model calibration with openDA. Specifically, in the study the Manning coefficients for the Western Scheldt are subject to change automatically through optimization scheme of openDA.

As described in §3.2.1, the modeller can freely change the **zomerbed** polygons which is essentially an important step to ensure efficient automatic model calibration using openDA (see details in §5.2.4 and §7).

4 Data

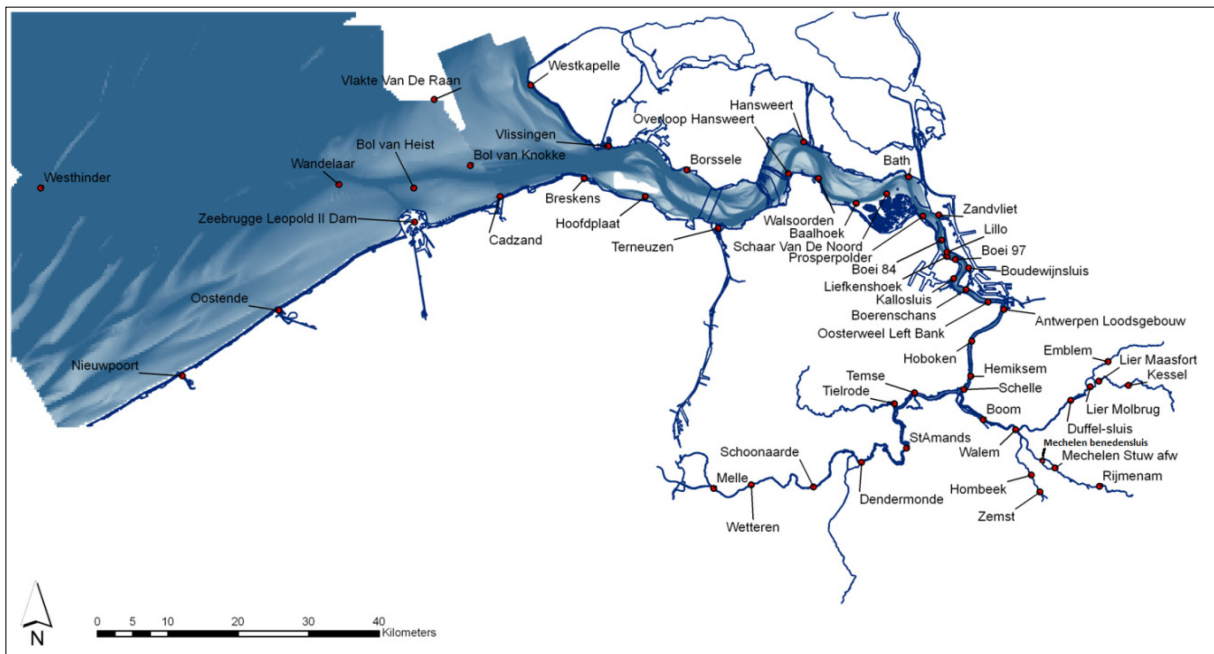
4.1 Water level

For the year 2007, 35 stations are available with water level measurements every 10 minutes, see Table 4. The stations are also shown in Figure 9. The water levels are used for the automatic calibration in OpenDA, and afterwards used to evaluate the model performance.

Table 4 – Available water level measurements for the year 2007.

No.	Station Name	Source	No.	Station Name	Source
1	Westhinder	HMCZ	19	Temse	HIC
2	Vlakte van de Raan	HMCZ	20	Tielrode	HIC
3	Westkapelle	HMCZ	21	Walem	HIC
4	Cadzand	HMCZ	22	StAmands	HIC
5	Vlissingen	HMCZ	23	Dendermonde	HIC
6	Breskens	HMCZ	24	Schoonaarde	HIC
7	Borssele	HMCZ	25	Wetteren	HIC
8	Terneuzen	HMCZ	26	Melle	HIC
9	Hansweert	HMCZ	27	Mechelen Benedensluis	HIC
10	Walsoorden	HMCZ	28	Hombeek	HIC
11	Baalhoek	HMCZ	29	Zemst	HIC
12	Bath	HMCZ	30	Duffel	HIC
13	Zandvliet	HIC	31	Rijmenam	HIC
14	Liefkenshoek	HMCZ	32	Lier Molbrug	HIC
15	Kallo	HMCZ	33	Lier Maasfort	HIC
16	Antwerpen	HMCZ	34	Emblem	HIC
17	Hemiksem	HIC	35	Kessel	HIC
18	Boom	HIC			

Figure 9 – Measurement locations of water level



4.2 Salinity

Salinity measurements with time interval of 10 minutes are available at 6 stations (Table 5). Salinity measurements are used to compare with the model predictions (§8.3). Note that the salinity measurement stations of Liefkenshoek, Hemiksem and Driegoten were deployed in 2009, thus no data available for the year 2007.

Table 5 – Overview of stations with salinity measurements of 2007.

Nr	Measuring station	Data source
1	Vlakte Van De Raan	HMCZ
2	Hoofdplaat	HMCZ
3	Baalhoek	HMCZ
4	Prosperpolder	HIC
5	Boei84	HIC
6	Oosterweel	HIC

4.3 Discharge

42 ADCP measurements of cross-sectional discharges are available (see Table 6 and Figure 10 to Figure 12) for model results comparison (§8.4).

Table 6 – Description of the 42 ADCP measurements of discharge.

No.	Campaign Names	No.	Campaign Names
1	R12 Wielingen 20020528	22	R3 Overloop van Valkenisse 20070814
2	R12 Wielingen 20070619	23	R3 Zimmermangeul 20070815
3	R11 Wielingen 20060517	24	R1 Vaarwater boven Bath 20061025
4	R11 Wielingen 20000605	25	Liefkenshoek_20090527
5	R12 Deurloo 20000605	26	Liefkenshoek_20100430
6	R12 Deurloo 20020528	27	Liefkenshoek_20130625
7	R12 Deurloo 20070703	28	Oosterweel_20090529
8	R12 Oostgat 20000605	29	Oosterweel_20100429
9	R12 Oostgat 20020528	30	Oosterweel_20130627
10	R12 Oostgat 20070618	31	Kruikeke_20090526
11	R11 Sardijneul 20060516	32	Kruikeke_20100414
12	R11 Sardijneul 20000605	33	Kruikeke_20130530
13	R10 Vaarwater langs hoofdplaat 20020516	34	Driegoten_20090623
14	R10 Vaarwater langs hoofdplaat 20071011	35	Driegoten_20100415
15	R9 Vaarwater langs hoofdplaat 20060913	36	Driegoten_20130612
16	R7 Everingen 20080604	37	Boom_20090622
17	R7 Pas van Terneuzen 20080605	38	Boom_20100427
18	R6 Gat van Ossensse 20041013	39	Schoonaarde_20090625
19	R6 Middelgat 20041013	40	Schoonaarde_20100414
20	R5 Schaar van Waarde 20051201	41	Schoonaarde_20130527
21	R5 Zuidergat 20051130	42	Terhagen_20130529

Figure 10 – Available measurements of discharge in the **Western Scheldt**.

Grey line represents the land boundary; red lines represent each transect. Note: for the purpose of concision, different ADCP transects (executed on different dates) at the same locations are labelled only once.

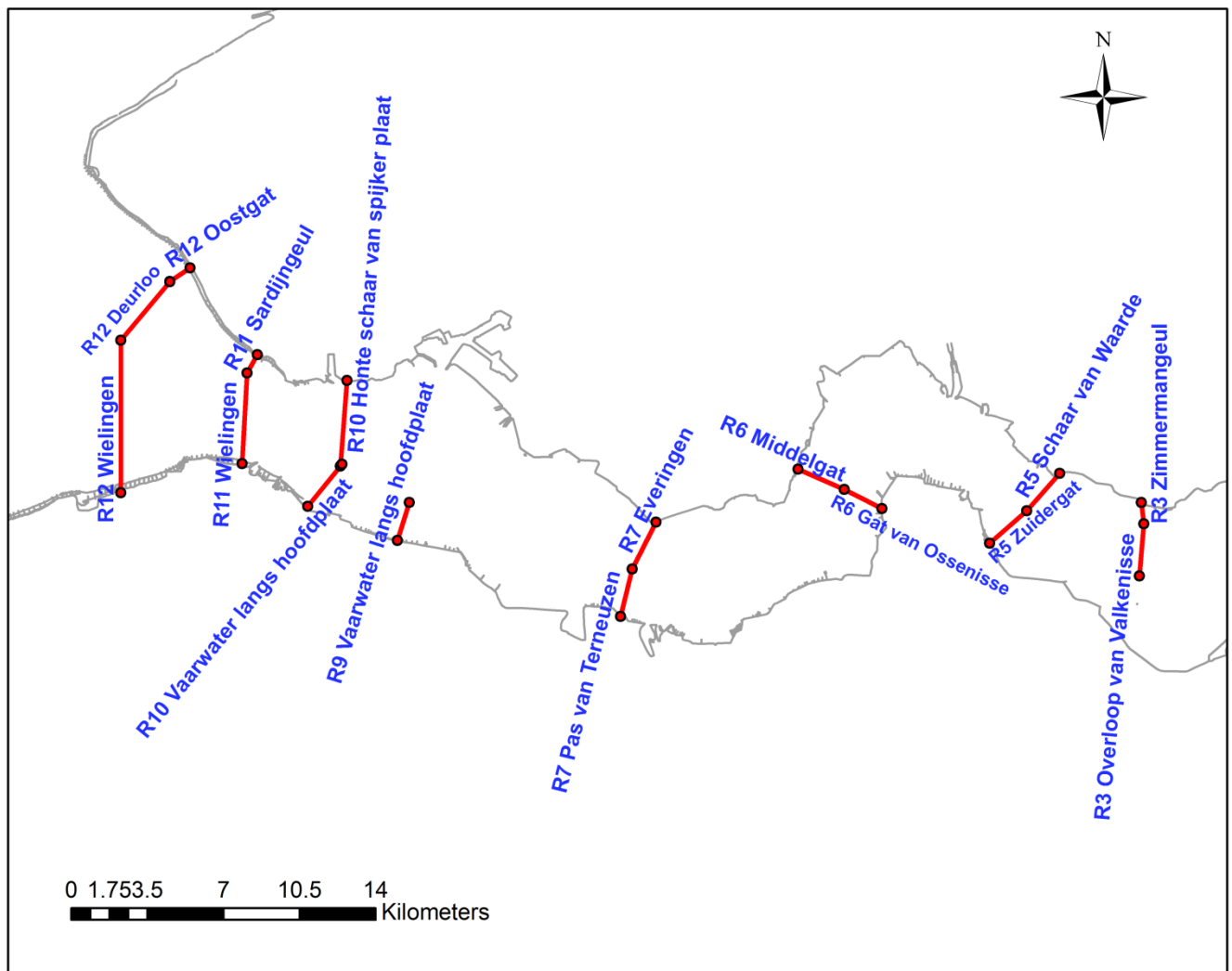


Figure 11 – Available measurements of discharge in the **Lower Sea Scheldt**.
Grey line represents the land boundary; red lines represent each transect. Note: for the purpose of concision, different ADCP transects (executed on different dates) at the same locations are labelled only once.

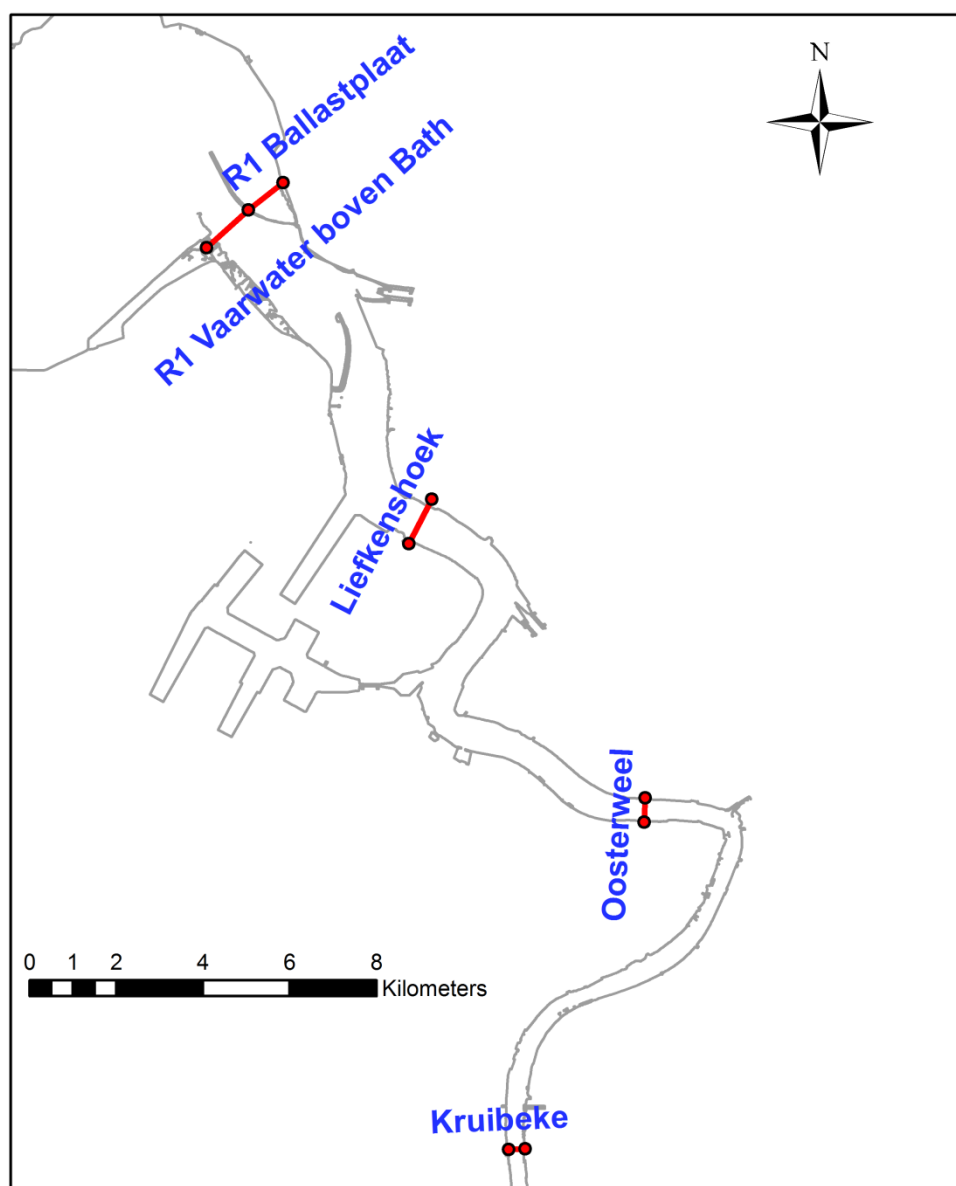
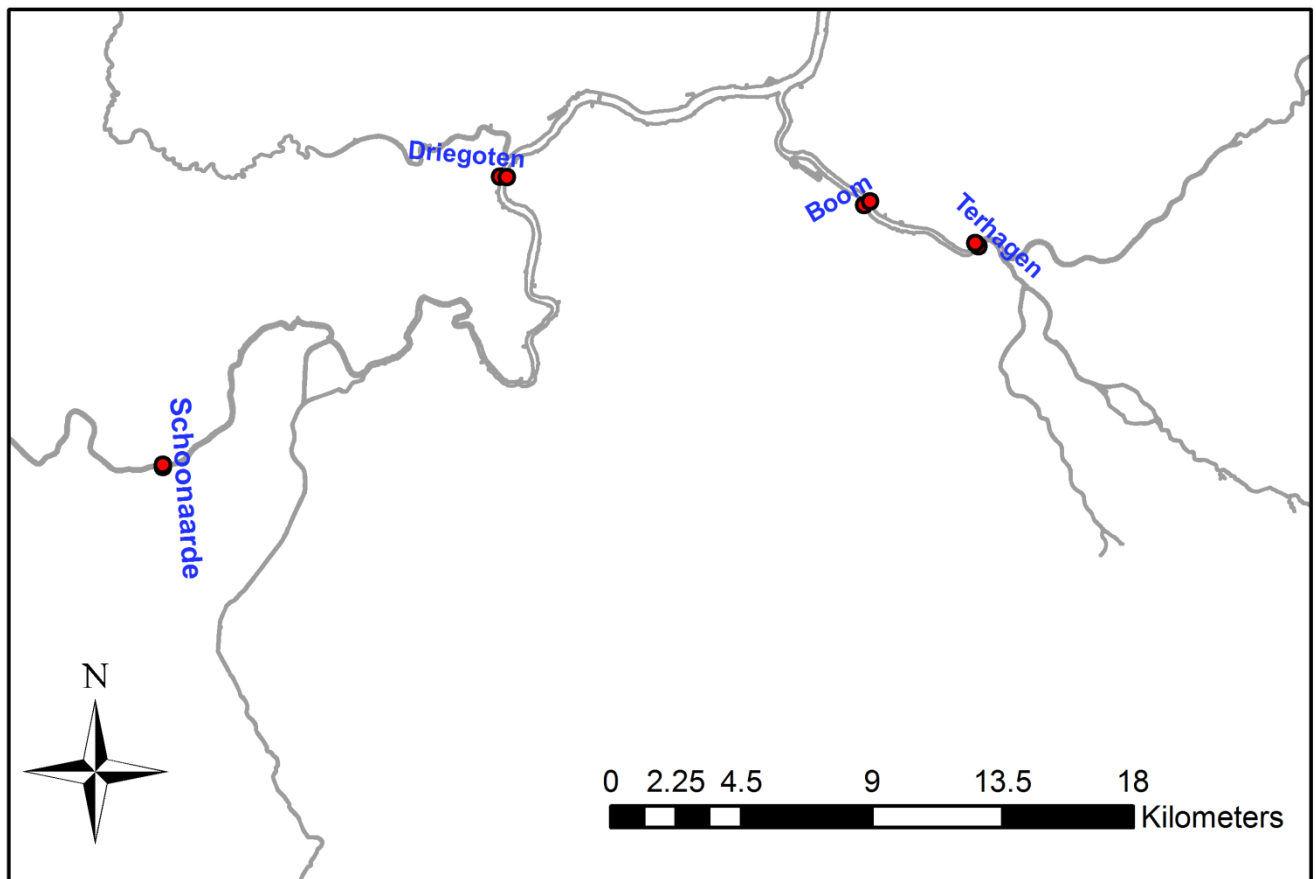


Figure 12 – Available measurements of discharge in the **Upper Sea Scheldt and Rupel**.
 Grey line represents the land boundary; red lines represent each transect. Note: for the purpose of concision, different ADCP transects (executed on different dates) at the same locations are labelled only once.



5 Baseline Tree

Baseline is a GIS database and application that makes it possible to unambiguously produce the spatial aspect of model scheduling for Waqua, SOBEK, SWAN and Delft3D. In Baseline, the spatial data is stored in such a way that an adequate geographical description of an area is obtained. That information is then converted into a schematic for hydraulic models using a number of conversion tools. For a detailed description of Baseline the reader is referred to the user manual (Deltares, 2016).

5.1 Description of j07_5-v4

The latest version of the Baseline database is **j07_5-v4** which contains the geographic information of the year 2007 and it is used for the 5th generation of WAQUA model of the Scheldt estuary. This baseline database was delivered to the FHR on **14-02-2017** and is used as a reference for this study.

j07_5-v4 was compiled in **August 2016** in Deltares based on a previous version of Baseline database **j07_5_v3** which is elaborated and reported by LievenseCSO (2015). The migration from v3 to v4 involves the following changes:

- Adjustment of double names along river-kilometre points in the Eastern Scheldt (maatregelen: **os_rkmpunt_a1**)
- Repair of kades (quays) and breuklijnen (rupture lines) in the Eastern Scheldt (maatregelen: **os_repOsch_a1**)

During this study, the baseline database **j07_5-v4** is upgraded to **j07_5-w4** with the repair of **hoogtepunten** (elevation points) in the Upper Sea Scheldt (see §5.2.1).

5.2 Migration to j07_5-w4

5.2.1 Adding bathymetric information

The bathymetry generated from Baseline database **j07_5-v4** showed unrealistic features in several parts of the Upper Sea Scheldt. Figure 13 exemplifies the TIN (Triangulated Irregular Network) generated in **j07_5-v4** at the upper part of Zenne river. The uneven pattern as shown in the TIN effectively blocks the river channel and consequently creates unrealistic bathymetry in the Schelde_Nevla model.

The main reason is that the summer bed bathymetric data are absent in the baseline tree **j07_5-v4** in the Nete, Dijle, Zenne, Durme and a small part of the Upper Sea Scheldt near Merelbeke (see the green polygons in Figure 14). In order to fix this problem, the existing bathymetry (**bathy2009_simG105.dep**) from the latest calibrated and validated NEVLA3D model **simG162** (Vanlede et al., 2015) are utilized to fill the summer bed data gap. Figure 15 shows the updated TIN (**j07_5-w4**) at the upper part of Zenne river.

However using the model bathymetry directly on the baseline tree is not a successful practice. Figure 16 exemplifies the model bathymetric samples at the upper end of the river Dijle which mismatches the geometric boundary of the river. This is due to the fact that the model bathymetry is highly depended on the structure and orientation of the model grid used by the model **simG162** (**simG36_simona.grd**). During the previous study, the meandering of the small river branches in the Upper Sea Scheldt were simplified in the model grid with more or less a straight streamline during the grid generation, to avoid large numbers of grid cells (also aspect ratios and grid smoothness etc) for the river bend. Although such kind of simplification is

deemed as unproblematic to solve the tidal propagation along the river Scheldt, a different approach is followed in this study.

The proposed solution is to shift the existing model bathymetric samples to follow the geometry of grid. Afterwards the bathymetry is slightly refined and smoothed. This methodology has been applied to fix the problem at all the locations (within the green polygons as shown in Figure 14) where model bathymetry mismatched the river geometry.

Note that the original bathymetric data are not directly used in this study because the original data are measured along the river transect, with large data gap in space along the direction of the river streamline. It is therefore not straightforward to perform spatial interpolation onto the model grid. The bathymetric data from the existing model are however already processed by linear interpolation along the river channel, thus have higher spatial resolution to use.

Figure 13 – Example of TIN generated in Baseline **j07_5-v4** in the upper part of Zenne river.

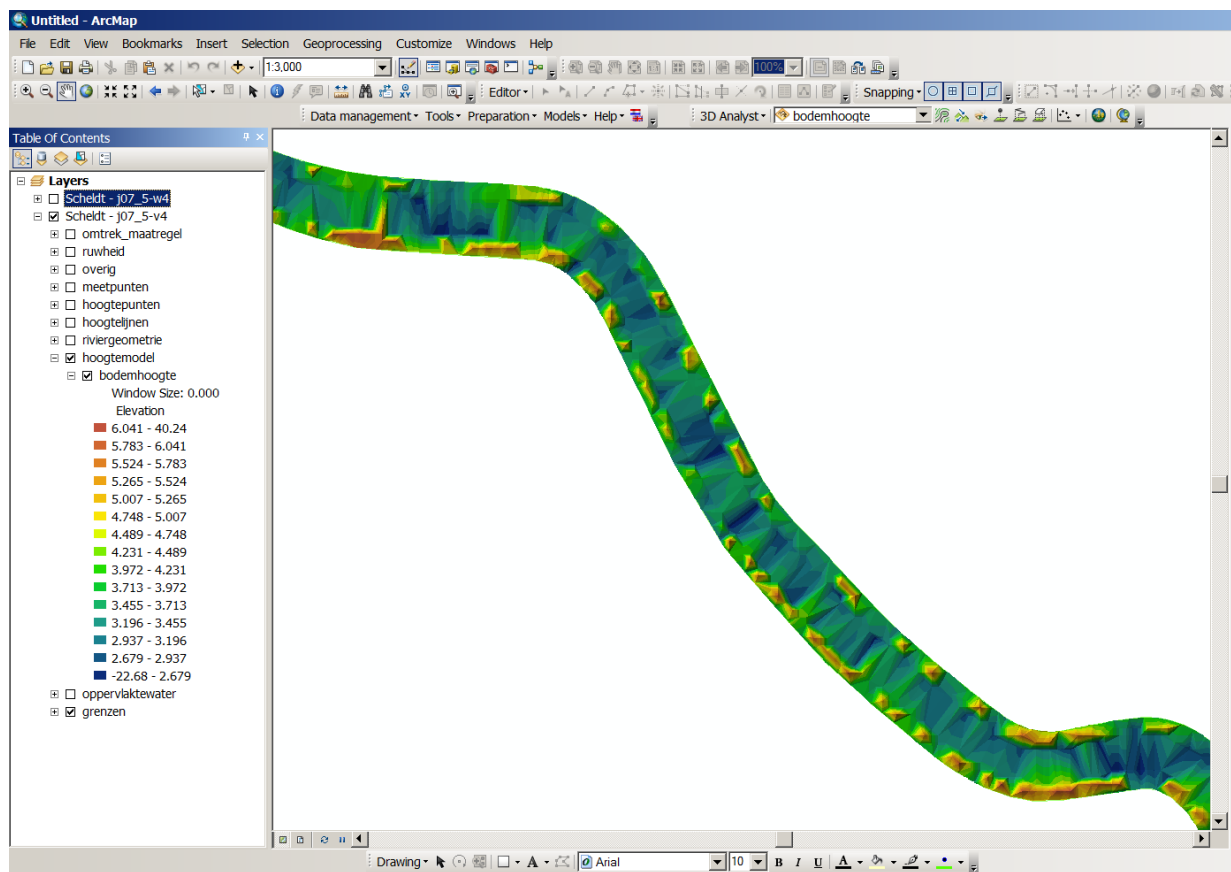


Figure 14 – Display of the winter bed data (in red) and summer bed data (in black) from Baseline tree **j07_5-v4**. The green polygons show the area without useful summer bed bathymetric data.

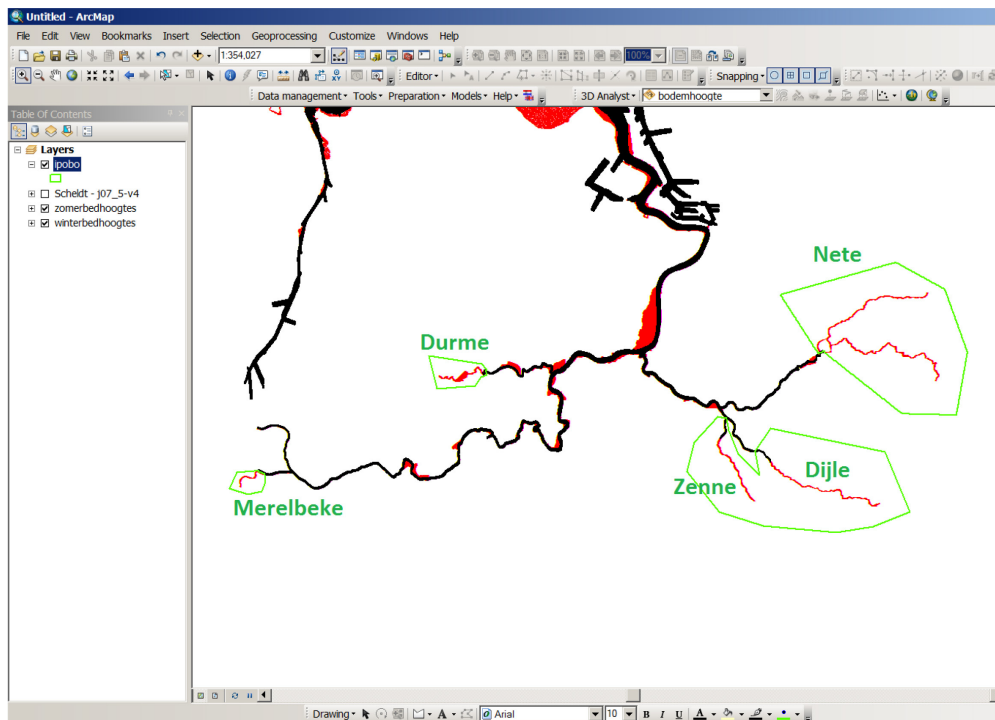


Figure 15 – Example of TIN generated in Baseline **j07_5-w4** in the upper part of Zenne river.

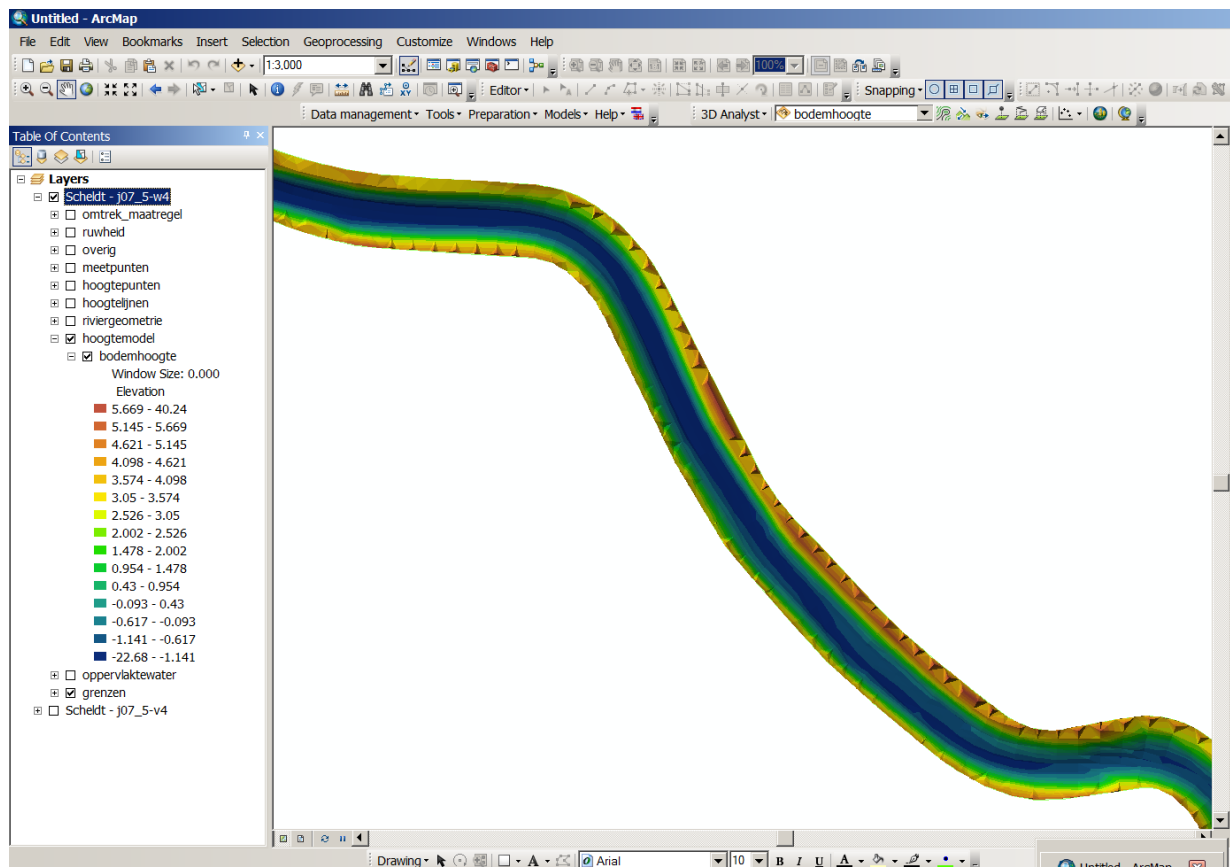
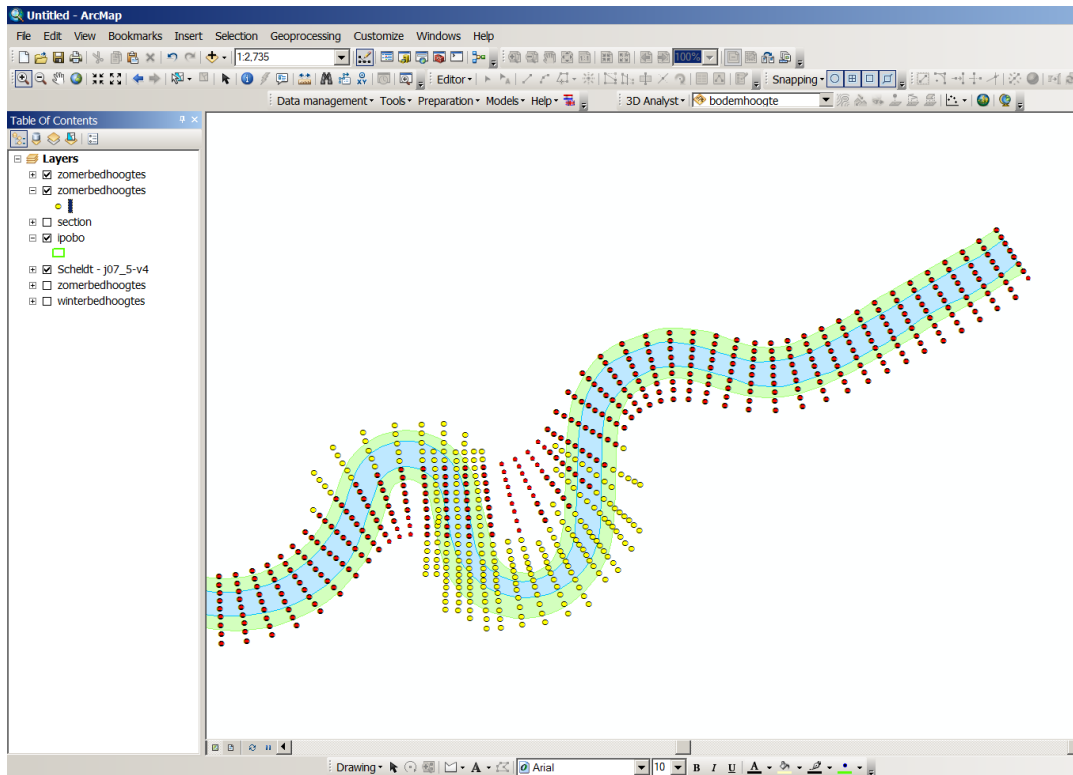


Figure 16 – Example of model bathymetric samples at the upper end of the river Dijle
 (red: model bathymetry from Vanlede et al., 2015; yellow: updated bathymetric data with shift and smooth).
 The green shadow (winter bed) and blue shadow (summer bed) represent the geometric boundary of the river.



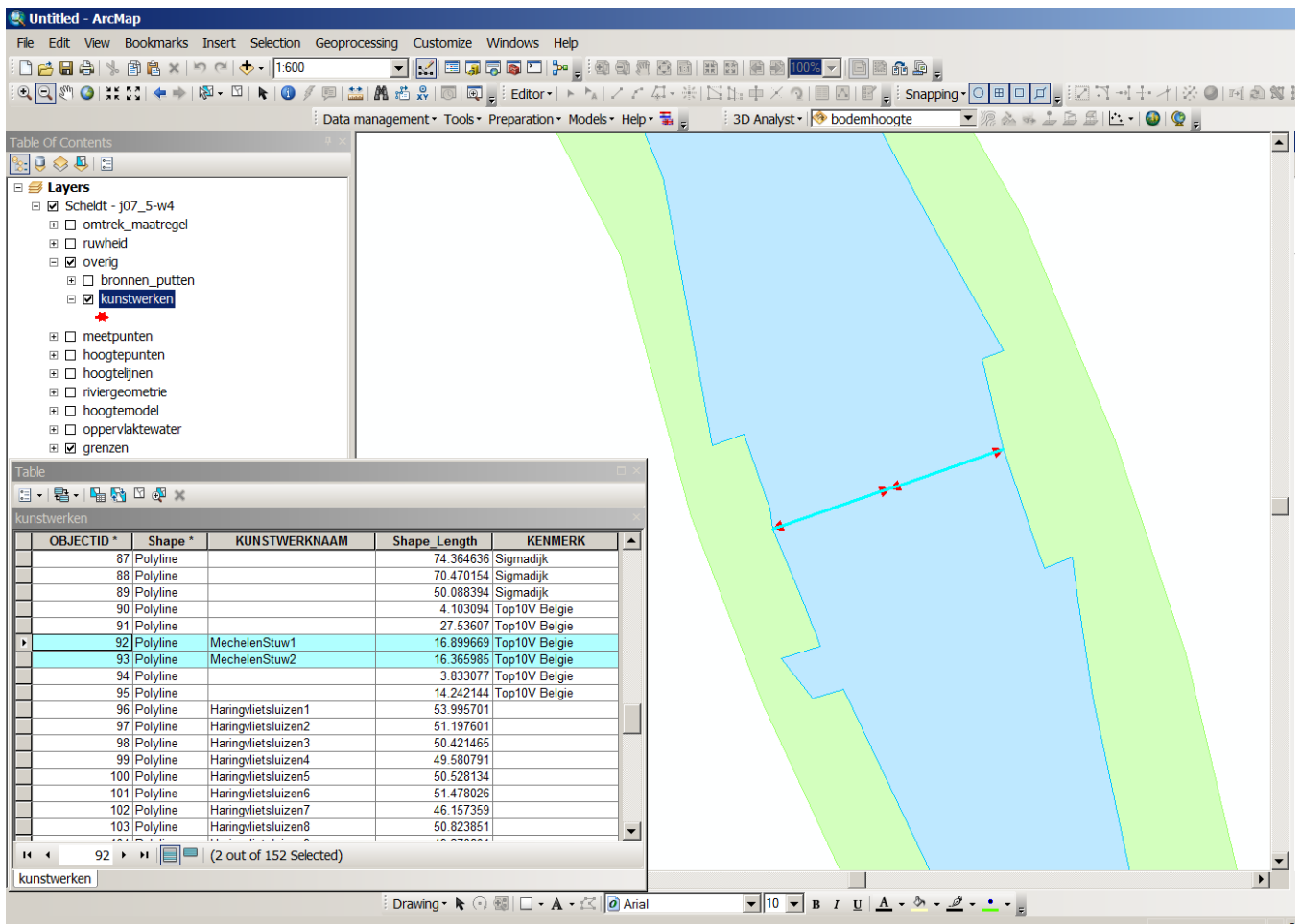
5.2.2 Assimilation of measure

The migration from **j07_5-v4** to **j07_5-w4** is done by assimilation of measure (**opname maatregel**) **ws_repWsch_a1**. This measure contains the information of polygons inside which the bathymetric data points should be erased firstly. The bathymetric data as described in §5.2.1 are added to this measure.

5.2.3 Adding KUNSTWERKNAAM at Mechelen.

After the upgrade of the Baseline tree, it has been detected that the **KUNSTWERKNAAM** of the hydraulic barrier at Mechelen is missing. The **KUNSTWERKNAAM** is therefore added by editing the attribute table under **overig-kunstwerken** (see snapshot in Figure 17).

Figure 17 – The KUNSTWERKNAAM of the hydraulic structure at Mechelen are added to the Baseline tree j07_5-w4.



5.2.4 Combining zomerbed roughness polygons

There are 33 roughness polygons of the **zomerbed** from Baseline database **j07_5-v4** as received from Deltares. The bottom roughness for the Western Scheldt (polygons with roughness codes 309 to 443) has been calibrated with OpenDA (Groenenboom et al., 2016). The calibration of bottom roughness with OpenDA from Zandvliet to Upper Sea Scheldt (polygons with roughness codes 450 to 468) is done in this study by FHR.

As described in §3.5, the polygons defining the roughness codes for the **zomerbed** can be changed by the modeller (e.g. merging or splitting). The choice of roughness polygons is an important step in the setup of the OpenDA calibration. More roughness polygons introduces more degrees of freedom in the model calibration.

In the Baseline database **j07_5-v4**, there are in total 19 polygons defined in the region between Zandvliet and Upper Sea Scheldt, which is deemed as too many. Therefore we combined some of the polygons, which leads to 10 polygons in the Baseline database **j07_5-w4** (see Figure 18 and Table 7).

The automatic calibration with OpenDA is described in §7.

Figure 18 – **zomerbed** polygons defined in **j07_5-w4** (left) and combined in **j07_5-v4** (right).
Top: **BeZS**; Middle: **BoZS**; Bottom: **Rupel**.

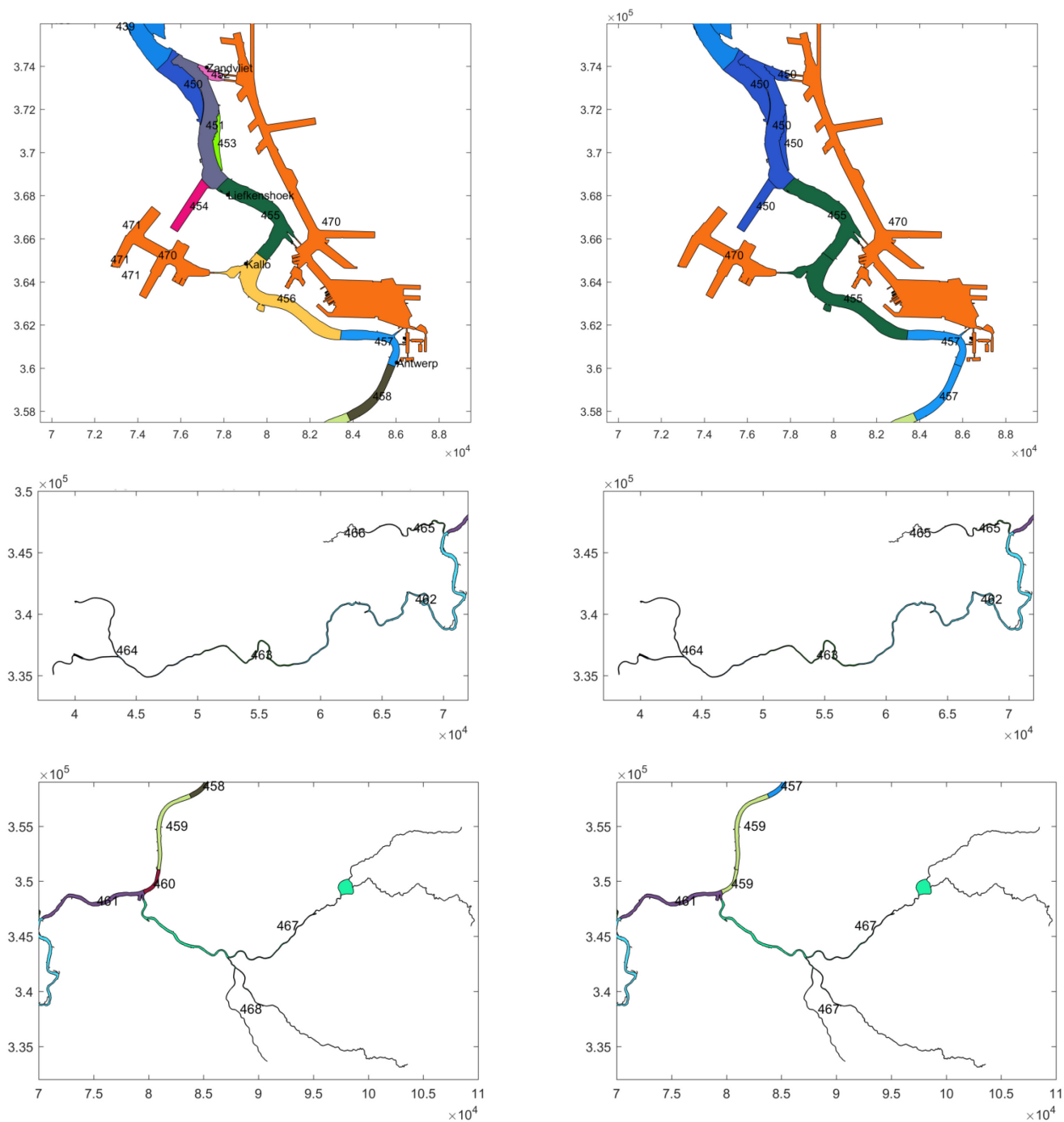


Table 7 – Merging **zomerbed** roughness polygons.

Existing Roughness Codes/Polygons	Combined Roughness Codes/Polygons	Water Level Stations (Figure 26)
450	450	Zandvliet
451		
452		
453		
454		
455	455	Liefkenshoek; Kallo
456		
457	457	Antwerp
458		
459	459	Hemiksem
460		
461	461	Temse
462	462	StAmands; Dendermond; Schoonaarde
463	463	Wetteren
464	464	Melle
465	465	Tielrode
466		
467	467	Boom; Wallem; Hombeek; Zemst; Mechelen_Benedensluis; Rijmenam; Duffel; Lier_Molbrug; Lier_Maasfort; Emblem; Kessel
468		

6 Model Update

6.1 Grid comparison

The grid used by the model waqua-schelde_nevla-j07_5-v4 is **grid-nevla_5-v2.grd**. It was created based on **NEVLAV07.grd** provided by FHR on 24-02-2015. The **NEVLAV07.grd** file stems from the operational forecasting system VSSKS (Voorspellingssysteem voor kust en Schelde) at FHR.

Deltares has adjusted this model grid. The orientation (M and N index) is shifted for the purpose of coupling with other model domains. Figure 19 shows the differences between the two model grids. The grid dimension remains unchanged (430×2945). Figure 20 shows the detailed differences at the upper end of the river Dijle. The **grid-nevla_5-v2.grd** is extended to the south to cover the realistic meandering of the river bend as discussed in §5.2.1. The detailed information of migration from **NEVLAV07.grd** to **grid-nevla_5-v2.grd** are summarized in Plieger (2015) and will not be elaborated here.

Figure 19 – Comparison of model grid **grid-nevla_5-v2.grd** and **NEVLAV07.grd**.

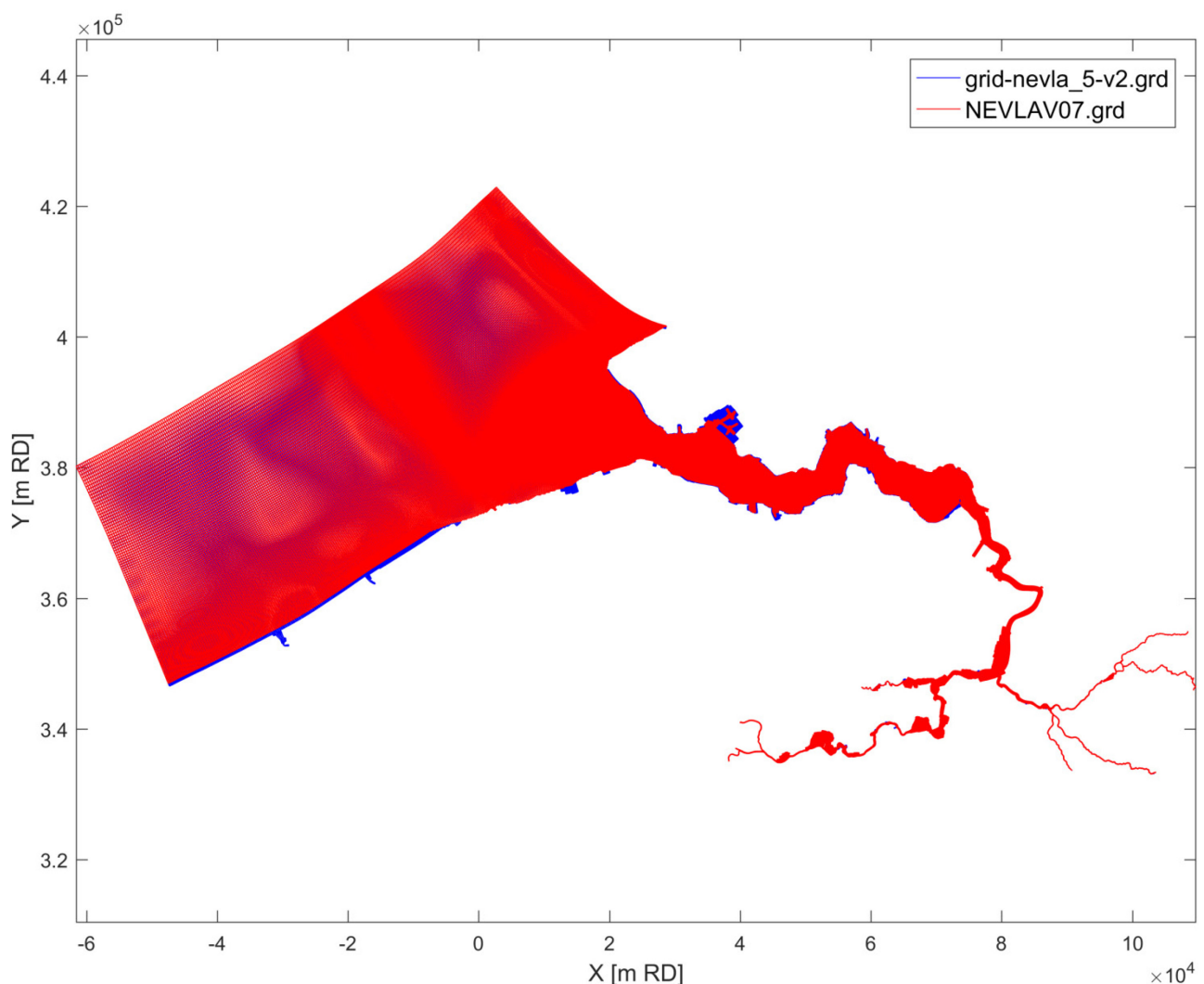
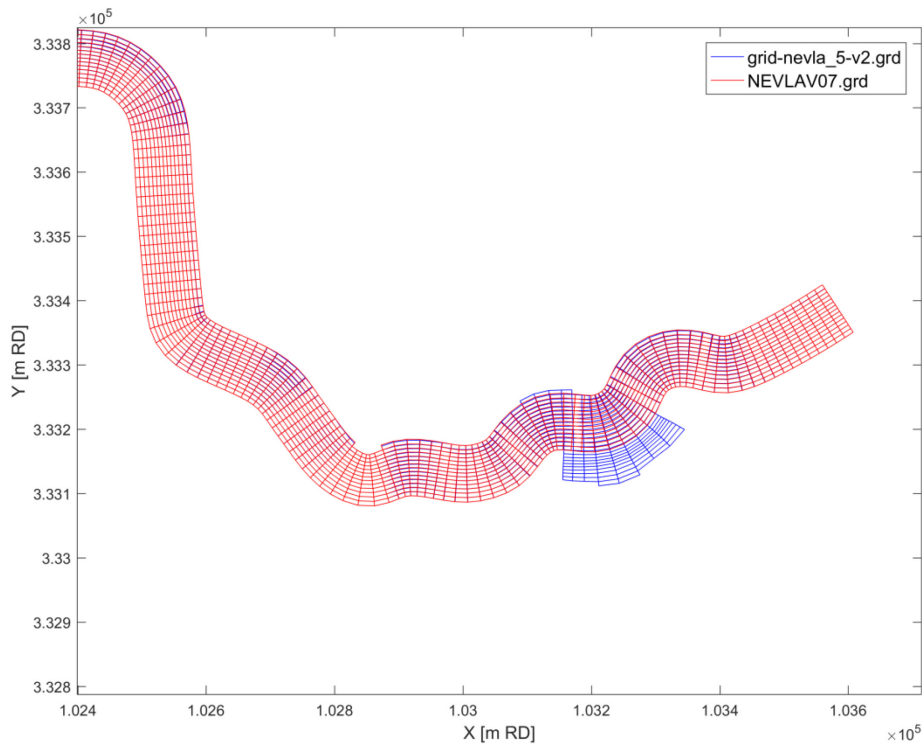


Figure 20 – Comparison of model grid **grid-nevla_5-v2.grd** and **NEVLAV07.grd** (zoomed into the upper end of the river Dijle).



As discussed in §5.2.1, the Baseline database uses existing model bathymetry in the area where there are no summer bed data. This model bathymetry is however associated with the model grid (**simG36_simona.grd**) used by the model run **simG162** in Vanlede et al., 2015. Figure 21 compares the this grid with the grid used in the Baseline database (**grid-nevla_5-v2.grd**). It shows that the **grid-nevla_5-v2.grd** is extended by inclusion of the flood control areas.

Note that although the **grid-nevla_5-v2.grd** is more similar to the model grid from VSSKS (**NEVLAV07.grd**), the model bathymetry (**bathy2009_simG105.dep**) from the latest calibrated and validated NEVLA3D model **simG162** (instead of the bathymetry from VSSKS) are utilized to fill the summer bed data gap as discussed in §5.2.1. The reason is that during the latest calibration and validation of the NEVLA3D model (**simG162** in Vanlede et al., 2015), extra efforts went into locally adjusting (e.g. smoothing) the model bathymetry of **bathy2009_simG105.dep**, to improve the model predictive abilities on water levels.

For a better overview, the different grid and bathymetry files used by different models are summarized in Table 8.

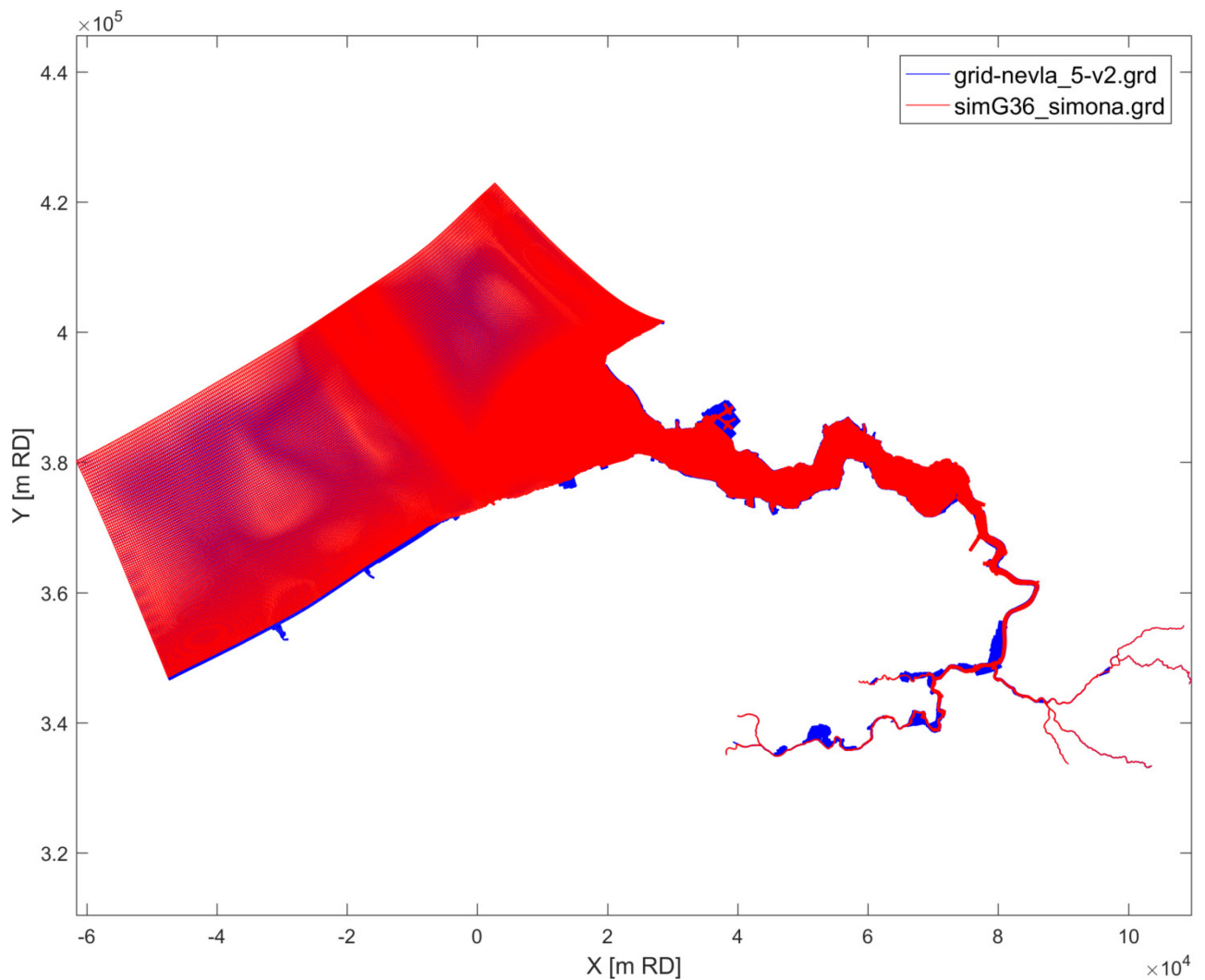
Figure 21 – Comparison of model grid **grid-nevla_5-v2.grd** and **simG36_simona.grd**.

Table 8 – Overview of different model grid and depth files used.

Model	grid file	depth file	reference of cal/val	year of bathymetry
Baseline	grid-nevla_5-v2.grd	bodem.j07_5-v4	LievenseCSO (2015)	2007
VSSKS	NEVLA07.grd	bathymetryv05	Chu et al., 2016	2013
Nevla3D	simG36_simona.grd	bathy2009_simG105.dep	Vanlede et al., 2015	2009

6.2 Grid adaptation around Tielrode

The bathymetry generated from Baseline database **j07_5-w4** (projection to **grid-nevla_5-v2.grd**) contains a hump around **Tielrode** (see Figure 22). This hump partially blocks tidal propagation during low water.

The main reason is that the local grid is too coarse along the N direction (grid resolution $[M \times N] \approx 16 \text{ m} \times 38 \text{ m}$) to resolve the tidal channel meandering from sample interpolation (Figure 22). A possible solution would be

to locally refine the grid along the N direction around Tielrode. However the grid refinement at Tielrode would also lead to local refinement on grid cells around **Walem** (because this is a structured grid).

In order to avoid this, **grid-nevla_5-v2.grd** is firstly split into two separate sub-grids. The submesh around Tielrode is locally refined along the N direction Tielrode with resulted local grid resolution $[M \times N] \approx 16 \text{ m} \times 16 \text{ m}$. Finally the two submeshes are pasted back in to one complete mesh **grid-nevla_5-v3-adjust.grd**. Following this method, the overall grid dimension remains unchanged while the unwanted changes at Walem is also avoided. Accordingly the grid smoothness along N direction of **grid-nevla_5-v3-adjust.grd** is improved (reduced to <1.3 , see Figure 23).

As the model grid has been changed, the MN – depended input files are also subject to change. A part of those files are automatically generated from Baseline tree via functionality of ‘conversion to WAQUA’. The rest files are prepared offline by modeller with projection of the same data from **grid-nevla_5-v2.grd** to **grid-nevla_5-v3-adjust.grd**. Figure 9 lists the input files which are adjusted to fit the new model grid.

Figure 22 – **Left Up:** Summerbed and winterbed data recorded in Baseline database **j07_5_w4**;
Left Bottom: Projection from Baseline database **j07_5_w4** to model grid **grid-nevla_5-v2.grd** (conversion to WAQUA).
The black circle shows the area where local bathymetry is humped.
Right Up: Model grid is locally refined in **grid-nevla_5-v3-adjust.grd**.
Right Bottom: Projection from Baseline database **j07_5_w4** to model grid **grid-nevla_5-v3-adjust.grd** (conversion to WAQUA).
The hump shown in the previous bathymetry disappears.

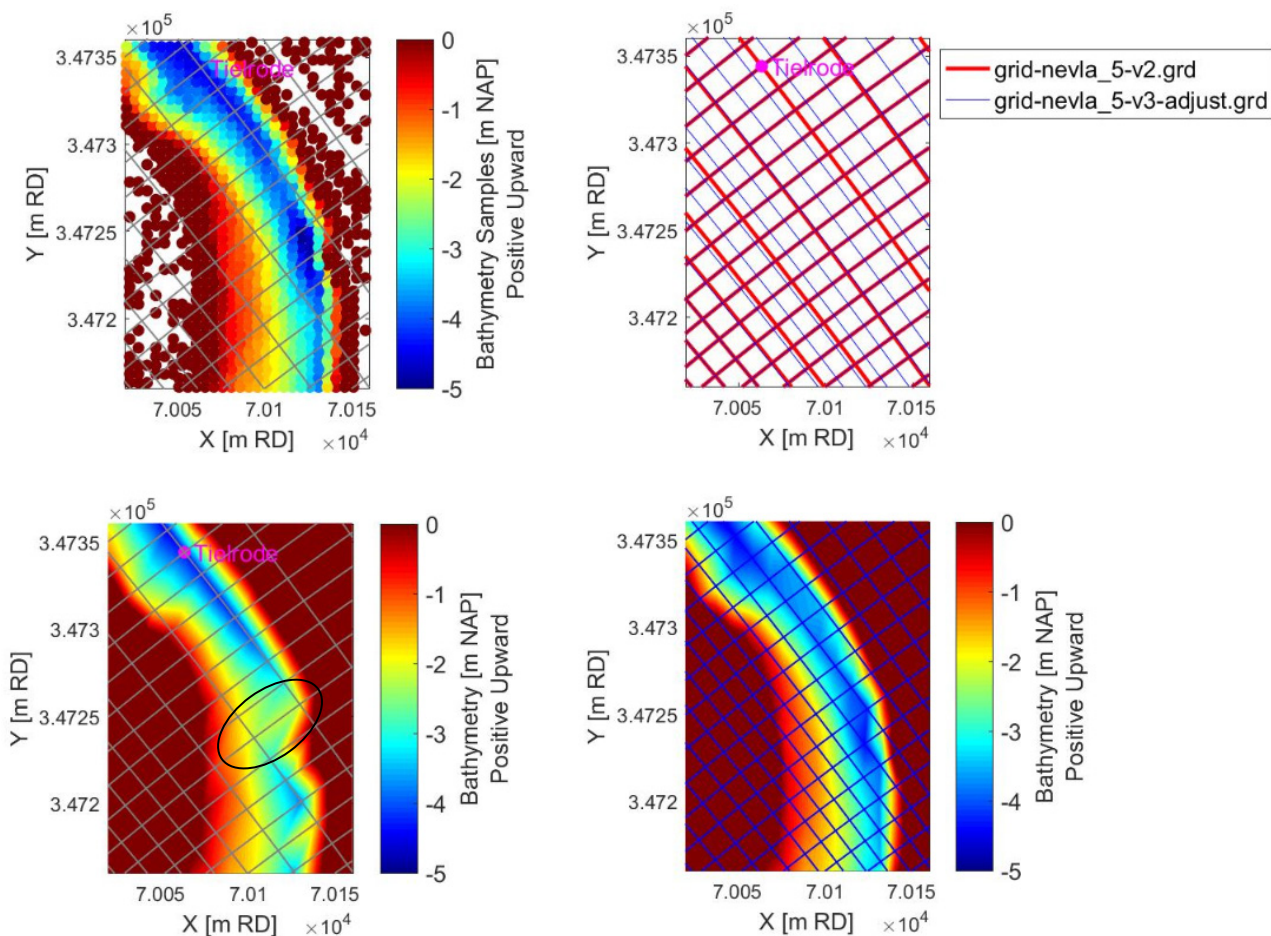
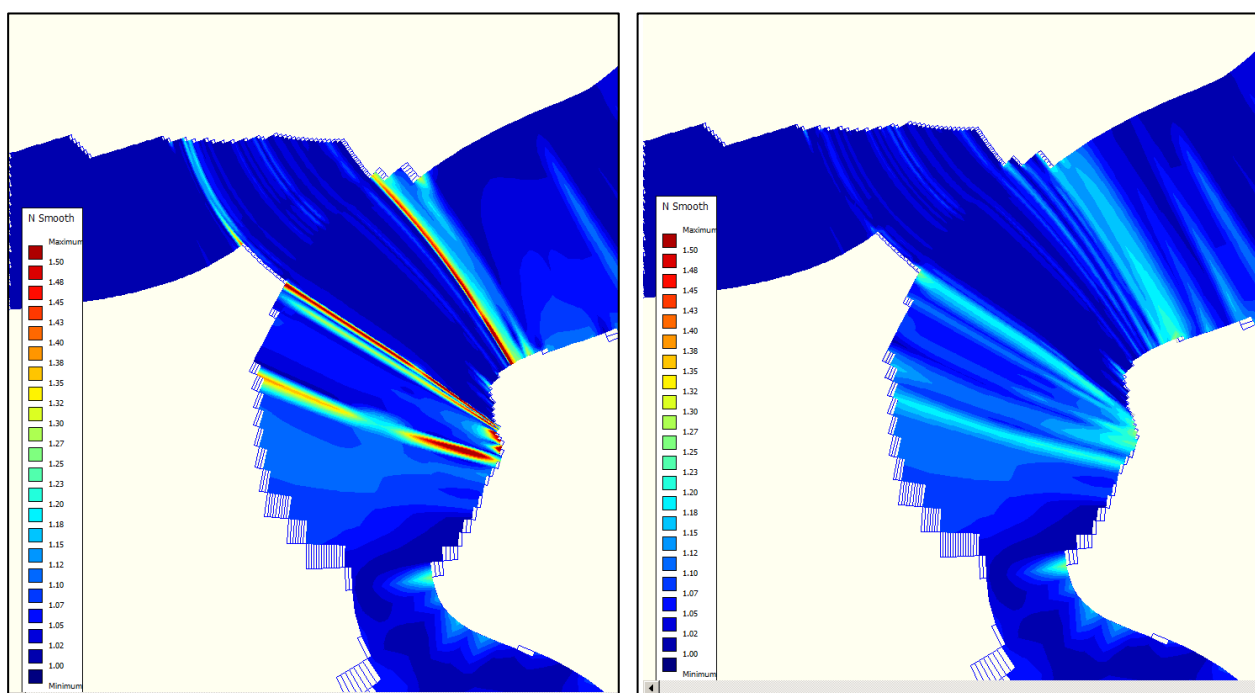


Figure 23 – Grid property of N Smoothness: **grid-nevla_5-v2.grd** (left) and **grid-nevla_5-v3-adjust.grd** (right).Table 9 – Changes of MN-depended input files associated with the new grid **grid-nevla_5-v3-adjust.grd**.

File Name	Description
ini-sal-HW-Vlissingen	Initial salinity map used to force the model
points-snelheden_debietraaien	Definition of points (MN) used to define cross-sections
siminp.nevla (steering file): 'Forcings – Initial WL – Local'	Initial water level used to force the model

6.3 Shift of MN index of output points

The MN index of output points are stored in the file **meetp.j07_5-w4** which is automatically generated from projection of Baseline tree **j07_5-w4** to the model grid of **grid-nevla_5-v3-adjust.grd**.

However, the local bathymetry at several output points are found to be too shallow (see Figure 10) which will lead to wrong calculation of low water levels, e.g. LW is cut off at a certain level. This is due to the fact that the tidal stations are usually installed close to the river bank where the local grid might be too coarse or the local bathymetric samples are not fine enough to resolve the side slope. Therefore the interpolated local bathymetry might be different from the bathymetry in reality. This is corrected by manual adjustment of the MN index to an adjacent deeper location (Figure 100). The shifted location is deemed as equally representative because a small shift in space will not lead to large differences in tidal predictions.

A new file **meetp.j07_5-w4-hand** is created, in which the 9 above-mentioned stations are indexed with an extension **'_waq'** added to the name (e.g. name = 'Melle_waq').

Table 10 – Update of M and N index at output stations.
Note: bathymetry is positive upward.

Station	X [m RD]	Y [m RD]	meetp.j07_5-w4		Bathymetry [m NAP]	Lowest Water Level [m NAP]	meetp.j07_5-w4-hand		Bathymetry [m NAP]
			M	N			M	N	
Tielrode	70046.5	347383.2	207	1693	-0.33	-2.71	209	1691	-3.91
Walem	87118.1	343117.7	364	1716	2.25	-2.41	365	1715	-3.57
StAmands	71554.4	341011.8	289	1540	-1.37	-2.41	290	1542	-3.65
Dendermonde	65102.4	339198.1	250	1377	-0.79	-1.81	251	1377	-4.57
Schoonaarde	58164.5	335910.5	256	1252	1.08	-1.15	255	1252	-2.37
Melle	43964.8	336168.3	255	973	1.48	-0.95	254	973	-2.30
Hombeek	89152.4	336610.4	341	1197	1.12	-0.33	342	1197	-0.55
Duffel	95065.3	347035.6	380	1473	-0.61	-1.54	376	1473	-1.86
LierMolbrug	97931.8	348868.6	406	1269	1.65	0.21	405	1270	-0.10

6.4 Barrier at Mechelen

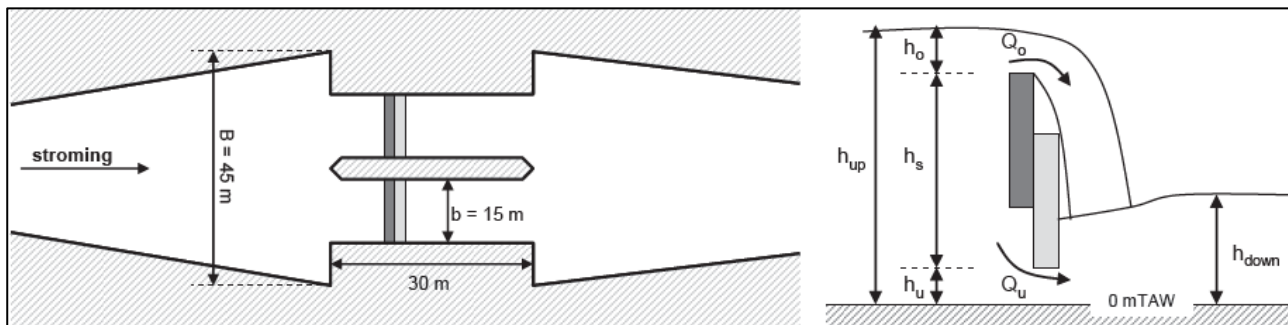
6.4.1 Physical Description

In reality there is a barrier near Mechelen which is not implemented in the present model. Figure 24 shows the schematization of the barrier which consists of two channels with width of 15 m. The total width of the bed is about 45 m (contracted). The bottom level of the weir is at 0 m TAW.

The barrier is controlled automatically or manually with both underflow and overflow. In case of low discharges, the barrier is controlled automatically. In case of high discharges (when the difference between water level upstream and downstream is less than 80 cm), manual control is implemented (Adema, 2006). Under normal circumstances, the bottom slider remains on the bottom and the flow passes over the upper slider. Water levels are maintained at 4.8 m TAW (2.47 m NAP) at the upstream (h_{up}).

Figure 24 – Schematization of the barrier at Mechelen in the Dijle river.

Left: top view; right: side view. h_o & Q_o = height of the water column and flow over the barrier; h_s = height of the sill;
 h_u & Q_u = height of the water column and flow rate under the barrier; h_{up} = upstream water level;
 h_{down} = downstream water level (after Vermeersch et al., 2016).



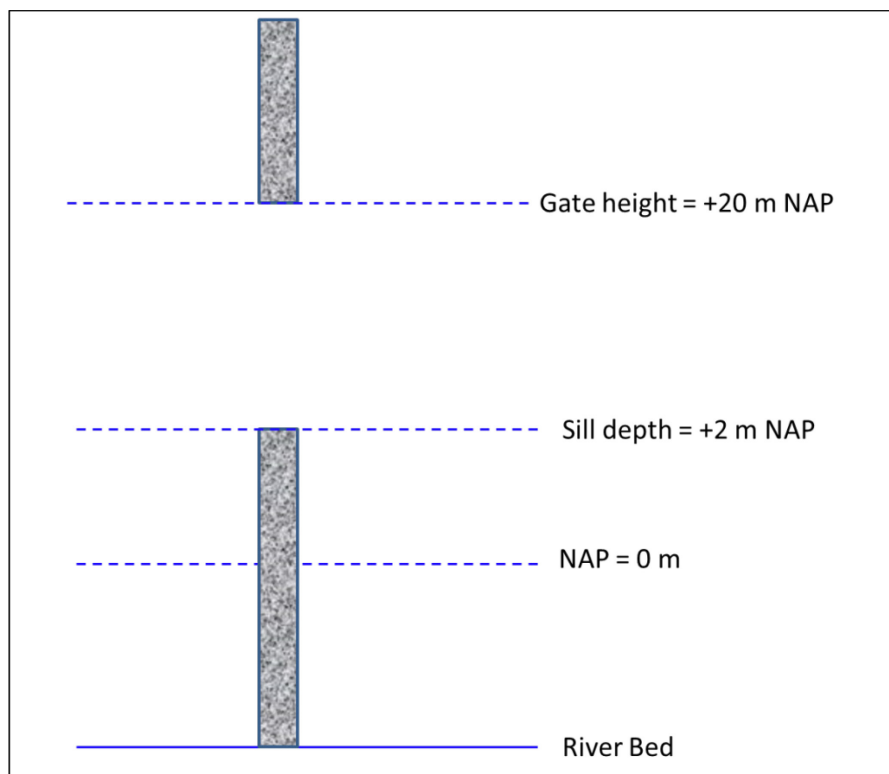
6.4.2 Implementation in the model

Accurate implementation of the hydraulic structure at Mechelen is important to guarantee correct water level predictions at MechelenSluis and Rijmenam. From the modelling point of view, it can be approximated by the use of barrier elements, weir structure or change of the local bathymetry in Simona.

A lot of efforts have been made by previous modelling studies. Maximova et al (2009a) implemented the structure by changing the local bathymetry with crest level defined at + 1.47m NAP, to be consistent with Adema (2006). It is however found that oscillations occur in the model and calculated water levels do not represent the reality. Thus, the implementation by the local change of bathymetry did not improve the model accuracy. Maximova et al (2009a) also attempted the use of weir structure in the SIMONA model. The horizontal V-weir with the crest at +2 m NAP is defined in the input files. This improved the low water levels at Rijmenam but does not give any significant improvement at Mechelen.

In this study, a barrier element is selected to represent the operation of the complex hydraulic structure at Mechelen. Unfortunately the time series data of the barrier operations is not available. Therefore the barrier is implemented in a static way with constant sill depth of +2 m NAP. The gate height is put at a height of +20 m NAP in order to exclude it from the simulation (see Figure 25). In the future if detailed operational data are available, the input parameters of the barrier can be completed to improve the representation in the model.

Figure 25 – Sketch of barrier element implemented in this study.



7 Calibration with OpenDA

7.1 Introduction

OpenDA (<http://www.openda.org>) is an open interface standard for (and free implementation of) a set of tools to quickly implement data-assimilation and calibration in arbitrary numerical models. OpenDA is a generic environment for parameter calibration and data assimilation application. It provides a platform that allows an easy interchange of algorithms and models.

In general, a complete OpenDA setup consists of one main input file and 3 data assimilation components: stochastic model factories, stochastic observers, and algorithms. OpenDA makes use of XML (Extensible Markup Language) format for the configuration files. All the template files **.xsd** (XML Schema Definition) can be found at <http://schemas.openda.org/>.

7.2 The input files of OpenDA

7.2.1 Main input file

The main input file is the top-level OpenDA configuration file that specifies the basic components and contains references to lower-level configuration files. It controls the overall configuration for an OpenDA application. There are 3 mandatory components, which make up an OpenDA application: `stochModelFactory`, `stochObserver` and `algorithm`. Each component is configured by specifying its `className` attribute, `workingDirectory` and `configFile/configString`.

An optional component is available for configuring the output of the results, and optional components for defining OpenDA restart input and output files.

The main input file uses **openDaApplication.xsd** as template. Below is an example of the main input file used in this study.

```
<openDaApplication xmlns="http://www.openda.org"
xmlns:xsi="http://www.w3.org/2001/XMLSchema-instance"
xsi:schemaLocation="http://www.openda.org
http://www.openda.org/schemas/openDaApplication.xsd">

  <stochModelFactory className="org.openda.blackbox.wrapper.BBStochModelFactory">
    <workingDirectory>./stochmodel</workingDirectory>
    <configFile>stochmodel_rough1.xml</configFile>
  </stochModelFactory>

  <stochObserver className="org.openda.observers.NoosTimeSeriesStochObserver">
    <workingDirectory>./stochobserver</workingDirectory>
    <configFile>obs_rough_20070101.xml</configFile>
  </stochObserver>

  <algorithm className="org.openda.algorithms.Dud">
    <workingDirectory>./algorithm</workingDirectory>
    <configString>dudAlgorithm.xml</configString>
  </algorithm>
```

```

<resultWriters>
  <resultWriter className="org.openda.resultwriters.MatlabResultWriter">
    <workingDirectory>.</workingDirectory>
    <configFile>results_gewonedud.m</configFile>
  </resultWriter>

  <resultWriter className="org.openda.resultwriters.TextTableWriter">
    <workingDirectory>.</workingDirectory>
    <configFile>results_gewonedud.csv</configFile>
  </resultWriter>
</resultWriters>

</openDaApplication>

```

7.2.2 Stochastic model factories

Stochastic model factories are configuration files for the black box model wrapper, subdivided in three layers.

- Outer layer - StochModel config ([blackBoxStochModelConfig.xsd](#))
- Middle layer - Model config ([blackBoxModelConfig.xsd](#))
- Inner layer - Wrapper config ([blackBoxWrapperConfig.xsd](#))

Outer layer - StochModel config

The outer layer stochastic model is configured by specifying the vectors of parameters, state, and/or predictor. It uses **blackBoxStochModelConfig.xsd** as template. Below is an example file used in this study (explanations are commented in green).

```

<vectorSpecification>
  <parameters> #Specify the model parameters vectors
    <regularisationConstant> #Specify which model parameters to adjust and how
      <stdDev value="0.002" transformation="identity"/>
      <vector id="A-455"/> #Identity of the vector
    </regularisationConstant>
  </parameters>
  # stdDev value: set the standard deviation of this parameter and the method how the parameter should be corrected.
  # Transformation: Two values are possible: 'identity' and 'ln'. The 'identity' means that the correction will be added
  directly without any transformation to the adjusted parameter. 'ln' means that correction is transformed logarithmically
  before it is added to the parameter;
  <predictor>
    <vector id="Zandvliet.waterlevel"/>
    <vector id="LIEF.waterlevel"/>
  </predictor>
  # Specify the predictor vectors. i.e. the model variables that correspond to the observer variables. This can contain three
  different types of mappings between model and observer variables: 1. a vector for a mapping between an observed
  scalar and a scalar in the model. In this case the coordinates are not used and no interpolation is done. (used in this
  study) 2. a vector for a mapping between an observed grid and a grid in the model. In this case the model values are
  interpolated to get values at the cell centers of the observed grid. This uses the coordinates of both grids and bilinear
  interpolation. 3. a sub-Vector for a mapping between an observed scalar and a cell of a grid in the model. In this case
  the coordinates are not used and no interpolation is done.
</vectorSpecification>

```

```

<modelConfig> # Specify a specific black box model configuration (Middle Layer). This can be either by writing directly
the model configuration or by referring to a black box model configuration file.
    <file>./detmodel/detmodel_rough1.xml</file> # Specify filename of the black box model configuration file.
</modelConfig>

```

Middle layer - Model config

The configuration of a specific black box model is exemplified here. It uses **blackBoxModelConfig.xsd** as template. Below is an example file used in this study (explanations are commented in green).

```

<aliasValues> # Specify the alias keys and (optionally) the corresponding actual values; The alias key name as defined
in the black box wrapper configuration
    <alias key="templateDir" value="base"/>
    <alias key="instanceDir" value="work"/>
    <alias key="runid" value="rough1"/>
    <alias key="netcdfoutput" value="waterlevelseries.nc"/>
    <alias key="inputFile" value="siminp.nevla"/>
    <alias key="roughParamsFile" value="roughcombination-westerschelde-2015_5-v1 openda2"/>
    <alias key="depthFile" value=""/>
    <alias key="roughness-U-File" value=""/>
    <alias key="roughness-V-File" value=""/>
</aliasValues>

<exchangeItems> # Specify the list of items to exchange between the model and OpenDA components.
    <vector id="A-450" ioObjectId="roughParams" elementId="Rough_CODE_450_A"/>
    # id Identity of the exchange item vector to be used in the stochastic model configuration.
    # ioObjectId is the corresponding object identity of the exchange item.
    # elementId is the corresponding identity of the exchange item as used internally within the model.
    <vector id="A-455" ioObjectId="roughParams" elementId="Rough_CODE_455_A"/>
    <vector id="A-457" ioObjectId="roughParams" elementId="Rough_CODE_457_A"/>
    <vector id="A-459" ioObjectId="roughParams" elementId="Rough_CODE_459_A"/>
    <vector id="A-461" ioObjectId="roughParams" elementId="Rough_CODE_461_A"/>
    <vector id="A-462" ioObjectId="roughParams" elementId="Rough_CODE_462_A"/>
    <vector id="A-463" ioObjectId="roughParams" elementId="Rough_CODE_463_A"/>
    <vector id="A-464" ioObjectId="roughParams" elementId="Rough_CODE_464_A"/>
    <vector id="A-465" ioObjectId="roughParams" elementId="Rough_CODE_465_A"/>
    <vector id="A-467" ioObjectId="roughParams" elementId="Rough_CODE_467_A"/>

    <vector id="Zandvliet.waterlevel" ioObjectId="%netcdfoutput%" elementId="Zandvliet.waterlevel"/>
    <vector id="LIEF.waterlevel" ioObjectId="%netcdfoutput%" elementId="LIEF.waterlevel"/>
    <vector id="KALO.waterlevel" ioObjectId="%netcdfoutput%" elementId="KALO.waterlevel"/>
</exchangeItems>

<wrapperConfig> # Specify the name of the black box wrapper configuration file (Inner Layer).
    <file>waquaWrapper.xml</file>
</wrapperConfig>

<doCleanUp>false</doCleanUp> # Specify whether to remove unnecessary files upon completion of a model run.

<skipModelActionsIfInstanceDirExists> true </skipModelActionsIfInstanceDirExists> # If set to true, no
actions are executed on a model instance that already exists.

```

Inner layer - Wrapper config

The configuration of a specific black box model is exemplified here. The configuration of a black box model wrapper contains of three main components: alias definitions, model run, and input-output definition. It uses **blackBoxWrapperConfig.xsd** as template. Below is an example file used in this study (explanations are commented in green).

```
<aliasDefinitions defaultKeyPrefix="%" defaultKeySuffix="%" >
# Define aliases for specific model information (directory names, file names etc.).
# Specify the prefix and suffix for the alias keys, default is '%';
  <alias key="SIMONADIR"/> # read alias SIMONADIR from environment variable.
  <alias key="templateDir"/>
  <alias key="instanceDir"/>
  <alias key="depthFile"/>
  <alias key="netcdfoutput"/>
  <alias key="inputFile" keyPrefix="${" keySuffix="}"/>
  <alias key="runid"/>
  <alias key="roughness-U-File" keyPrefix="${" keySuffix="}"/>
  <alias key="roughness-V-File" keyPrefix="/" keySuffix="/" />
  <alias key="roughParamsFile" keyPrefix="${" keySuffix="}"/>
</aliasDefinitions> # END

<run> #Specify the initialize/compute/finalize actions that direct the model
  <initializeActionsUsingDirClone instanceDir="%instanceDir%%instanceNumber%"
templateDir="%templateDir%"/> # The directory, in which the model executables and input files are located, will
be cloned to a new working directory. The actions are executed in this new working directory.
  <computeActions> # Configure the method for model computation
    <action exe="%SIMONADIR%/bin/waqpre.pl" workingDirectory="%instanceDir%"> #waqpre
      # Specify a list of input arguments of the model executable.
      <arg>-runid</arg> # Run ID
      <arg>%runid%</arg>
      <arg>-input</arg> # siminp file
      <arg>${inputFile}</arg>
      <arg>-isddh</arg> # domain decomposition (y/n)
      <arg>n</arg>
      <arg>-back</arg> # execute in background (y/n)
      <arg>n</arg>
      <checkOutput file="waqpre-m.%runid%" expect="SIMONA --- program ended successfully"/>
      <checkOutput file="SDS-%runid%"/> # should exist
      # checkOutput file: Specify list of output files to be checked after the command execution has finished
      # expect: expected content of the output file when the action is successful
    </action>
    <action exe="%SIMONADIR%/bin/waqpro.pl" workingDirectory="%instanceDir%">#waqpro
      <arg>-runid</arg> # Run ID
      <arg>%runid%</arg>
      <arg>-isddh</arg> # domain decomposition (y/n)
      <arg>n</arg>
      <arg>-back</arg> # execute in background (y/n)
      <arg>n</arg>
      <arg>-npart</arg> # MPI
      <arg>32</arg> # Parallel with 32 processors.
      <checkOutput file="waqpro-m.%runid%" expect="SIMONA --- program ended successfully"/>
      <checkOutput file="SDS-%runid%"/> # should exist
```



```

</action>
<action exe="%SIMONADIR%/bin/getdata.pl" workingDirectory="%instanceDir%"> #getdata
    <arg>-f</arg>
    <arg>SDS-%runid%</arg> # name of the SDS file, including the full path
    <arg>-v</arg> # the list of chosen variables (comma-separated)
    <arg>ZWL,NAMWL,MWL,NWL,XZETA,YZETA,ITDATE</arg>
    <arg>-o</arg> # output format
    <arg>netcdf</arg>
    <arg>-d</arg> # output file
    <arg>%netcdfoutput%</arg>
    <checkOutput file="%netcdfoutput%">
</action>
</computeActions>
<finalizeActions/>
</run>

<inputOutput> # Specify the input/output object
    <ioObject className="org.openda.blackbox.io.SimonaRoughParamsFile">
        <file>${roughParamsFile}</file> # Name of input/output file (e.g. roughness file)
        <id>roughParams</id> # Identity of the input/output object
        <arg>roughParams</arg> # Input argument for the corresponding OpenDA class
    </ioObject>
    <ioObject className="org.openda.blackbox.io.SimonaNetcdfFile"> #water level output NetCDF.
        <file>%netcdfoutput%</file>
        <id>%netcdfoutput%</id>
    </ioObject>
</inputOutput>

```

7.2.3 Stochastic observers

Stochastic observers is a configuration file for a number of possible stochastic observers (time series of water level with standard deviation, see explanations in box below).

The configuration of stochastic observers is exemplified here. It uses **noosObservations.xsd** as template. Below is an example file used in this study (explanations are commented in green). The observation data stored in different files at different observing locations are listed here.

```

<noosObserver xmlns:xsi="http://www.w3.org/2001/XMLSchema-instance">

    <timeSeries status="use" location="Zandvliet" standardDeviation="0.5" minDateTime="200701010000"
maxDateTime="200712312350">
        Zandvliet.waterlevel # Specify the file name of the NOOS data time series. The path is written relative to the
directory where this xml file is stored.
    </timeSeries>

    # standardDeviation specify the observational error standard deviation of this time series. The value is given in the
same units as the observations. Also see it in the cost function in §7.4
    # minDateTime is the begin time for observation selection
    # maxDateTime is the end time for observation selection

    <timeSeries status="use" location="Hemiksem" standardDeviation="0.5" minDateTime="200701010000"
maxDateTime="200712312350">

```



```

    Hemiksem.waterlevel
  </timeSeries>

</noosObserver>

```

7.2.4 Algorithms

This part contains the configuration files for the calibration and assimilation algorithms that are available in OpenDA.

The configuration of optimization algorithm of DUD is exemplified here, **dudConfig.xsd** as template. Below is an example file used in this study (explanations are commented in green). The detailed descriptions are referred to §7.3.

```

<DudConfig>
  <costFunction weakParameterConstraint="false"
class="org.openda.algorithms.SimulationKwadraticCostFunction" biasRemoval="false" />
# Specify whether to use weak constraint (weakParameterConstraint=true) or strong constraint
(weakParameterConstraint=false). The difference is that in case of strong constrained optimization you do not get a
penalty when the parameter moves away from the initial value (background term in cost function).
# biasRemoval Specify whether bias should be removed (true) from the cost computation. Default: false.

  <outerLoop maxIterations="100" absTolerance="0.001" relTolerance="0.001"
relToleranceLinearCost="0.0001" />
# maxIterations: how many times a new choice for a parameter set is made.
# absTolerance Maximum absolute difference between the costs of 2 best parameter estimates  $|J_{\text{new}} - J_{\text{previous}}|$ .
# relTolerance Maximum relative difference between the costs of 2 best parameter estimates  $|J_{\text{new}} - J_{\text{previous}}| / J_{\text{new}}$ .
# relToleranceLinearCost Maximum relative difference between the linearized costs of two best parameter
estimates.  $|J_{\text{new}} - J_{\text{linear}}| / (J_{\text{previous}} - J_{\text{linear}})$ ;

  <lineSearch maxIterations="30" maxRelStepSize="5.0" >
    <backtracking shorteningFactor="0.5" startIterationNegativeLook="3" />
  </lineSearch>
# maxIterations Maximum number of inner iterations.
# maxRelStepSize Maximum relative step size. This indicates how much the parameters may change from one outdoor
rotation to the other.
# backtracking Back tracking if the line search produces estimate with larger cost.
# shorteningFactor Factor for shortening step size.
# startIterationNegativeLook Maximum number of iterations before searching in opposite direction.
</DudConfig>

```

7.3 The Optimization Algorithm - DUD

For the present study, the DUD (Doesn't Use Derivative) algorithm is used (Ralston and Jennrich, 1978). DUD is a derivative-free algorithm for nonlinear least squares. It can be seen as a Gauss-Newton method, in the sense that it transforms the nonlinear least square problem into the well-known linear square problem. DUD evaluates and optimizes uncertain model parameters by minimizing a cost function. The parameter values corresponding to the minimum value of the cost function are considered as the optimal parameter values for the given analysis.

The general DUD implementation is given by the following steps:

- Start running first guess and modify each parameter;
- Linearize the model around these values and solve a linear problem;
- If this is an improvement, update linearization with new point (so called outer iteration);
- Or, do a line-search (only until there is improvement), which is the inner iteration.

The detailed description and mathematical calculation is given in ANNEX1.

7.4 Cost function

The cost function used by this study is **org.openda.algorithms.SimulationKwadraticCostFunction** which is a quadratic cost function over the complete timeseries. It is essentially a total sum of squares, made dimensionless with the measurement uncertainty

$$J = \frac{1}{2} \sum_{r=1}^{R_{max}} \sum_{s=1}^{S_{max}} \sum_{n=1}^{N_{max}} \frac{(H_{r,s,n}^{sim}(t) - H_{r,s,n}^{obs}(t))^2}{(\sigma_{H_{r,s}^{obs}})^2}$$

where:

H(t) - water level at time t;

sim - results obtained from model simulations over the simulation period;

obs - observation values;

n, N_{max} - number of time steps in the time series (**52560**);

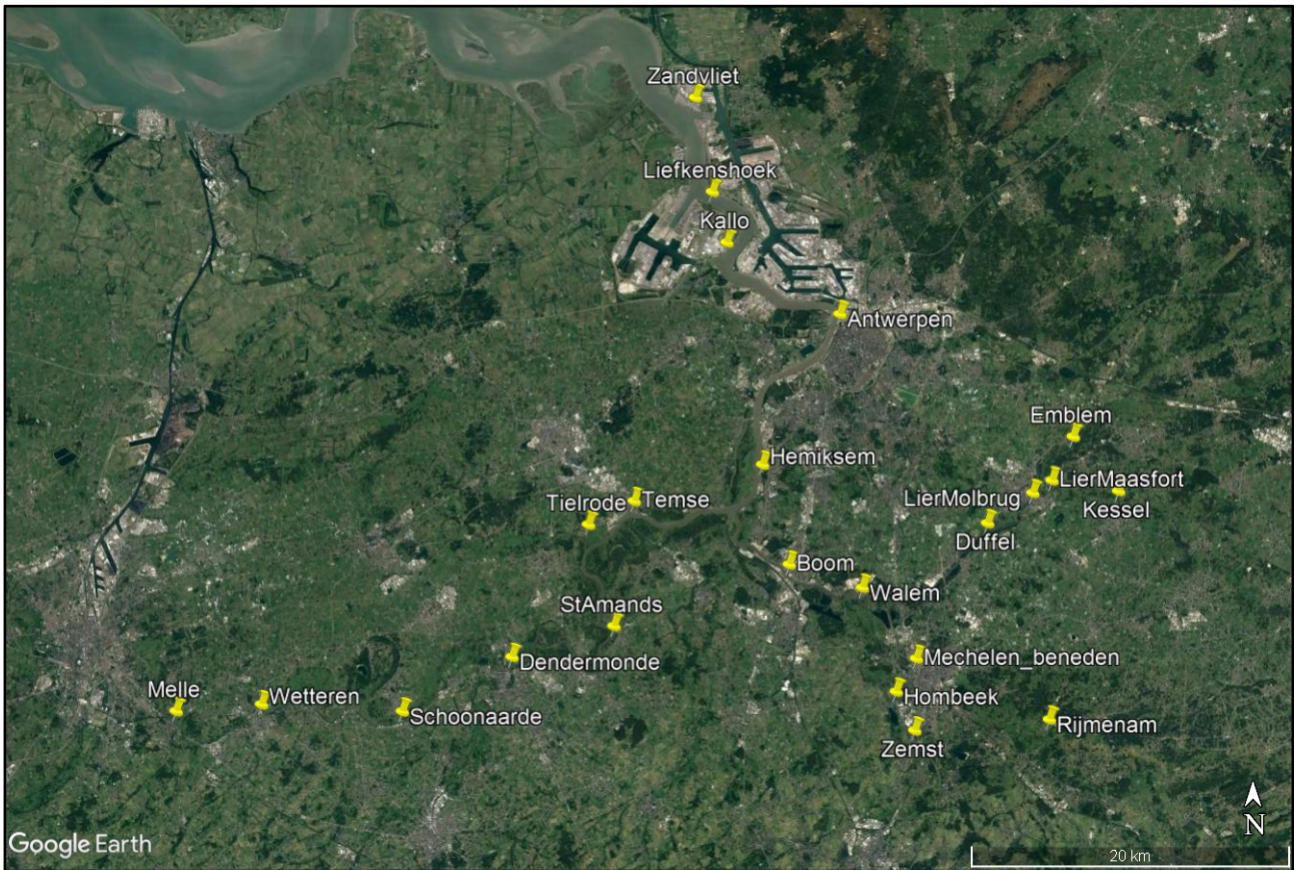
s, S_{max} - number of stations in region r;

r, R_{max} - number of polygons for which observations are included (**10**, see Table 7);

$\sigma_{H_{r,s}^{obs}}$ - uncertainties assigned to the observations (**0.5 m**).

In this study, time series of water level measurement at **23** stations (as shown in Figure 26) are employed to the OpenDA calibration. The calibration period is the year 2007 (2007/01/01 00:00 – 2007/12/31 23:50) with time step of 10 minutes, giving the total number of time steps equal to **52560 (N_{max})**.

Figure 26 – Map of water level stations involved in the OpenDA calibration.



7.5 Stop Criterion

As described in §7.3, the DUD algorithm starts with running a first guess and then modifies each parameter. Afterwards the model is linearized around these values and a linear optimisation problem is solved. The inner workings of the DUD algorithm are briefly described in Annex 1.

If the linearization yields a new parameter setting with a better (lower) cost, this is called an **outer iteration** which can stop on the various criteria:

- **outerLoop maxIterations = 100**
The maximum iteration numbers of the outer loop which is set to 100 in this study.
- **absTolerance = 0.001**
The maximum absolute difference between the costs resulted from the 2 best parameter estimates $|J_{\text{new}} - J_{\text{previous}}|$.
- **relTolerance = 0.001**
The maximum relative difference between the costs resulted from the 2 best parameter estimates $|J_{\text{new}} - J_{\text{previous}}| / J_{\text{new}}$.
- **relToleranceLinearCost = 0.0001**
The maximum relative difference between the linearized costs resulted from the 2 best parameter estimates $|J_{\text{new}} - J_{\text{linear}}| / (J_{\text{previous}} - J_{\text{linear}})$;

However if the linearization does *not* produce a better estimate, DUD will perform a line search until a better estimate is found. The procedure is stopped when one of the stopping criteria of **inner iteration** is fulfilled.

- **lineSearch maxIterations = 30**
The maximum iteration number of the inner loops which is set to 30 in this study.
- **maxRelStepSize = 5**
Maximum size of relative step. This indicates how much the parameters may change from one iteration to the other.
In practice, the searching step is preferably not set too large so that the searching is still in the surroundings of the initial guess. When the norm of α (see ANNEX 1) is larger than maxRelStepSize, α will be reduced in such a way that: $\alpha_{\text{new}} = |\alpha| / \text{maxRelStepSize}$.
- **backtracking shorteningFactor (η) = 0.5**
Factor for shortening step size.
- **startIterationNegativeLook = 3**
Maximum number of iterations before searching in opposite direction. This determines when parameter $\beta = \pm 1$ changes sign.

7.6 Initial guess of roughness

The definition of initial friction map is inspired from an analysis of previous hydrodynamic modelling studies carried out at FHR. Figure 27 shows the comparison of bottom friction values of Manning coefficient along the navigation channel of the River Scheldt. The spatial distribution of manning coefficient show differences with different modeling software and different calibration/validation modelling studies. The latest NEVLA2D calibration (simT31) has been done by Maximova et al (2009b), from which the initial roughness map is constructed by averaging the values of Manning coefficient within each combined polygons (see output in Table 11). The combination of roughness polygons is described in §5.2.4.

Be aware that the initial guess is only applied to the area which are subject to calibration (polygons with roughness codes 450 to 468). The bottom roughness for the Western Scheldt (polygons with roughness codes 309 to 443) has been calibrated with OpenDA (Groenenboom et al., 2016). Therefore the existing roughness in those areas are taken as the initial roughness, and they are not changed throughout the model calibration.

Figure 27 – Comparison of Manning coefficient used by existing 2D and 3D hydrodynamic models along the navigation channel of the River Scheldt.

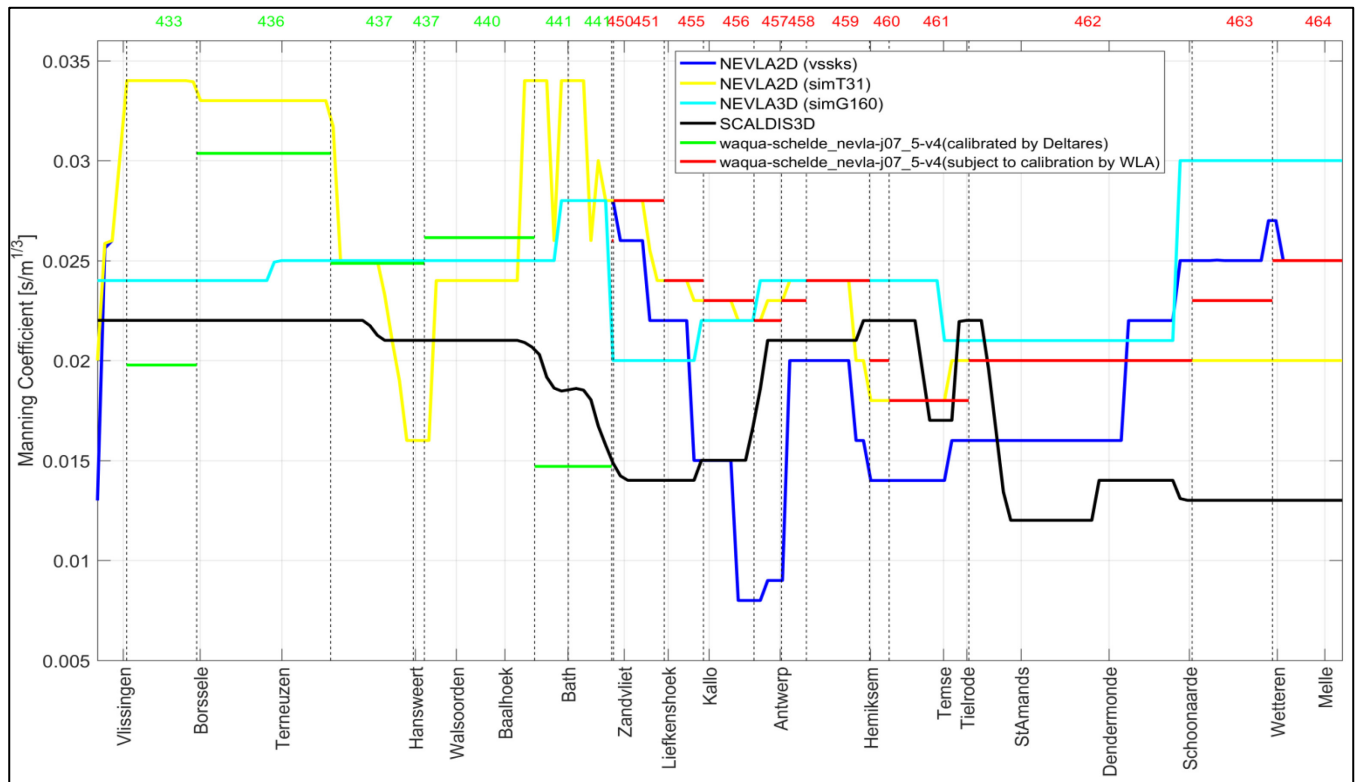


Table 11 – Combined roughness polygons with initial estimation of manning coefficients used by OPENDA. The combination of roughness polygons is described in §5.2.4

Existing Roughness Polygons	Combined Roughness Polygons	Manning Coefficient (Initial Guess)
450	450	0.029
451		
452		
453		
454		
455	455	0.024
456	457	0.023
457		
458	459	0.022
459		
460		
461	461	0.018
462	462	0.020
463	463	0.020
464	464	0.020
465	465	0.024
466		
467	467	0.019
468		

7.7 Results

Table 12 shows the changes of cost function and calibration parameter (in this case Manning coefficient) during the OpenDA calibration after 55 iterations. As described in §7.3, the first 11 runs are the preparation for the optimization algorithm. The actual optimization procedure (e.g. linearization and line search) starts from iteration number 12. The cost function drops gradually until iteration number 25, at which the minimum cost function is found of 75996.43. Afterwards the cost function cannot further decrease beyond 75996.43.

The iterations from 26 to 55 are actually the extensive line search (see explanation in §7.3) which however could not lead to any further improvement. It is likely that the cost function is almost minimized and the optimal parameter estimations are already found with iteration run 25. If so, the OpenDA calibration should have been stopped after 25 iterations.

However, the automatic calibration did not stop probably because the stop criterion are set too strict to be met in this study (see definition in §7.2.4). For example, the cost function after 25 iterations is 75996.43 while the previous lowest cost function is 76105.97 (iteration 24). Before the 25th iteration run, the linearized model leads to linearized cost of 75054.26. Below the calculation showing that none of the stop criterion is met.

For future studies, the predefinition of a more reasonable stop criterion should be considered.

$$\text{outerLoop maxIterations} = 25 < 100$$

$$\text{absTolerance} = |\text{new cost} - \text{previous cost}| = |75996.43 - 76105.97| = 109.54 > 0.001$$

$$\text{relTolerance} = \frac{|\text{new cost} - \text{previous cost}|}{|\text{new cost}|} = \frac{|75996.43 - 76105.97|}{75996.43} = 0.0014 > 0.001$$

$$\text{relToleranceLinearCost} = \frac{|\text{new cost} - \text{linearized cost}|}{|\text{previous cost} - \text{linearized cost}|} = \frac{|75996.43 - 75054.27|}{|76105.97 - 75054.27|} = 0.895 > 0.001$$

In order to check if the cost function is close to minimal, the modeler terminated the OpenDA calibration run when the total iteration number reached to 55 (Stage I). The whole calibration restarts (stage II) with the roughness field after 25 iterations in Phase I, just to further check if the cost function could further reduce. The calibration stops after 14 iterations when the stop criterion **relTolerance** is met (see numbers in Table 13):

$$\frac{|\text{new cost} - \text{previous cost}|}{|\text{new cost}|} = \frac{|75927.76 - 75953.42|}{75927.76} = 3.38E - 4 < 0.001 (\text{relTolerance})$$

Table 13 shows that the final cost function slightly reduced to 75927.76. The evolution of the cost function during the OpenDA calibration are demonstrated in Figure 28. The cost function is reduced by 20% during the entire calibration study. Table 14 compares the Manning coefficients before and after OpenDA calibration. The main changes are found within roughness polygons of 461, 462, 463, 465 and 467.

Table 12 – Changes of cost function and parameter (manning coefficient) during the OpenDA calibration stage I.

Iteration	Cost	A-450	A-455	A-457	A-459	A-461	A-462	A-463	A-464	A-465	A-467
1	93764.04	0	0	0	0	0	0	0	0	0	0
2	93774.96	0.002	0	0	0	0	0	0	0	0	0
3	93683.68	0	0.002	0	0	0	0	0	0	0	0
4	93379.2	0	0	0.002	0	0	0	0	0	0	0
5	93173.57	0	0	0	0.002	0	0	0	0	0	0
6	93365.14	0	0	0	0	0.002	0	0	0	0	0
7	99763.76	0	0	0	0	0	0.002	0	0	0	0
8	95440.79	0	0	0	0	0	0	0.002	0	0	0
9	93929.84	0	0	0	0	0	0	0	0.002	0	0
10	93675.36	0	0	0	0	0	0	0	0	0.002	0
11	89441.32	0	0	0	0	0	0	0	0	0	0.002
12	85320.41	1.934E-04	1.377E-04	2.662E-04	3.142E-04	7.014E-04	-1.704E-03	-3.908E-04	2.153E-04	4.049E-04	1.514E-03
13	83924.62	1.079E-04	-5.079E-05	2.070E-04	2.729E-04	1.229E-03	-1.920E-03	-1.058E-03	1.839E-04	5.595E-04	2.012E-03
14	81774.54	3.483E-05	-2.699E-04	1.623E-04	2.118E-04	1.887E-03	-2.765E-03	-1.169E-03	1.689E-04	7.724E-04	2.351E-03
15	79887.65	-1.304E-05	-5.195E-04	1.290E-04	1.176E-04	2.744E-03	-3.706E-03	-1.579E-03	2.864E-04	1.080E-03	2.609E-03
16	78402.3	3.394E-05	-8.094E-04	9.607E-05	-3.320E-06	3.638E-03	-4.565E-03	-1.960E-03	3.440E-04	1.394E-03	2.733E-03
17	77384.04	1.789E-05	-1.057E-03	9.532E-05	-1.319E-04	4.476E-03	-5.257E-03	-2.273E-03	3.885E-04	1.728E-03	2.770E-03
18	76687.9	-2.362E-06	-1.116E-03	5.080E-05	-3.096E-04	5.146E-03	-5.746E-03	-2.503E-03	4.163E-04	1.958E-03	2.741E-03
19	76495.49	-1.992E-05	-1.245E-03	7.007E-05	-4.324E-04	5.739E-03	-6.090E-03	-2.668E-03	4.347E-04	2.028E-03	2.731E-03
20	76173.91	-3.338E-05	-1.330E-03	3.575E-05	-5.318E-04	6.133E-03	-6.284E-03	-2.766E-03	4.437E-04	2.112E-03	2.716E-03
21	76296.51	-3.669E-05	-1.378E-03	2.811E-05	-3.887E-04	6.081E-03	-6.420E-03	-2.829E-03	4.527E-04	2.171E-03	2.782E-03
22	76230.21	-3.504E-05	-1.354E-03	3.193E-05	-4.603E-04	6.107E-03	-6.352E-03	-2.797E-03	4.482E-04	2.142E-03	2.749E-03
23	76244.41	-3.421E-05	-1.342E-03	3.384E-05	-4.960E-04	6.120E-03	-6.318E-03	-2.782E-03	4.459E-04	2.127E-03	2.732E-03
24	76105.97	-3.380E-05	-1.336E-03	3.479E-05	-5.139E-04	6.127E-03	-6.301E-03	-2.774E-03	4.448E-04	2.120E-03	2.724E-03
25	75996.43	-3.788E-05	-1.406E-03	2.541E-05	-5.237E-04	6.267E-03	-6.516E-03	-2.873E-03	4.594E-04	2.209E-03	2.834E-03
26	76214.3	-3.685E-05	-1.427E-03	2.667E-05	-5.380E-04	6.378E-03	-6.615E-03	-2.918E-03	4.672E-04	2.245E-03	2.831E-03
27	76057.84	-3.737E-05	-1.417E-03	2.604E-05	-5.308E-04	6.322E-03	-6.566E-03	-2.895E-03	4.633E-04	2.227E-03	2.833E-03
28	76308.77	-3.763E-05	-1.411E-03	2.573E-05	-5.273E-04	6.295E-03	-6.541E-03	-2.884E-03	4.614E-04	2.218E-03	2.833E-03
29	76130.2	-3.775E-05	-1.409E-03	2.557E-05	-5.255E-04	6.281E-03	-6.529E-03	-2.878E-03	4.604E-04	2.214E-03	2.833E-03
30	76031.2	-3.782E-05	-1.407E-03	2.549E-05	-5.246E-04	6.274E-03	-6.522E-03	-2.876E-03	4.599E-04	2.211E-03	2.834E-03
31	76240.23	-3.792E-05	-1.405E-03	2.537E-05	-5.233E-04	6.263E-03	-6.513E-03	-2.871E-03	4.592E-04	2.208E-03	2.834E-03
32	76045.88	-3.787E-05	-1.406E-03	2.543E-05	-5.239E-04	6.269E-03	-6.518E-03	-2.873E-03	4.596E-04	2.210E-03	2.834E-03
33	76261.82	-3.789E-05	-1.406E-03	2.540E-05	-5.236E-04	6.266E-03	-6.515E-03	-2.872E-03	4.594E-04	2.209E-03	2.834E-03
34	76248.33	-3.788E-05	-1.406E-03	2.542E-05	-5.238E-04	6.267E-03	-6.517E-03	-2.873E-03	4.595E-04	2.209E-03	2.834E-03
35	76098.82	-3.789E-05	-1.406E-03	2.541E-05	-5.237E-04	6.267E-03	-6.516E-03	-2.873E-03	4.594E-04	2.209E-03	2.834E-03
36	76061.57	-3.788E-05	-1.406E-03	2.541E-05	-5.237E-04	6.267E-03	-6.516E-03	-2.873E-03	4.594E-04	2.209E-03	2.834E-03
37	76184.81	-3.788E-05	-1.406E-03	2.541E-05	-5.237E-04	6.267E-03	-6.516E-03	-2.873E-03	4.594E-04	2.209E-03	2.834E-03
38	76239.28	-3.788E-05	-1.406E-03	2.541E-05	-5.237E-04	6.267E-03	-6.516E-03	-2.873E-03	4.594E-04	2.209E-03	2.834E-03
39	76237.99	-3.788E-05	-1.406E-03	2.541E-05	-5.237E-04	6.267E-03	-6.516E-03	-2.873E-03	4.594E-04	2.209E-03	2.834E-03
40	76175.88	-3.788E-05	-1.406E-03	2.541E-05	-5.237E-04	6.267E-03	-6.516E-03	-2.873E-03	4.594E-04	2.209E-03	2.834E-03
41	76110.5	-3.788E-05	-1.406E-03	2.541E-05	-5.237E-04	6.267E-03	-6.516E-03	-2.873E-03	4.594E-04	2.209E-03	2.834E-03
42	76096.01	-3.788E-05	-1.406E-03	2.541E-05	-5.237E-04	6.267E-03	-6.516E-03	-2.873E-03	4.594E-04	2.209E-03	2.834E-03
43	76216.15	-3.788E-05	-1.406E-03	2.541E-05	-5.237E-04	6.267E-03	-6.516E-03	-2.873E-03	4.594E-04	2.209E-03	2.834E-03
44	75996.43	-3.788E-05	-1.406E-03	2.541E-05	-5.237E-04	6.267E-03	-6.516E-03	-2.873E-03	4.594E-04	2.209E-03	2.834E-03
45	76062.93	-3.254E-05	-1.418E-03	2.939E-05	-5.374E-04	6.355E-03	-6.596E-03	-2.894E-03	4.685E-04	2.238E-03	2.807E-03
46	76266.94	-4.055E-05	-1.400E-03	2.342E-05	-5.168E-04	6.223E-03	-6.476E-03	-2.862E-03	4.549E-04	2.195E-03	2.847E-03
47	76209.78	-3.655E-05	-1.409E-03	2.641E-05	-5.271E-04	6.289E-03	-6.536E-03	-2.878E-03	4.617E-04	2.216E-03	2.827E-03
48	76017.79	-3.855E-05	-1.405E-03	2.491E-05	-5.220E-04	6.256E-03	-6.506E-03	-2.870E-03	4.583E-04	2.206E-03	2.837E-03
49	76123.84	-3.755E-05	-1.407E-03	2.566E-05	-5.246E-04	6.272E-03	-6.521E-03	-2.874E-03	4.600E-04	2.211E-03	2.832E-03
50	76139.19	-3.805E-05	-1.406E-03	2.529E-05	-5.233E-04	6.264E-03	-6.514E-03	-2.872E-03	4.592E-04	2.208E-03	2.835E-03
51	76100.06	-3.780E-05	-1.406E-03	2.547E-05	-5.239E-04	6.268E-03	-6.518E-03	-2.873E-03	4.596E-04	2.210E-03	2.833E-03
52	76166.53	-3.793E-05	-1.406E-03	2.538E-05	-5.236E-04	6.266E-03	-6.516E-03	-2.873E-03	4.594E-04	2.209E-03	2.834E-03
53	76059.58	-3.786E-05	-1.406E-03	2.543E-05	-5.238E-04	6.267E-03	-6.517E-03	-2.873E-03	4.595E-04	2.209E-03	2.834E-03
54	76042.25	-3.789E-05	-1.406E-03	2.540E-05	-5.237E-04	6.267E-03	-6.516E-03	-2.873E-03	4.594E-04	2.209E-03	2.834E-03
55	76008.11	-3.788E-05	-1.406E-03	2.542E-05	-5.237E-04	6.267E-03	-6.516E-03	-2.873E-03	4.594E-04	2.209E-03	2.834E-03

Table 13 – Changes of cost function and parameter (manning coefficient) during the OpenDA calibration stage II.

Iteration	Cost	A-450	A-455	A-457	A-459	A-461	A-462	A-463	A-464	A-465	A-467
1	75996.43	0	0	0	0	0	0	0	0	0	0
2	76576.21	0.002	0	0	0	0	0	0	0	0	0
3	77112.58	0	0.002	0	0	0	0	0	0	0	0
4	76687.53	0	0	0.002	0	0	0	0	0	0	0
5	77365.69	0	0	0	0.002	0	0	0	0	0	0
6	75985.22	0	0	0	0	0.002	0	0	0	0	0
7	77216.72	0	0	0	0	0	0.002	0	0	0	0
8	76969.92	0	0	0	0	0	0	0.002	0	0	0
9	76580.14	0	0	0	0	0	0	0	0.002	0	0
10	76141.95	0	0	0	0	0	0	0	0	0.002	0
11	79391.06	0	0	0	0	0	0	0	0	0	0.002
12	76137.76	1.44E-04	-4.19E-05	1.01E-04	-1.28E-04	5.52E-04	2.40E-04	4.84E-05	1.61E-04	3.91E-04	9.36E-05
13	75953.42	7.19E-05	-2.10E-05	5.06E-05	-6.41E-05	0.001276	1.20E-04	2.42E-05	8.05E-05	1.96E-04	4.68E-05
14	75927.76	1.34E-04	-6.11E-05	8.57E-05	-1.58E-04	7.28E-04	2.25E-04	3.37E-05	1.54E-04	4.01E-04	9.38E-06

Figure 28 – Evolution of cost function during OpenDA calibration stage I (left panel) and II (right panel).

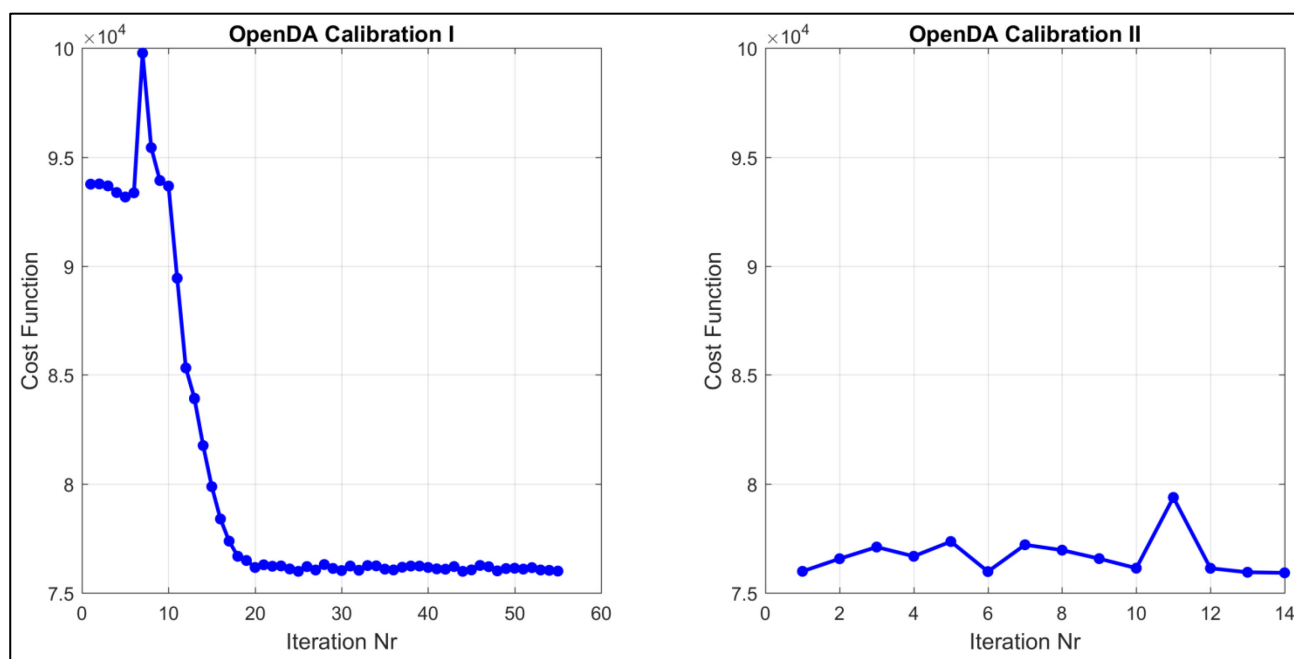


Table 14 – Comparison of manning coefficient before and after the automatic calibration with OpenDA.

Legend	Manning Coefficient
	0.01-0.015
	0.015-0.02
	0.02-0.025
	>0.025

Existing Roughness Polygons (Roughness Code)	Combined Roughness Polygons	Water Level Stations (Figure 28)		Manning Coefficient (Initial Guess)	Manning Coefficient (after automatic calibration)
450	450	Zandvliet	Lower Sea Scheldt	0.029	0.0291
451					
452					
453					
454					
455	455	Liefkenshoek; Kallo		0.024	0.0225
456					
457	457	Antwerp		0.023	0.0231
458					
459	459	Hemiksem		0.022	0.0213
460					
461	461	Temse	Upper Sea Scheldt	0.018	0.0249
462	462	StAmands; Dendermonde; Schoonaarde		0.02	0.0137
463	463	Wetteren		0.02	0.0172
464	464	Melle		0.02	0.0206
465	465	Tielrode		0.024	0.0266
466					
467	467	Boom; Wallem; Hombeek; Zemst;		0.019	0.0218
468		Mechelen_Benedensluis; Rijmenam; Duffel; Lier_Molbrug; Lier_Maasfort; Emblem; Kessel			

8 Validation with VIMM

In this Chapter, the model performance is evaluated with the in-house postprocessing tool VIMM written in MATLAB. VIMM is a toolbox developed in-house at Flanders Hydraulics to assist the modeller during calibration and validation of hydraulic models.

We compare the model performance between 3 different model runs (Table 15).

Table 15 – Description of model runs involved in the model validation.

Run001	Model as received from Deltares on 14/02/2017; constructed from Baseline database j07_5-v4 .
Run002	Model constructed from Baseline database j07_5-w4 (after changes described in chapter 5); with initial roughness guess as described in §7.5.
Run003	Calibrated model using OpenDA (Iteration 14 of Stage II in Table 13).

8.1 Water Level Timeseries

The water level data used for validation is referred to §4.1.

8.1.1 Validation

Table 17, Table 18 and Table 19 compare the statistics of Bias, RMSE and RMSE0 (see definitions in ANNEX2) of the complete time series, high water levels and low water levels respectively. The statistical values are color-coded by the definition shown in Table 16.

In the Upper Sea Scheldt, the statistical errors from Run 001 are rather high (e.g. Bias of complete time series is 485.2 cm at Lier Maasfort), this is mainly due to the poor quality of bathymetric data as discussed in §5.2.1. For readability, Figure 29 to Figure 37 only show the statistical comparison between Run002 and Run003.

The model predictions offshore and in the Western Scheldt are good in all 3 runs (these stations are marked in green in Table 17). This implies that the modelling activities carried out in this study (e.g. updating Baseline database to **j07_5-w4**, updating the model grid, OpenDA calibration in the Sea Scheldt) have a negligible impact on the model quality in the Western Scheldt.

The model quality in the Lower Sea Scheldt from **Zandvliet** until **Hemiksem** doesn't change much. This is logical because OpenDA does not change the bottom friction much within the polygon 450, 455, 457 and 459 (see resulting roughness of OpenDA in Table 14).

The model quality in the area of Rupel (**Boom** and **Walem**) and Upper Sea Scheldt (**Temse** to **Melle**) is improved noticeably.

- The bias of high water level are slightly reduced at **Boom** (from 10.2 cm to 8.6 cm) and **Walem** (from 11.2 cm to 8.2 cm). The bias of low water level are substantially reduced at **Boom** (from -16.7 cm to -10.4 cm) and **Walem** (from -19.3 cm to -7.9 cm). The comparison of RMSE and RMSE0 also imply improvements on the model quality.

- By increasing the Manning coefficient from 0.018 to 0.0249 in polygon 461, the bias of high water level at **Temse** reduced significantly from 10.6 cm to 5.5 cm while the bias of low water level reduced from -9.7 cm to -3.1 cm. The comparison of RMSE and RMSE0 also imply improvements on the model quality.
- By decreasing the Manning coefficient from 0.02 to 0.0137 in polygon 462, the bias of high water level reduced significantly at **StAmands** (from 10.9 cm to 5.7 cm), **Dendermonde** (from -6.2 cm to -4.7 cm) and **Schoonaarde** (from -10.9 cm to 1.8 cm). The bias of low water level at **Dendermonde** reduced significantly from 42.2 cm to 21.6 cm, although still substantial. The bias of low water level does not change much at **StAmands** and **Schoonaarde**. The comparison of RMSE and RMSE0 show similar trend.
- The bias of high water level reduced significantly at **Wetteren** (from -16.6 cm to -1.3 cm), **Melle** (from -18.2 cm to -5 cm) and **Tielrode** (from 7.9 cm to 0.9 cm). The bias of low water level also reduced significantly at **Wetteren** (from 21.2 cm to -4.5 cm), **Melle** (from 21.6 cm to 1.9 cm) and **Tielrode** (from -4.6 cm to 0.8 cm). The comparison of RMSE and RMSE0 also imply improvements on the model quality.

The model quality in the Zenne (**Hombeek** and **Zemst**), Dijle (**Mechelen_Benedensluis** and **Rijmenam**), Lower Nete (**Duffel**), Grote Nete (**Lier_Molbrug**, **Lier_Maasfort** and **Kessel**) and Kleine Nete (**Emblem**) show complex characteristics. Firstly of all, as described in §6.4, the implementation of the barrier at Mechelen is not perfect in this study due to the lack of operational data. This will introduce uncertainties to the water level predictions in the river Dijle. Secondly, river Zenne, Dijle and Nete are all within one polygon 467, in which the Manning coefficient is slightly increased from 0.019 to 0.0218. The degrees of freedom on the model calibration is limited, which restrains the possibility to find ONE value of Manning coefficient leads to satisfactory results at all the stations. Improvements can be foreseen if splitting the roughness polygons of 467 to more smaller polygons. This might be considered for the future studies.

- In the Zenne, the bias of high water level is slightly reduced at **Hombeek** (from 10.8 cm to 6.8 cm) and **Zemst** (from 16.2 cm to 14 cm). The bias of low water level is reduced at **Zemst** (from -14.3 cm to -7 cm) but it is increased at **Hombeek** (from 2.4 cm to 10.1 cm).
- In the Dijle and Nete, the bias of high water level is slightly increased while the bias of low water level is slightly decreased. The bias of the complete time series of water level drops at all stations. The comparison of RMSE and RMSE0 show similar trend.

Table 16 – Definition of colour code in terms of bias, RMSE and RMSE0.

Legend	Bias [cm]	RMSE [cm]	RMSE0 [cm]
	0-5	0-5	0-5
	5-10	5-10	5-10
	10-15	10-15	10-15
	15-20	15-20	15-20
	>20	>20	>20

Table 17 – Comparison of Bias, RMSE and RMSE0 of the complete time series.

The 12 stations marked in green (**Westhinder to Bath**) represent the areas where the bottom roughness are already calibrated with OpenDA by Deltares (Western Scheldt). The 23 stations marked in brown (**Zandvliet to Kessel**) represent the areas where the bottom roughness is calibrated with OpenDA in this study (Sea Scheldt and tributaries).

Stations	Complete TimeSeries								
	Run001			Run002			Run003		
	BIAS [cm]	RMSE [cm]	RMSE_0 [cm]	BIAS [cm]	RMSE [cm]	RMSE_0 [cm]	BIAS [cm]	RMSE [cm]	RMSE_0 [cm]
Westhinder	-0.3	2.6	2.6	-0.3	2.6	2.6	-0.3	2.6	2.6
Vlakte van de Raan	-1.4	4.6	4.4	-1.4	4.6	4.4	-1.4	4.6	4.4
Westkapelle	-0.4	4.1	4.1	-0.4	4.1	4.1	-0.4	4.1	4.1
Cadzand	2.0	5.8	5.5	2.0	5.8	5.5	2.0	5.8	5.5
Vlissingen	-1.4	4.8	4.6	-1.4	4.8	4.6	-1.4	4.8	4.6
Breskens	-0.6	5.0	5.0	-0.6	5.0	5.0	-0.6	5.0	4.9
Borssele	-0.5	5.1	5.1	-0.5	5.2	5.1	-0.5	5.2	5.2
Terneuzen	-1.6	5.7	5.4	-1.6	5.7	5.5	-1.6	5.7	5.5
Hansweert	1.0	5.5	5.4	1.1	5.5	5.4	1.1	5.5	5.4
Walsoorden	0.7	6.0	5.9	0.7	6.0	6.0	0.7	6.0	6.0
Baalhoek	1.5	6.2	6.1	1.5	6.3	6.1	1.6	6.2	6.0
Bath	3.9	8.0	7.0	4.0	8.2	7.1	4.0	8.2	7.2
Zandvliet	2.3	8.6	8.3	2.4	8.8	8.4	2.5	8.9	8.6
Liefkenshoek	4.5	8.6	7.3	4.6	8.7	7.3	4.7	8.7	7.4
Kallo	6.1	10.0	7.9	6.3	10.1	7.9	6.2	10.1	7.9
Antwerpen	6.1	10.1	8.1	6.5	10.3	8.0	6.3	10.3	8.1
Hemiksem	-1.8	9.0	8.8	-1.8	8.3	8.1	-1.8	8.7	8.5
Boom	-3.7	14.4	13.9	-2.2	10.7	10.5	-0.7	8.9	8.9
Temse	-1.5	12.7	12.6	-1.5	11.6	11.6	0.8	8.0	8.0
Tielrode	75.3	118.7	91.8	-2.7	13.0	12.7	-0.3	10.0	10.0
Walem	185.1	231.5	139.1	-2.3	12.5	12.3	0.7	8.7	8.7
StAmands	7.0	24.5	23.5	-5.3	19.3	18.5	-5.7	16.5	15.5
Dendermonde	18.8	35.8	30.4	14.2	26.9	22.8	8.7	21.4	19.5
Schoonaarde	55.5	86.6	66.5	1.7	16.6	16.6	-6.9	15.2	13.5
Wetteren	7.5	24.2	23.0	5.1	24.0	23.5	-0.4	16.1	16.1
Melle	122.2	173.0	122.4	9.1	29.3	27.9	6.1	23.1	22.3
MechelenSluis	-3.3	26.2	26.0	7.4	18.8	17.2	12.2	22.2	18.5
Hombeek	173.6	203.9	107.0	6.6	16.9	15.6	10.0	20.3	17.6
Zemst	297.7	311.1	90.2	9.0	27.3	25.7	13.1	29.6	26.6
Duffel	-0.2	36.8	36.8	-7.5	14.8	12.8	-3.6	9.8	9.1
Rijmenam	332.8	334.6	34.7	-3.1	23.1	22.8	-2.1	23.2	23.1
Lier Molbrug	160.5	192.6	106.5	-17.8	26.2	19.2	-16.8	23.3	16.1
Lier Maasfort	485.2	491.0	75.2	-17.2	27.7	21.7	-17.4	25.4	18.6
Emblem	351.1	356.0	58.9	-19.0	31.0	24.5	-16.6	25.5	19.3
Kessel	459.4	463.0	57.9	-9.8	21.9	19.6	-8.5	19.5	17.6

Table 18 – Comparison of Bias, RMSE and RMSE0 of high water levels.

The 12 stations marked in green (Westhinder to Bath) represent the areas where the bottom roughness are already calibrated with OpenDA by Deltares (Western Scheldt). The 23 stations marked in brown (Zandvliet to Kessel) represent the areas where the bottom roughness is calibrated with OpenDA in this study (Sea Scheldt and tributaries).

Stations	High Water Level								
	Run001			Run002			Run003		
	BIAS [cm]	RMSE [cm]	RMSE_0 [cm]	BIAS [cm]	RMSE [cm]	RMSE_0 [cm]	BIAS [cm]	RMSE [cm]	RMSE_0 [cm]
Westhinder	-1.7	2.7	2.1	-1.7	2.7	2.1	-1.7	2.7	2.1
Vlakte van de Raan	-6.1	6.6	2.5	-6.1	6.6	2.5	-6.1	6.6	2.5
Westkapelle	-3.9	4.6	2.4	-3.9	4.6	2.4	-3.9	4.6	2.4
Cadzand	-0.7	3.6	3.6	-0.6	3.6	3.6	-0.6	3.6	3.6
Vlissingen	-4.0	5.4	3.6	-4.0	5.4	3.6	-4.0	5.4	3.6
Breskens	-4.0	5.3	3.6	-4.0	5.3	3.6	-3.9	5.3	3.6
Borssele	0.1	4.8	4.8	0.1	4.8	4.8	0.1	4.8	4.8
Terneuzen	-3.4	5.4	4.2	-3.4	5.4	4.3	-3.2	5.3	4.3
Hansweert	1.3	5.1	4.9	1.3	5.1	5.0	1.5	5.2	5.0
Walsoorden	-2.5	5.5	4.9	-2.4	5.4	4.8	-2.3	5.4	4.8
Baalhoek	0.1	4.9	4.9	0.2	4.9	4.9	0.2	4.9	4.9
Bath	6.5	8.4	5.3	6.6	8.5	5.3	6.5	8.4	5.4
Zandvliet	8.9	11.0	6.5	8.8	11.0	6.6	8.8	11.0	6.6
Liefkenshoek	8.8	10.7	6.2	8.1	10.2	6.2	8.1	10.2	6.2
Kallo	11.1	13.0	6.7	10.2	12.2	6.7	10.6	12.6	6.8
Antwerpen	11.2	13.0	6.6	9.2	11.3	6.6	10.5	12.4	6.6
Hemiksem	4.3	7.8	6.5	3.4	7.4	6.5	4.1	7.7	6.5
Boom	13.4	15.4	7.6	10.2	12.6	7.5	8.6	11.4	7.5
Temse	12.1	13.9	6.9	10.6	12.7	6.9	5.5	8.5	6.5
Tielrode	9.2	11.7	7.3	7.9	10.8	7.3	0.9	7.0	6.9
Walem	19.5	20.8	7.2	11.2	13.2	7.1	8.2	10.7	6.9
StAmands	11.3	13.5	7.4	10.9	13.3	7.6	5.7	9.1	7.1
Dendermonde	-4.0	8.9	8.0	-6.2	10.0	7.9	-4.7	9.1	7.8
Schoonaarde	-5.6	9.8	8.0	-10.9	13.5	7.9	1.8	8.3	8.1
Wetteren	-7.7	14.0	11.7	-16.6	20.2	11.5	-1.3	11.6	11.5
Melle	47.6	68.2	48.8	-18.2	25.7	18.2	-5.0	17.8	17.1
MechelenSluis	25.6	26.9	8.3	0.0	8.0	8.0	-3.3	8.9	8.3
Hombeek	34.6	41.7	23.4	10.8	13.7	8.5	6.8	10.7	8.2
Zemst	127.5	137.3	51.0	16.2	23.4	16.9	14.0	21.5	16.4
Duffel	32.5	33.9	9.6	-1.1	6.8	6.7	-6.0	8.9	6.5
Rijmenam	290.7	292.2	29.9	-11.7	18.0	13.7	-12.7	19.3	14.5
Lier Molbrug	61.5	64.4	19.0	-10.9	14.6	9.8	-16.3	19.0	9.7
Lier Maasfort	368.6	370.2	34.8	-2.6	8.8	8.4	-8.8	11.8	7.9
Emblem	246.4	249.5	39.2	2.9	8.5	8.0	-3.0	8.8	8.3
Kessel	370.1	372.4	41.7	-1.5	9.0	8.9	-7.4	12.3	9.8

Table 19 – Comparison of Bias, RMSE and RMSE0 of low water levels.

The 12 stations marked in green (**Westhinder to Bath**) represent the areas where the bottom roughness are already calibrated with OpenDA by Deltares (Western Scheldt). The 23 stations marked in brown (**Zandvliet to Kessel**) represent the areas where the bottom roughness is calibrated with OpenDA in this study (Sea Scheldt and tributaries).

Stations	Low Water Level								
	Run001			Run002			Run003		
	BIAS [cm]	RMSE [cm]	RMSE_0 [cm]	BIAS [cm]	RMSE [cm]	RMSE_0 [cm]	BIAS [cm]	RMSE [cm]	RMSE_0 [cm]
Westhinder	2.1	3.0	2.2	2.1	3.0	2.2	2.1	3.0	2.2
Vlakte van de Raan	1.7	3.0	2.4	1.7	2.9	2.4	1.7	2.9	2.4
Westkapelle	3.9	4.5	2.3	3.9	4.5	2.3	3.8	4.5	2.3
Cadzand	5.8	6.4	2.7	5.8	6.4	2.7	5.8	6.4	2.7
Vlissingen	0.8	3.3	3.2	0.8	3.3	3.2	0.7	3.3	3.2
Breskens	1.0	3.4	3.3	1.0	3.4	3.3	0.9	3.4	3.3
Borssele	1.7	4.1	3.7	1.7	4.1	3.8	1.6	4.1	3.8
Terneuzen	2.2	4.6	4.0	2.2	4.6	4.0	2.1	4.6	4.0
Hansweert	0.4	4.7	4.7	0.5	4.8	4.7	0.5	4.8	4.8
Walsoorden	0.1	5.2	5.2	0.3	5.3	5.2	0.3	5.3	5.3
Baalhoek	-0.1	5.1	5.1	0.2	5.1	5.1	0.3	5.2	5.2
Bath	-0.6	5.7	5.7	0.0	5.7	5.7	0.1	5.8	5.8
Zandvliet	-4.0	7.6	6.4	-3.2	7.2	6.4	-3.1	7.2	6.5
Liefkenshoek	0.0	6.0	6.0	1.2	6.0	5.9	1.3	6.1	6.0
Kallo	1.8	6.3	6.1	3.2	6.8	6.0	3.1	6.8	6.0
Antwerpen	0.6	6.3	6.2	3.1	6.6	5.9	2.8	6.7	6.1
Hemiksem	-11.1	12.8	6.5	-9.4	11.3	6.3	-8.8	11.0	6.6
Boom	-23.0	24.5	8.4	-16.7	18.1	7.1	-10.4	12.1	6.2
Temse	-11.1	18.7	15.1	-9.7	17.2	14.3	-3.1	11.3	10.8
Tielrode	205.3	209.9	43.8	-4.6	19.5	18.9	0.8	14.3	14.3
Walem	190.3	190.3	0.0	-19.3	20.8	7.8	-7.9	10.4	6.8
StAmands	60.2	67.0	29.4	-29.2	30.3	8.2	-28.3	29.6	8.7
Dendermonde	66.5	70.1	22.2	42.2	43.3	9.9	21.6	23.5	9.2
Schoonaarde	67.3	78.1	39.6	17.9	21.6	12.1	-18.5	22.5	12.8
Wetteren	20.6	26.8	17.2	21.2	27.2	17.1	-4.5	18.7	18.1
Melle	77.1	97.4	59.5	21.6	31.4	22.8	1.9	23.4	23.3
MechelenSluis	-21.3	29.4	20.3	0.2	17.1	17.1	14.8	22.4	16.8
Hombeek	242.9	244.4	27.1	2.4	19.7	19.5	10.1	23.5	21.2
Zemst	366.0	366.5	19.1	-14.3	31.1	27.6	-7.0	28.8	27.9
Duffel	43.2	55.1	34.2	-27.7	28.8	8.1	-10.4	13.2	8.1
Rijmenam	357.1	358.1	26.3	-1.5	25.6	25.5	1.0	25.8	25.8
Lier Molbrug	173.7	182.6	56.4	-30.1	38.5	24.0	-26.2	33.3	20.6
Lier Maasfort	557.4	558.8	39.9	-30.7	41.4	27.8	-29.6	37.9	23.7
Emblem	410.8	411.4	21.7	-44.8	46.8	13.4	-35.7	38.0	12.9
Kessel	509.5	511.0	38.3	-27.2	31.5	16.0	-20.3	25.3	15.1

Figure 29 – Bias of complete time series of water levels along the Scheldt.

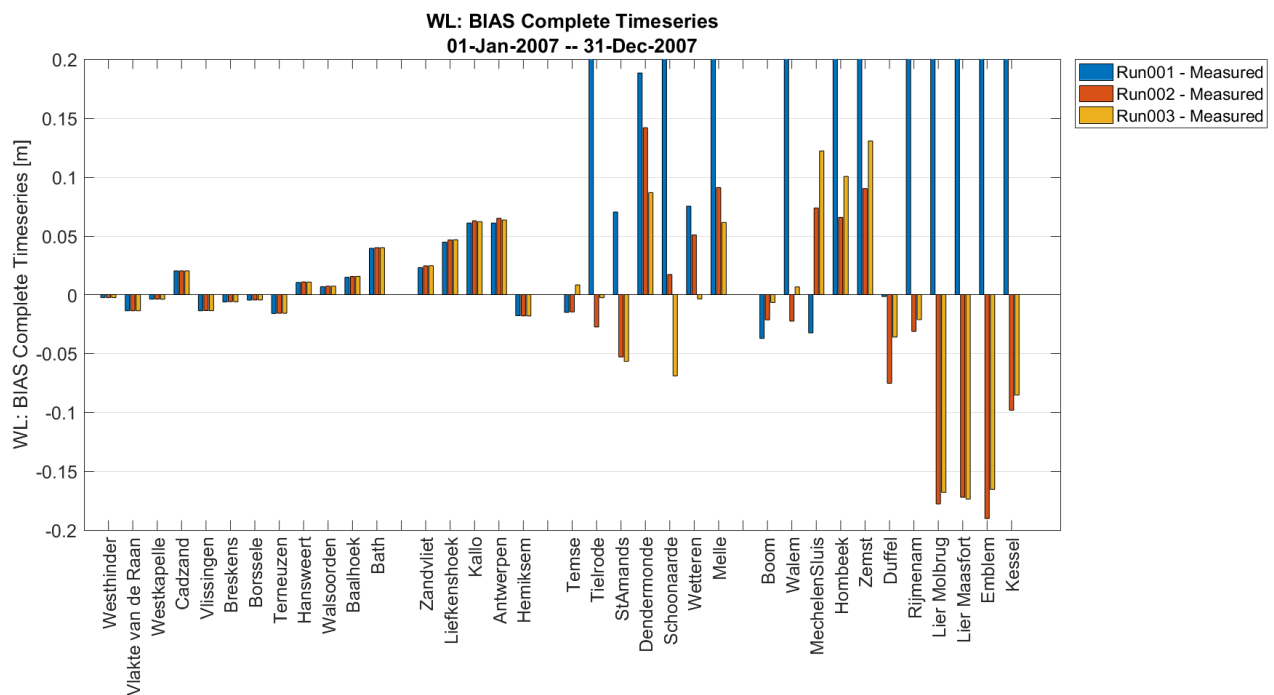


Figure 30 – RMSE of complete time series of water levels along the Scheldt.

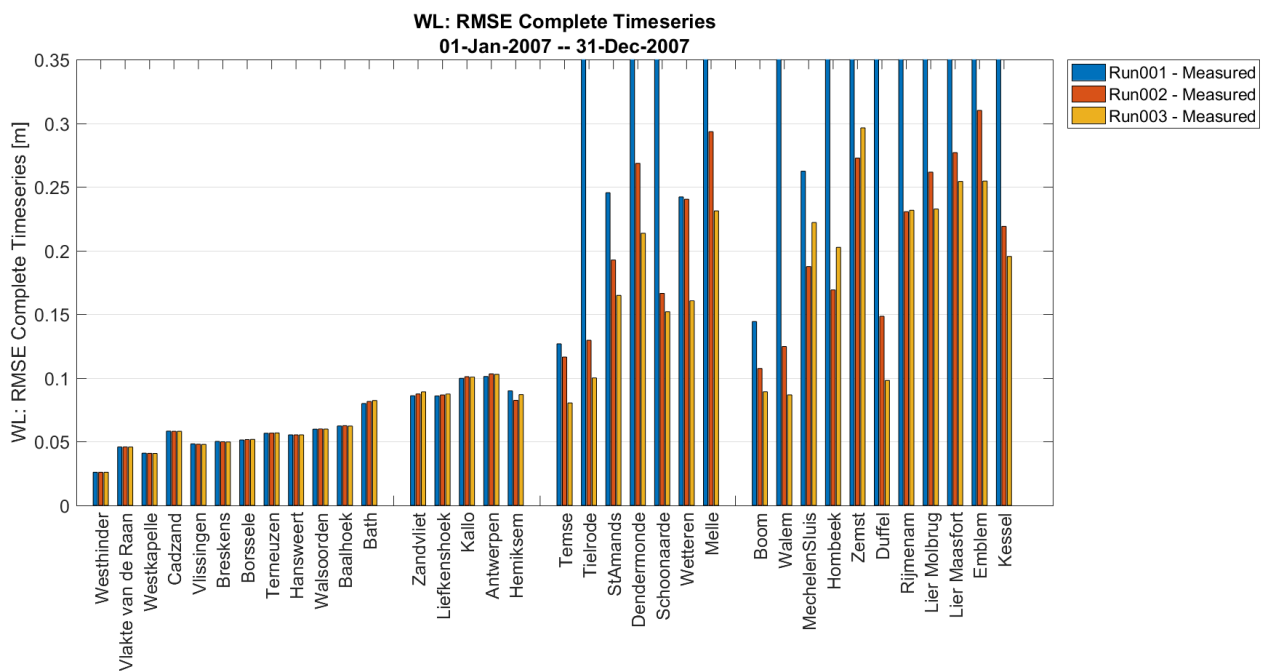


Figure 31 – RMSE0 of complete time series of water levels along the Scheldt.

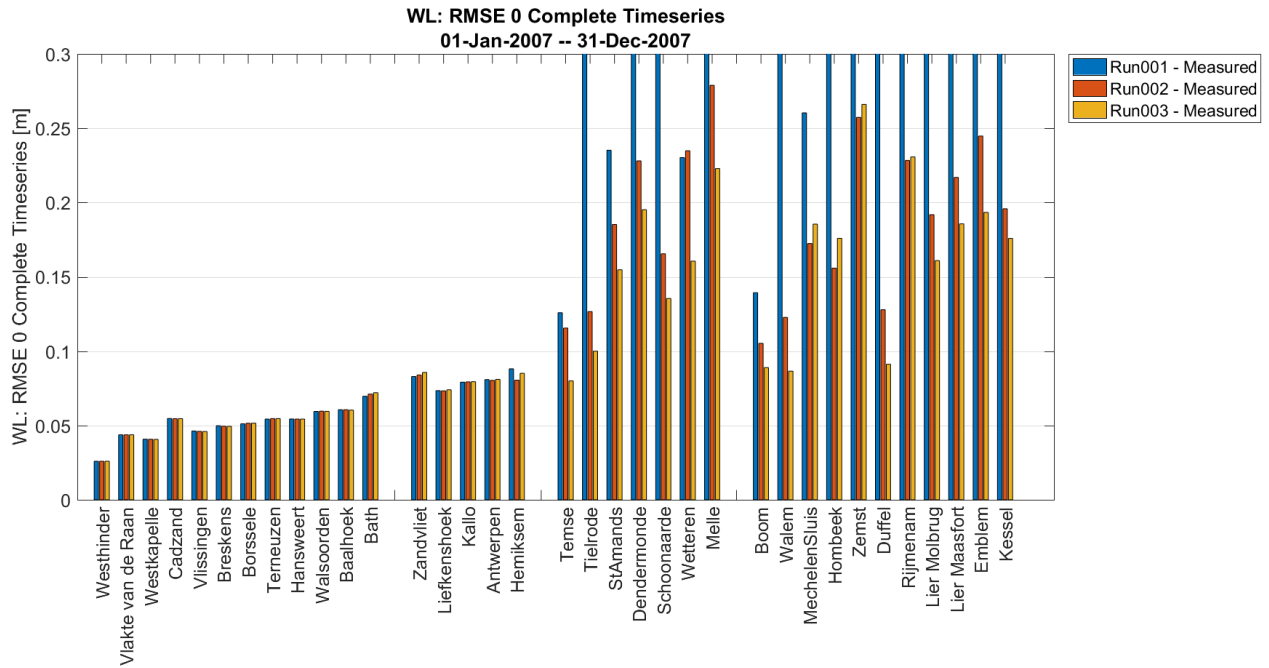


Figure 32 – Bias of high water levels along the Scheldt.

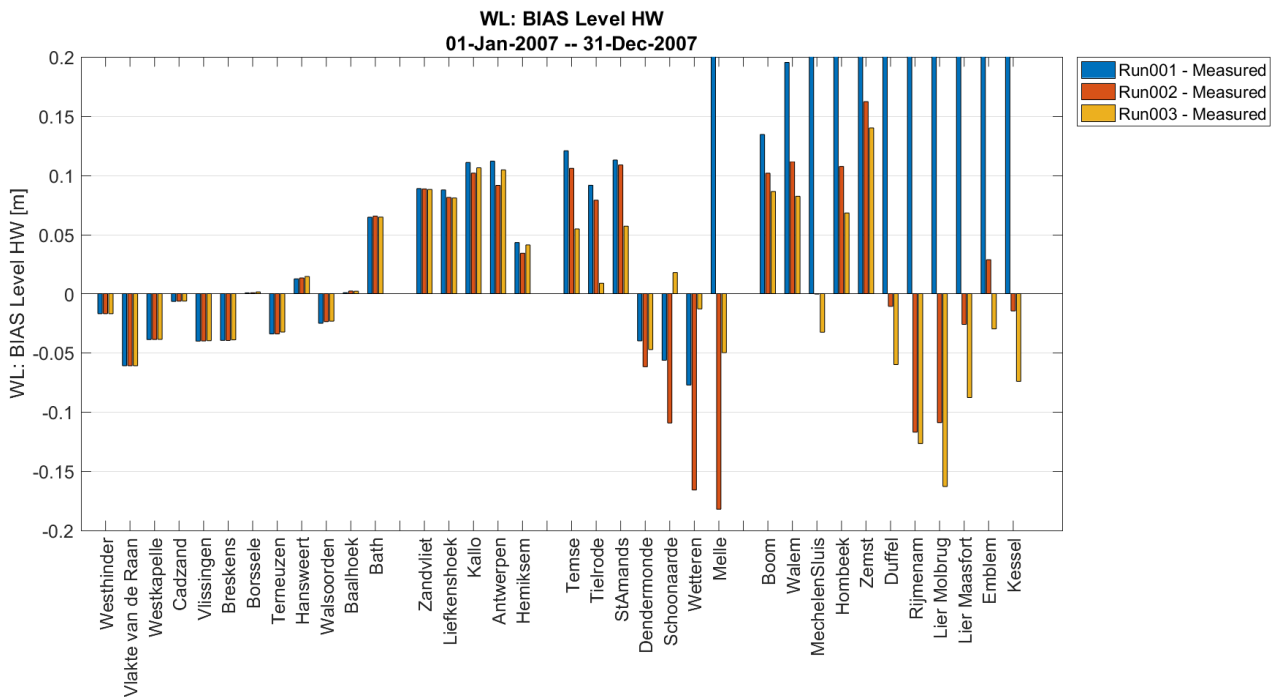


Figure 33 – RMSE of high water levels along the Scheldt.

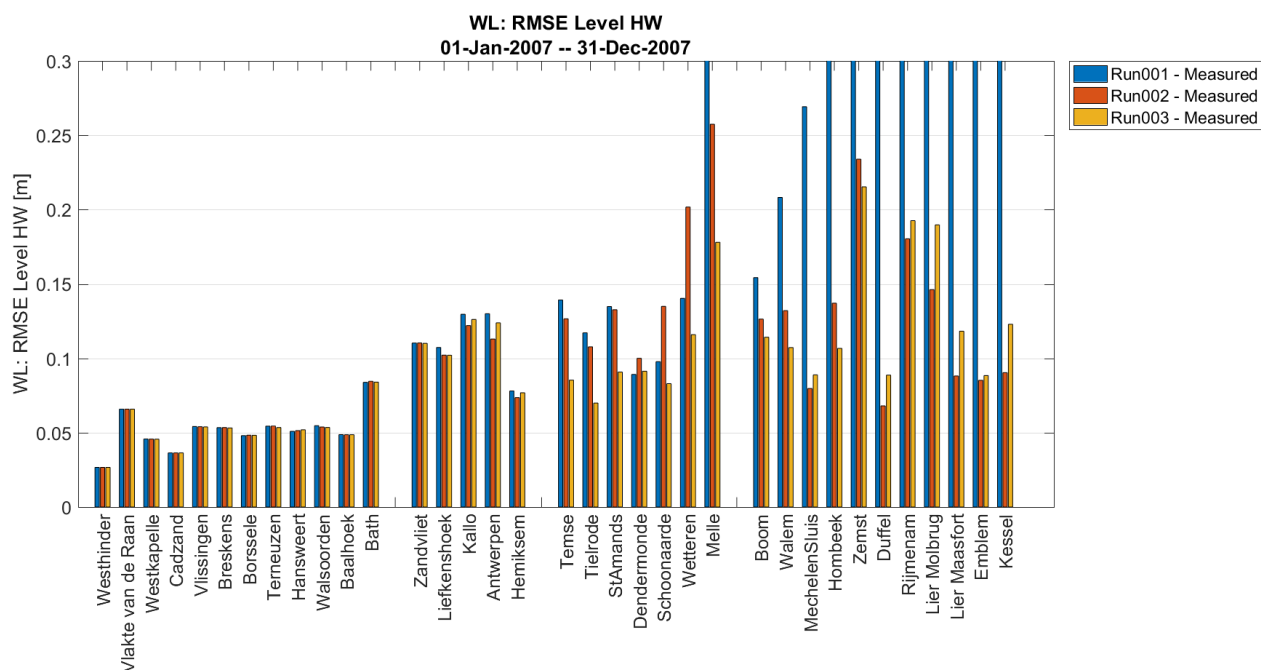


Figure 34 – RMSE0 of high water levels along the Scheldt.

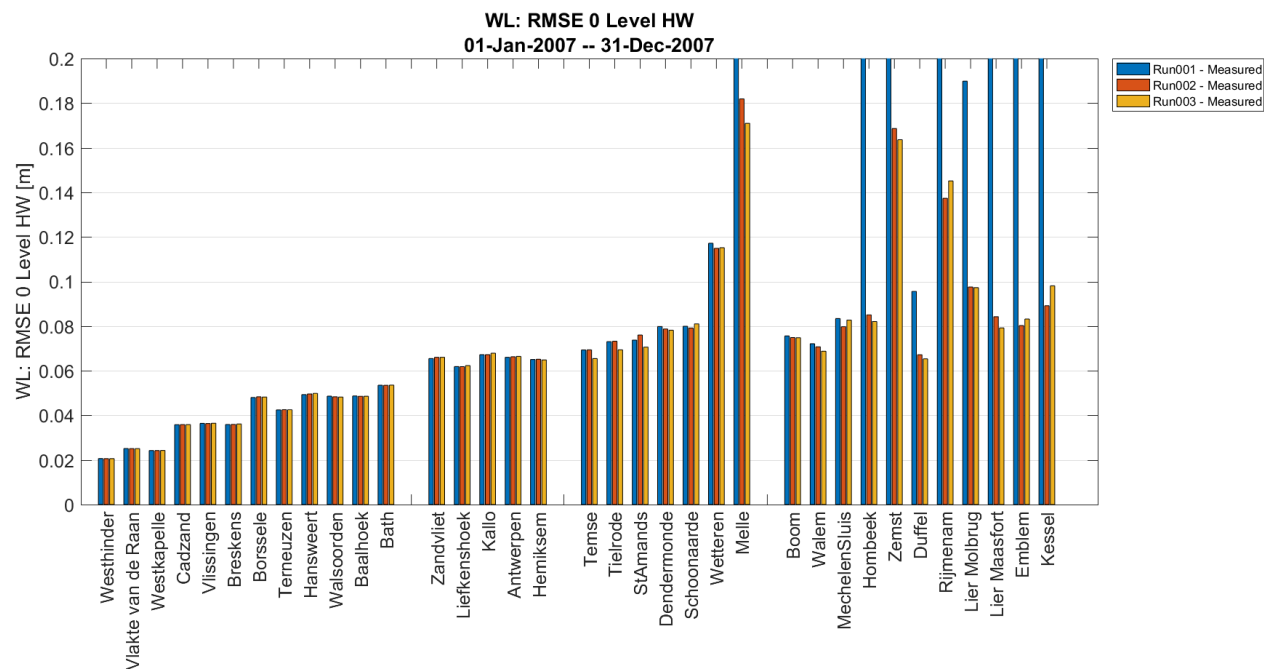


Figure 35 – Bias of low water levels along the Scheldt.

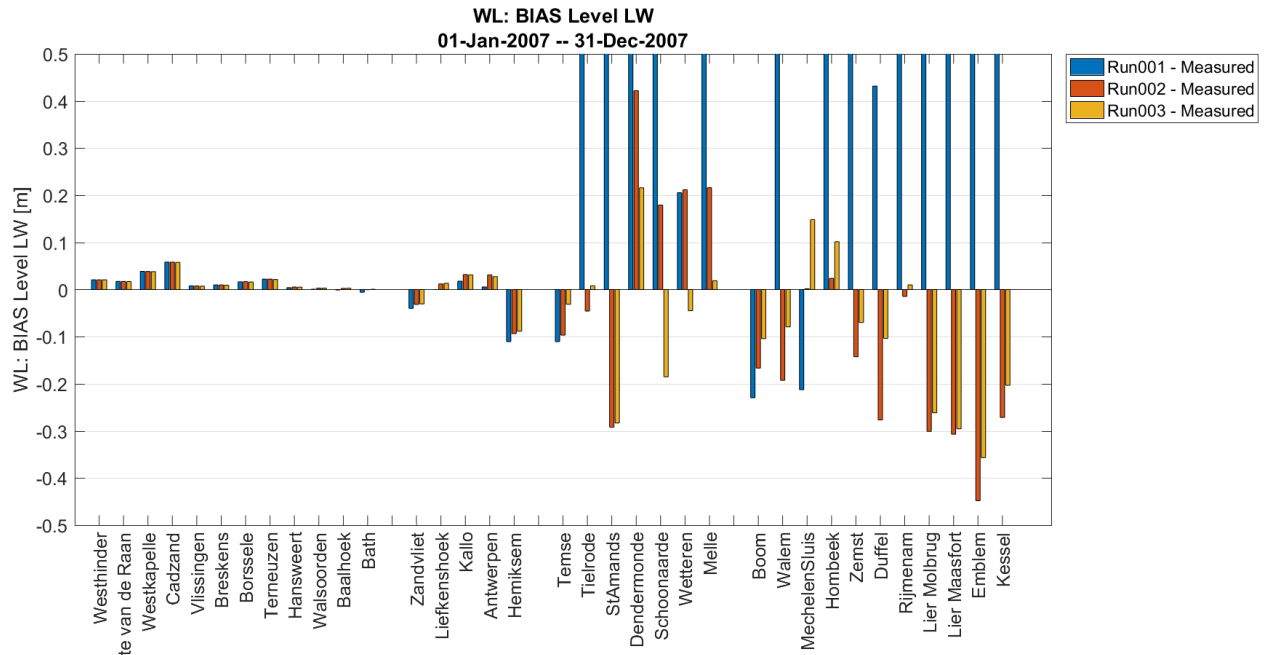


Figure 36 – RMSE of low water levels along the Scheldt.

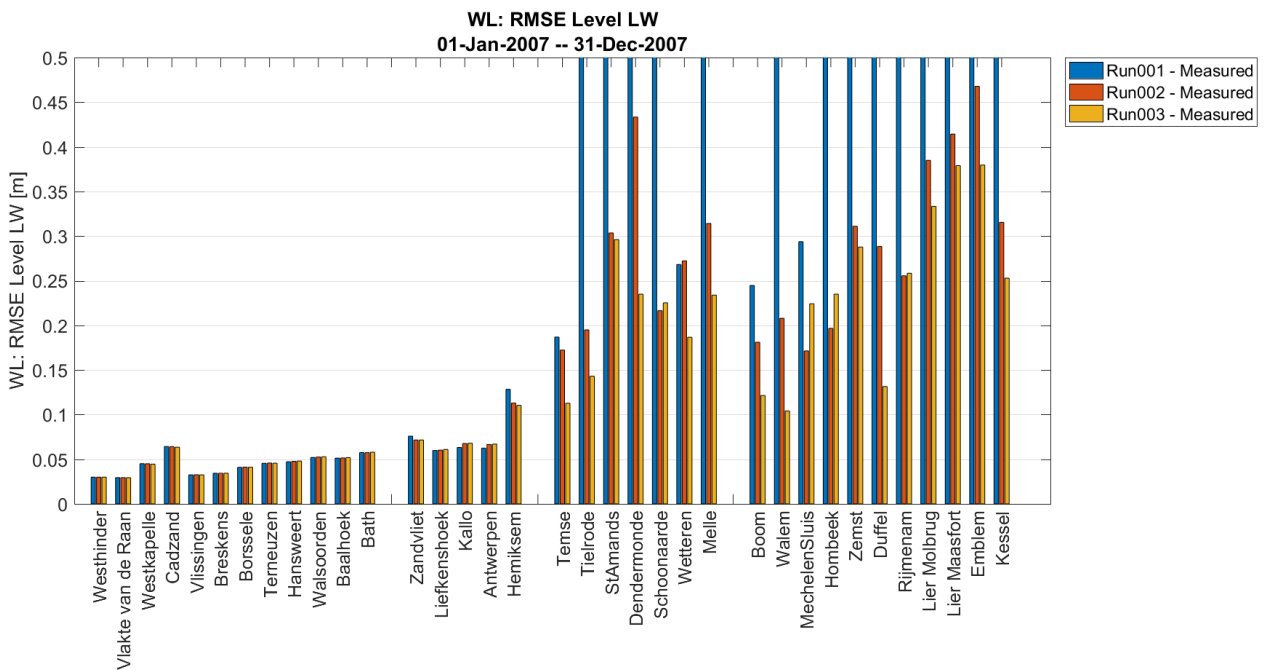
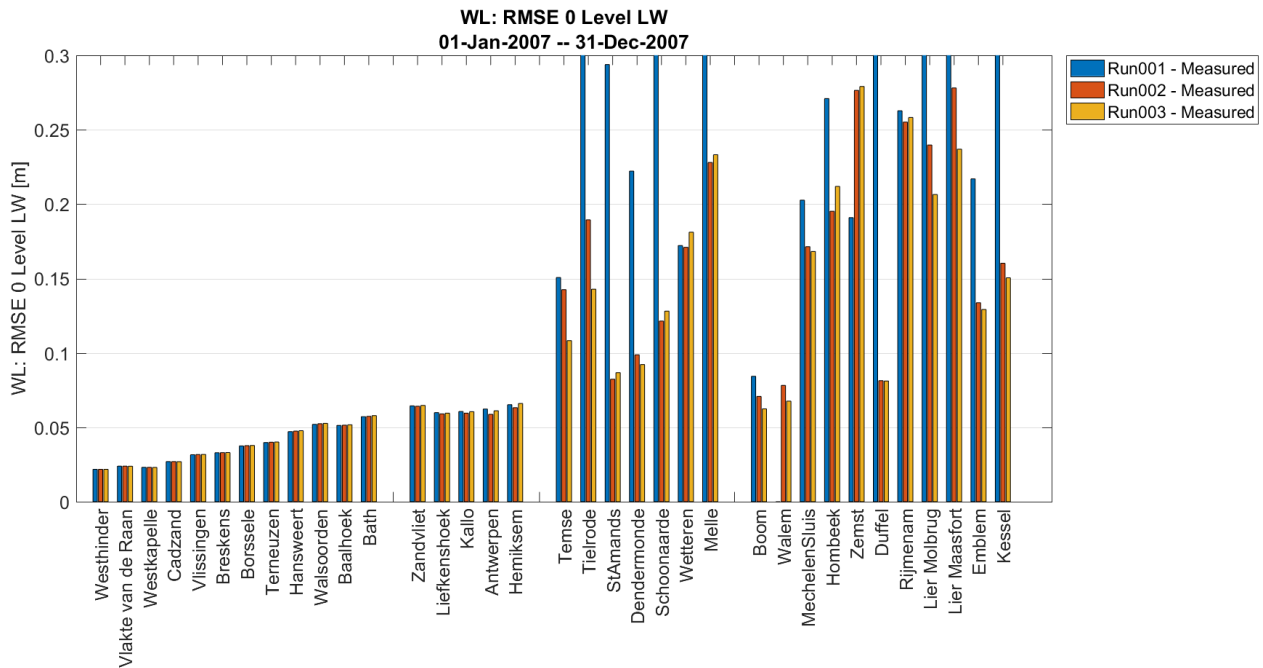


Figure 37 – RMSE0 of low water levels along the Scheldt.



8.1.2 Benchmark against manually calibrated 2D hindcast model

The error statistics are also inter-compared with the results of Maximova et al (2009b) which is a NEVLA2D model out of manual calibration. We didn't perform a new NEVLA2D run, instead we used the existing simulation results.

Be aware that there are many differences of the two models such as the simulation periods. Besides, Maximova et al (2009b) uses measured water level at Cadzand – Westkapelle as offshore boundary conditions (Run 003 is nested from ZUNO) and time series of measured wind data at Hansweert to force the model (Run 003 is forced by Hirlam wind field data). Therefore the comparison is essentially not one on one.

Table 20 shows that high water level is better predicted from Run003 in the Western Scheldt and the Upper Sea Scheldt. In the Lower Sea Scheldt, Maximova (2009b) leads to better predictions on the high water level. In terms of low water level, Run003 leads to similar or slightly better predictions in the Western Scheldt and Lower Sea Scheldt while Maximova (2009b) leads to slightly better results in **Schoonaarde** and **Wetteren**. Table 21 shows that the high water time is slightly better predicted by Maximova (2009b) and the low water time is slightly better predicted by Run003.

Table 20 – Comparison of Bias of high water and low water between Run003 and Maximova et al (2009b).

Stations	Bias of High Water [cm]		Bias of Low Water [cm]	
	Run003 (From 01-01-2007 to 12-31-2007)	Maximova 2009b (From 19-06-2002 to 17-07-2002)	Run003 (From 01-01-2007 to 12-31-2007)	Maximova 2009b (From 19-06-2002 to 17-07-2002)
Vlissingen	-4.0	2.6	0.7	0.6
Terneuzen	-3.2	-5.7	2.1	-0.3
Hansweert	1.5	-3.8	0.5	-1.5
Baalhoek	0.2	-6	0.3	-6.1
Bath	6.5	1.1	0.1	-4.6
Liefkenshoek	8.1	-3	1.3	-1.9
Antwerpen	10.5	-3.4	2.8	1
Hemiksem	4.1	-2	-8.8	-6
Boom	8.6	-4.7	-10.4	-13
Temse	5.5	-9.2	-3.1	-20.2
Walem	8.2	-8.8	-7.9	-24.7
Schoonaarde	1.8	6	-18.5	0.6
Wetteren	-1.3	1.5	-4.5	-1.6
Melle	-5.0	-22.1	1.9	-7.7
Kessel	-7.4	12.2	-20.3	-

Table 21 – Comparison of Bias of high water and low water time between Run003 and Maximova et al (2009b).

Stations	Bias of High Water Time [min]		Bias of Low Water Time [min]	
	Run003 (From 01-01-2007 to 12-31-2007)	Maximova 2009b (From 19-06-2002 to 17-07-2002)	Run003 (From 01-01-2007 to 12-31-2007)	Maximova 2009b (From 19-06-2002 to 17-07-2002)
Vlissingen	-5	0	-3	3
Terneuzen	-6	1	-4	5
Hansweert	-9	3	-2	5
Baalhoek	-7	0	-2	2
Bath	-8	-1	-3	1
Liefkenshoek	-3	1	-2	4
Antwerpen	-2	5	-3	5
Hemiksem	-8	2	-2	3
Boom	-6	3	-2	4
Temse	-2	1	-4	0
Walem	-7	4	-1	4
Schoonaarde	2	-3	8	11
Wetteren	5	-3	13	16
Melle	11	0	14	21
Kessel	9	-3	1	-

8.1.3 Benchmark against manually calibrated 2D forecast model (VSSKS)

In addition, the error statistics are inter-compared with the results of the NEVLA2D model running operationally on the forecasting system VSSKS (see calibration and validation report of Chu et al., 2016). The NEVLA2D model is calibrated for one spring-neap cycle between 20-09-2013 and 04-10-2013, with more weights assigned to the high water levels and less weights assigned to the low water levels. This is logical in a sense that the VSSKS is mainly configured for flooding forecast, so that the predictions on high water levels require more accuracy.

Table 22 shows that the high water levels are better (or similar) predicted by VSSKS for the Western Scheldt to Lower Sea Scheldt (from **Viissingen** to **Hemiksem**). Be aware that the simulation period of the 2 compared models are different. For the Upper Sea Scheldt, the VSSKS model predictive ability on high water levels slightly drops. The VSSKS model typically performs worse on low water levels, especially in the Upper Sea Scheldt.

Table 22 – Comparison of error statistics of water levels between Run003 and VSSKS.

Stations	TS						HW						LW					
	Bias		RMSE		RMSE0		Bias		RMSE		RMSE0		Bias		RMSE		RMSE0	
	Run003	VSSKS	Run003	VSSKS	Run003	VSSKS	Run003	VSSKS	Run003	VSSKS	Run003	VSSKS	Run003	VSSKS	Run003	VSSKS	Run003	VSSKS
Westkapelle	-0.4	5.6	4.1	16.5	4.1	15.5	-3.9	8.1	4.6	8.9	2.4	3.7	3.8	1.2	4.5	6.5	2.3	6.4
Cadzand	2.0	7.2	5.8	16.1	5.5	14.4	-0.6	5.6	3.6	7.4	3.6	4.9	5.8	7.5	6.4	10.7	2.7	7.6
Breskens	-0.6	2.9	5.0	19.0	4.9	18.7	-3.9	1.6	5.3	4.0	3.6	3.7	0.9	1.9	3.4	7.1	3.3	6.9
Viissingen	-1.4	5.7	4.8	16.2	4.6	15.1	-4.0	6.4	5.4	7.4	3.6	3.9	0.7	3.3	3.3	7.4	3.2	6.7
Borsele	-0.5	4.3	5.2	15.0	5.2	14.4	0.1	2.5	4.8	4.6	4.8	3.8	1.6	3.5	4.1	7.7	3.8	6.8
Terneuzen	-1.6	2.0	5.7	15.2	5.5	15.0	-3.2	-1.8	5.3	4.6	4.3	4.2	2.1	2.7	4.6	7.7	4.0	7.2
Hansweert	1.1	-0.5	5.5	9.8	5.4	9.8	1.5	-1.4	5.2	4.4	5.0	4.2	0.5	-1.1	4.8	6.9	4.8	6.8
Walsoorden	0.7	-1.4	6.0	11.5	6.0	11.4	-2.3	-2.5	5.4	5.4	4.8	4.8	0.3	-3.0	5.3	7.6	5.3	6.9
Baalhoek	1.6	-0.5	6.2	14.0	6.0	14.0	0.2	-0.3	4.9	4.3	4.9	4.3	0.3	-4.1	5.2	7.9	5.2	6.7
Bath	4.0	1.5	8.2	13.1	7.2	13.0	6.5	2.2	8.4	5.4	5.4	5.0	0.1	-1.8	5.8	6.9	5.8	6.7
Zandvliet	2.5	3.0	8.9	13.8	8.6	13.5	8.8	3.4	11.0	6.5	6.6	5.5	-3.1	-2.0	7.2	7.6	6.5	7.4
Liefkenshoek	4.7	4.1	8.7	13.3	7.4	12.7	8.1	2.0	10.2	7.3	6.2	7.0	1.3	0.2	6.1	6.9	6.0	6.9
Kallo	6.2	2.8	10.1	12.5	7.9	12.2	10.6	-1.0	12.6	7.9	6.8	7.8	3.1	-2.3	6.8	7.9	6.0	7.5
Antwerpen	6.3	-4.1	10.3	16.8	8.1	16.3	10.5	0.2	12.4	7.9	6.6	7.9	2.8	-15.3	6.7	16.8	6.1	7.0
Hemiksem	-1.8	-0.9	8.7	22.9	8.5	22.9	4.1	5.0	7.7	8.9	6.5	7.3	-8.8	-21.2	11.0	22.2	6.6	6.7
Temse	0.8	-10.1	8.0	37.6	8.0	36.3	5.5	0.6	8.5	9.7	6.5	9.7	-3.1	-45.8	11.3	46.5	10.8	8.4
Sint Amands	-5.7	-5.8	16.5	45.3	15.5	44.9	5.7	4.5	9.1	12.2	7.1	11.3	-28.3	-65.1	29.6	66.1	8.7	11.6
Dendermonde	8.7	32.0	21.4	44.2	19.5	30.4	-4.7	6.2	9.1	13.8	7.8	12.4	21.6	91.7	23.5	92.7	9.2	13.2
Schoonarde	-6.9	26.7	15.2	34.5	13.5	21.8	1.8	3.1	8.3	17.6	8.1	17.3	-18.5	47.8	22.5	48.8	12.8	9.8
Wetteren	-0.4	50.4	16.1	60.5	16.1	33.5	-1.3	-0.5	11.6	13.0	11.5	13.0	-4.5	109.3	18.7	110.2	18.1	14.1
Melle	6.1	42.6	23.1	54.0	22.3	33.2	-5.0	-11.4	17.8	17.3	17.1	13.0	1.9	96.6	23.4	97.6	23.3	14.3
Duffel	-3.6	-0.4	9.8	17.5	9.1	17.5	-6.0	1.6	8.9	6.1	6.5	5.9	-10.4	-3.1	13.2	7.2	8.1	6.5

8.1.4 Comparison to the sensitivity analysis of NEVLA3D

Vanlede et al (2008) carried out a sensitivity analysis of NEVLA3D model to investigate the influence of bottom roughness in 10 different zones on model predicted water levels (e.g. M2 and M4 tidal amplitude). The roughness field proved to be of the utmost importance for the gradient of the harmonic components along the Scheldt estuary. The sensitivity of this, linked to the geographical influences was identified. The sensitivity analysis showed that the gradient of the M2 amplitude changes in the region where the local alteration of the roughness takes place. In the regions up and down of the region concerned, the gradient remains almost constant. Similar effects were observed for the M4 amplitude in the most downstream regions. In the rest of the Westerschelde, the Baarland - Liefkenshoek section, a local roughness change has no significant effect on M4. This does not apply to the Zeeschelde, where larger changes in amplitude occur with roughness variations. In the Upper Zeeschelde the influence zone is limited to the zone in which the roughness was changed. In contrast, an inversion situation occurs with roughness changes in the Lower Zeeschelde. With a locally smaller roughness, the amplitude in the relevant area increases as expected. However, the M4 amplitude decreases downwards.

During the automatic calibration with OpenDA in this study, the first 11 runs can be used to test the sensitivity, see Table 23. The resulting changes on M2 and M4 amplitude along the Scheldt estuary can be found in ANNEX 3. Changing roughness in a zone has also an influence upstream. The most sensitive area is zone 462 and 467 where the M2 amplitude decreased by 6 cm and 4 cm respectively. M4 is however not very sensitive to the roughness changes.

The above-mentioned findings do not fully agree with the findings from Vanlede et al (2008). A possible reason is that the Manning coefficient from Vanlede et al (2008) is changed by ± 0.005 , to be able to make sufficient distinctions with the reference situation. The roughness changes from this study is however smaller (0.002). Additionally, Vanlede et al (2008) investigated a NEVLA3D model while a NEVLA2D model is adopted by this study. The 2D and 3D models respond differently to changes in bottom roughness.

Table 23 – 11 runs of NEVLA2D model out of the automatic calibration with OpenDA.
The initial roughness (Manning coefficient) is increased by 0.002 in one zone in each run.

Iteration	A-450	A-455	A-457	A-459	A-461	A-462	A-463	A-464	A-465	A-467
1 (Reference)	0	0	0	0	0	0	0	0	0	0
2	+0.002	0	0	0	0	0	0	0	0	0
3	0	+0.002	0	0	0	0	0	0	0	0
4	0	0	+0.002	0	0	0	0	0	0	0
5	0	0	0	+0.002	0	0	0	0	0	0
6	0	0	0	0	+0.002	0	0	0	0	0
7	0	0	0	0	0	+0.002	0	0	0	0
8	0	0	0	0	0	0	+0.002	0	0	0
9	0	0	0	0	0	0	0	+0.002	0	0
10	0	0	0	0	0	0	0	0	+0.002	0
11	0	0	0	0	0	0	0	0	0	+0.002

8.2 Harmonic Analysis of Water Levels

Figure 38 to Figure 41 compare the model predicted tidal components of M2 and S2 along the River Scheldt (results for the river tributaries are summarized in Table 24). Run003 shows better predictions on both M2 and S2 amplitude and phase from Antwerp to Melle.

Figure 42 shows that the vector difference (see definition in ANNEX 4) from Run003 is also dropped significantly from at stations between Antwerp and Melle. However the it is increased in the River Zenne and Dijle.

Figure 38 – M2 amplitude along the River Scheldt.

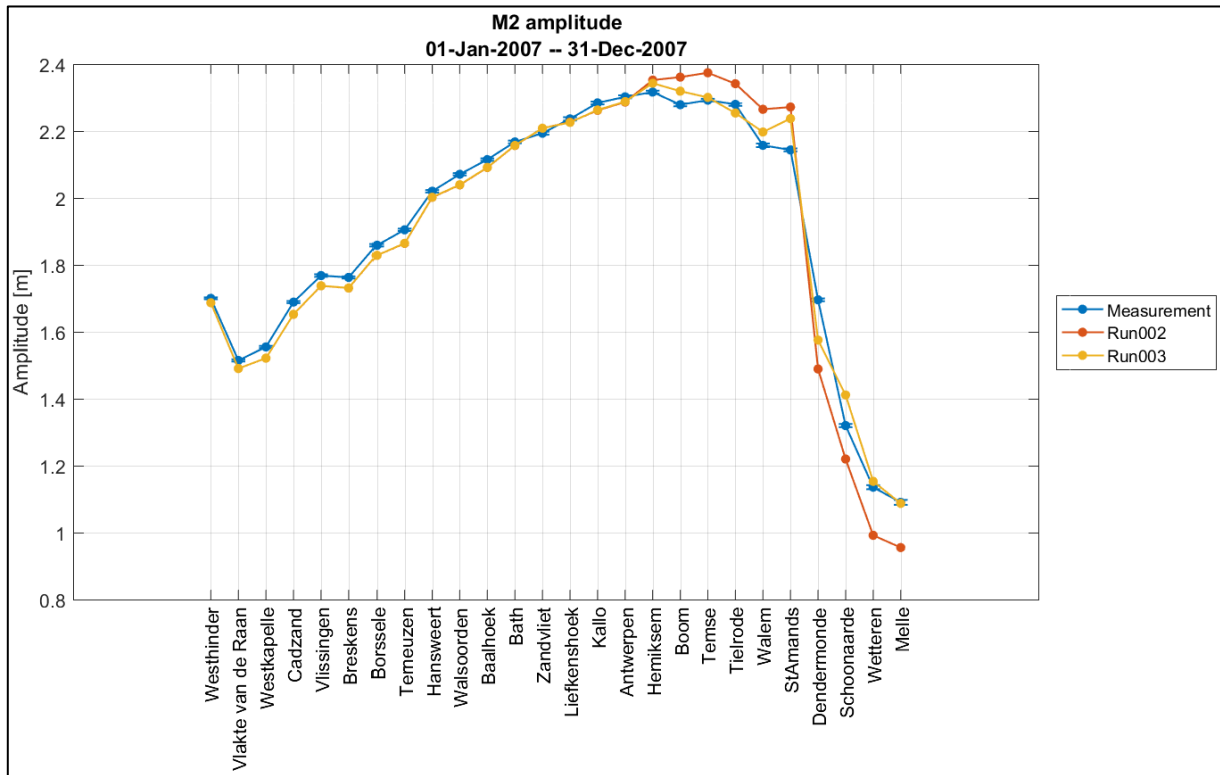


Figure 39 – M2 phase along the River Scheldt.

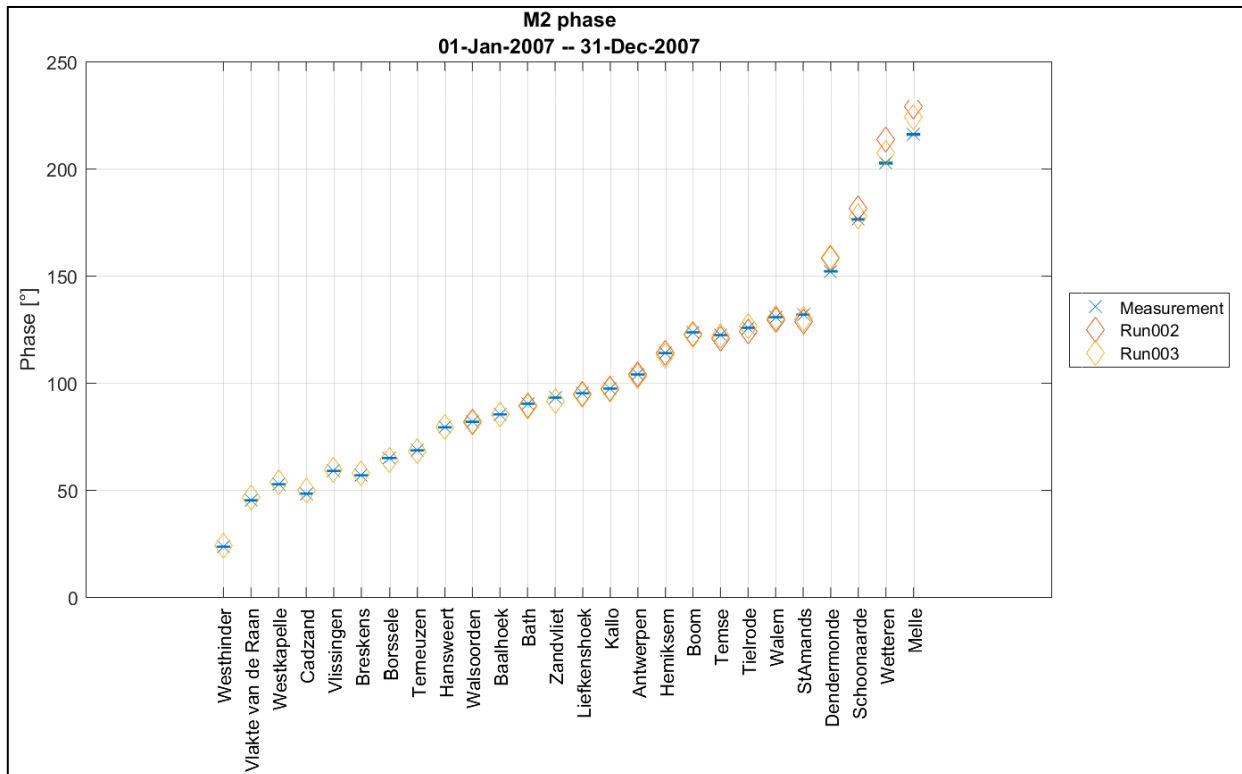


Figure 40 - S2 amplitude along the River Scheldt.

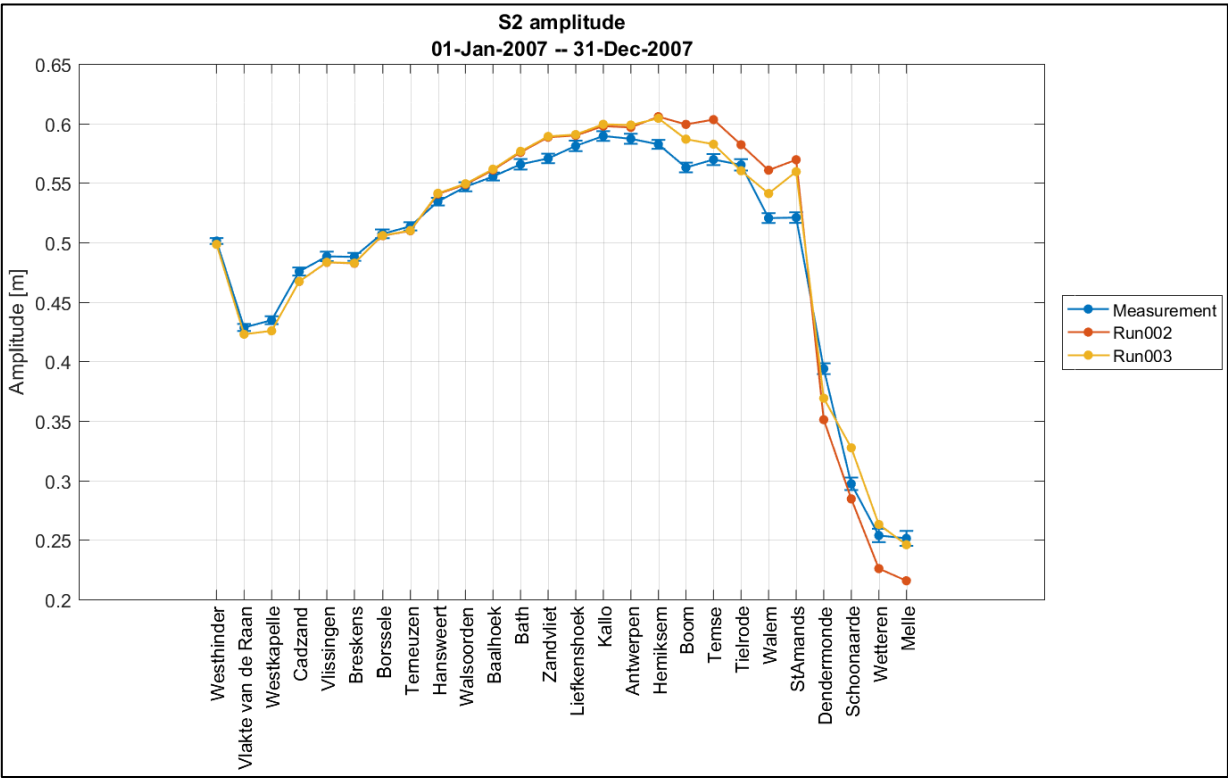


Figure 41 – S2 phase along the River Scheldt.

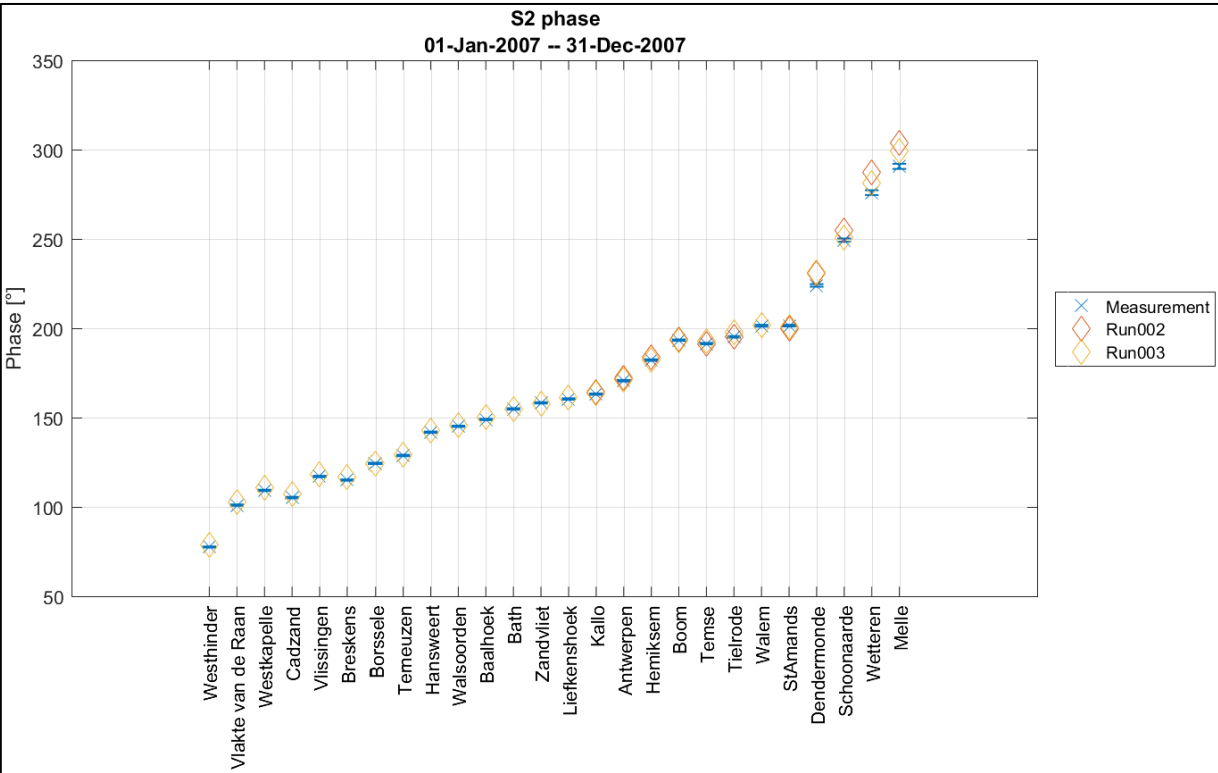


Figure 42 – Vector differences along the River Scheldt.

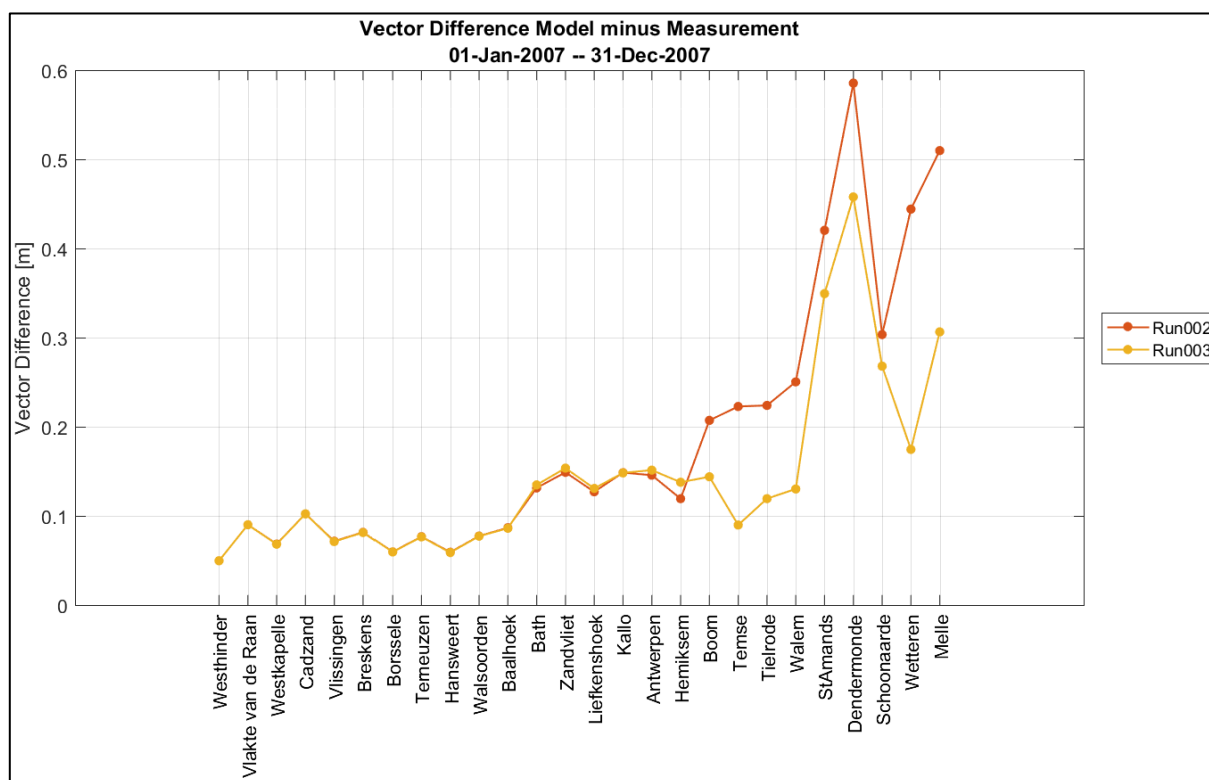


Table 24 – Harmonic components of M2, S2 and vector differences for the tributaries of Scheldt.

Stations	M2 Amplitude			M2 Phase			S2 Amplitude			S2 Phase			Vector Difference	
	Obs	Run002	Run003	Obs	Run002	Run003	Obs	Run002	Run003	Obs	Run002	Run003	Run002	Run003
MechelenSluis	1.83	1.86	1.78	139.8	142.4	144.0	0.43	0.45	0.43	210.7	217.7	218.7	0.36	0.45
Hombeek	1.50	1.52	1.45	145.8	147.3	149.3	0.38	0.39	0.37	216.3	219.3	220.9	0.18	0.29
Zemst	0.99	1.03	0.98	148.1	150.6	152.7	0.28	0.29	0.28	215.2	219.5	221.2	0.23	0.32
Duffel	1.77	1.87	1.77	148.3	147.3	149.2	0.41	0.44	0.41	219.9	221.0	222.4	0.30	0.15
Rijmenam	0.24	0.21	0.20	176.3	191.2	192.1	0.09	0.09	0.08	237.8	250.0	250.5	0.24	0.24
Lier Molbrug	1.12	1.27	1.22	164.2	161.9	164.8	0.26	0.31	0.30	234.9	236.6	239.1	0.49	0.41
Lier Maasfort	0.84	1.00	0.97	179.0	175.8	179.0	0.20	0.25	0.24	247.9	250.3	253.4	0.46	0.42
Emblem	0.66	0.93	0.85	191.3	188.3	191.9	0.16	0.23	0.21	258.9	263.5	266.1	0.60	0.45
Kessel	0.55	0.71	0.65	202.8	207.8	211.3	0.14	0.18	0.16	272.1	282.3	284.9	0.35	0.31

8.3 Salinity

The comparison of the modeled and measured salinity time series (§4.2) are presented in Figure 43 to Figure 48. The statistical analysis results are presented in Table 25. Salinity is in general well reproduced by the model along the estuary. There are no substantial differences on salinity between the 3 different runs. This is logical because the salinity is only compared where measurement data are available (Vlakte van de Raan to Oosterweel). The bottom roughness in this area is not modified much by OpenDA.

Figure 43 – Comparison of salinity between measurement and model runs at Vlake Van De Raan.

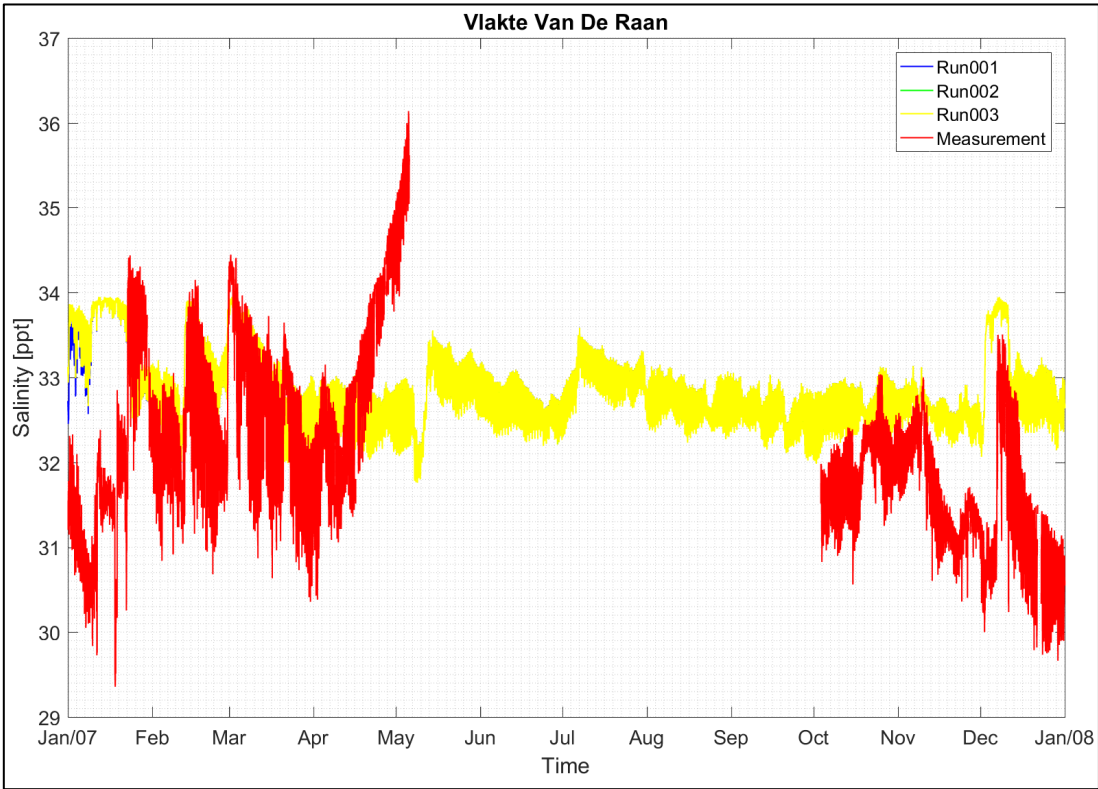


Figure 44 – Comparison of salinity between measurement and model runs at Hoofdplaat.

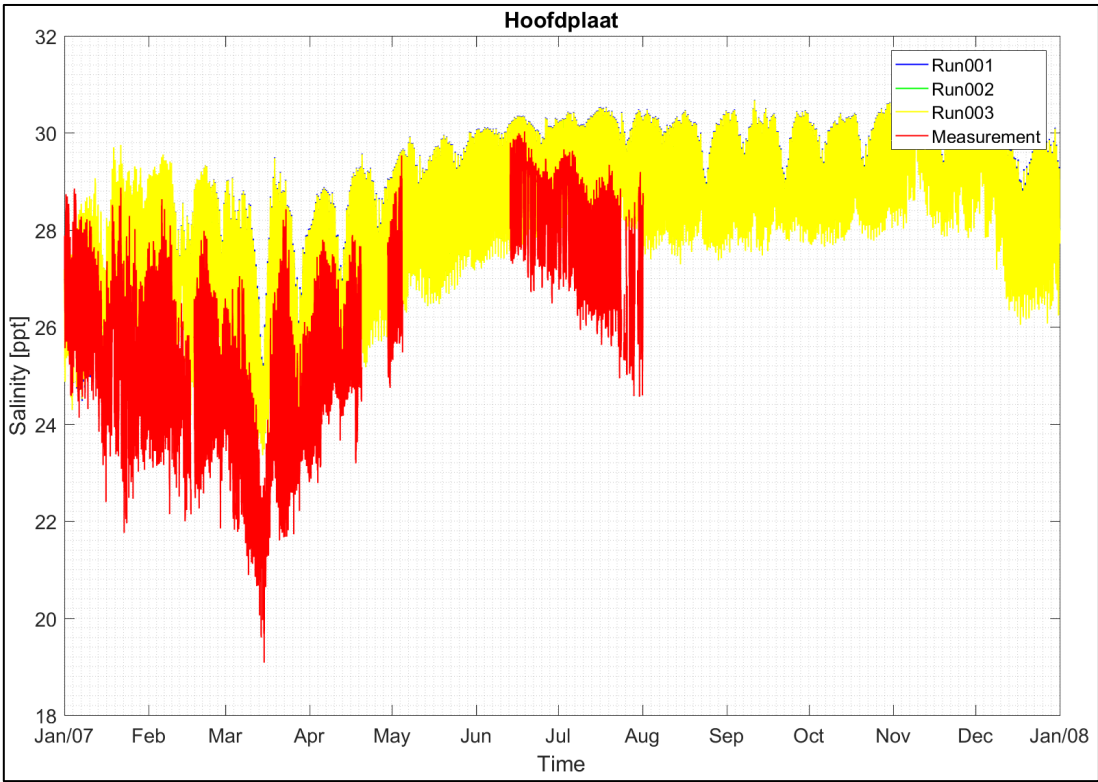


Figure 45 – Comparison of salinity between measurement and model runs at Baalhoek.

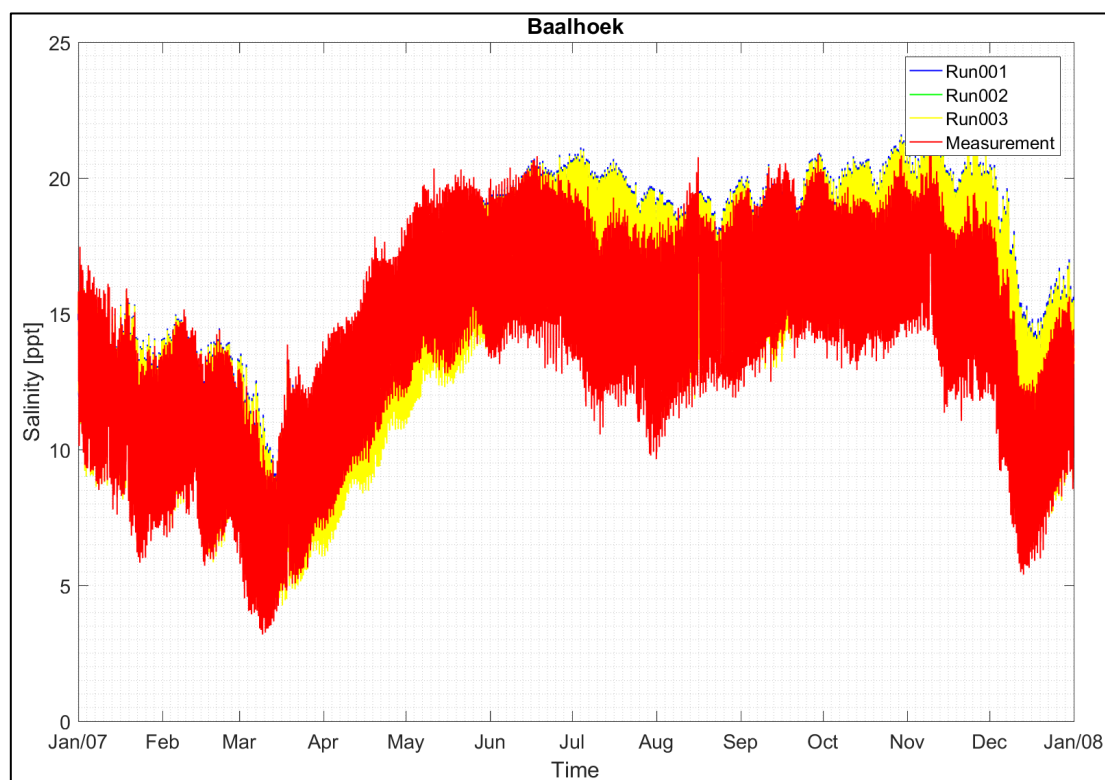


Figure 46 – Comparison of salinity between measurement and model runs at Prosperpolder.

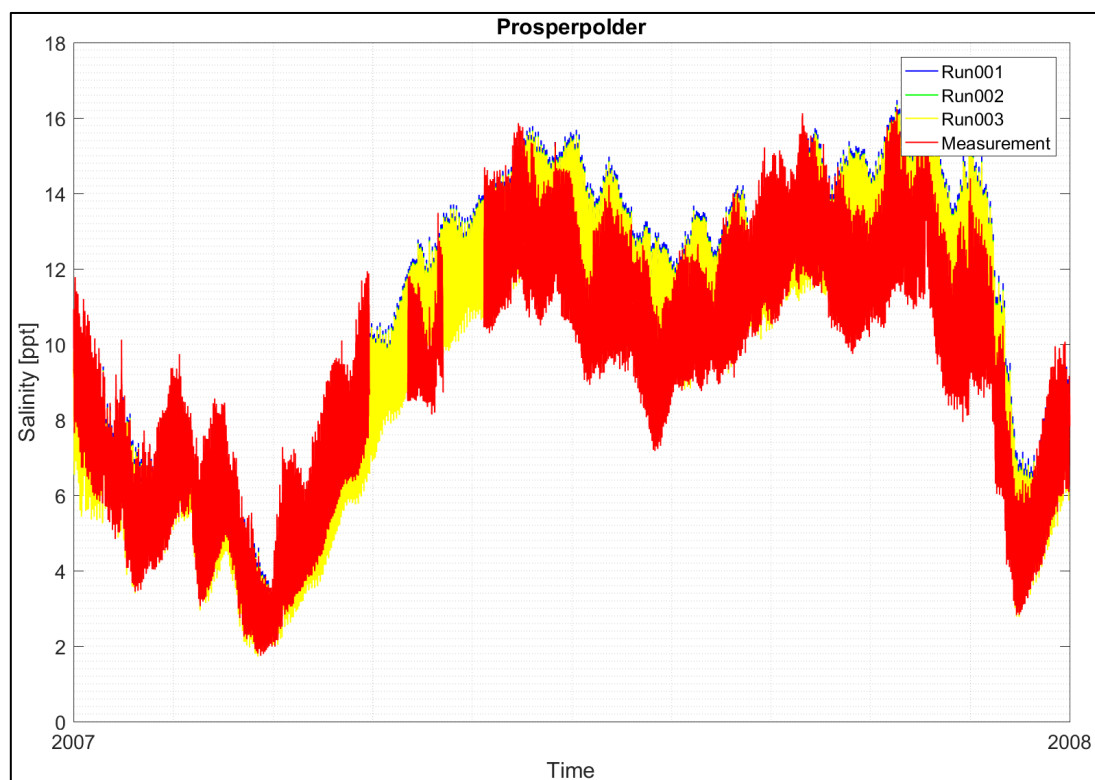


Figure 47 – Comparison of salinity between measurement and model runs at Boei84.

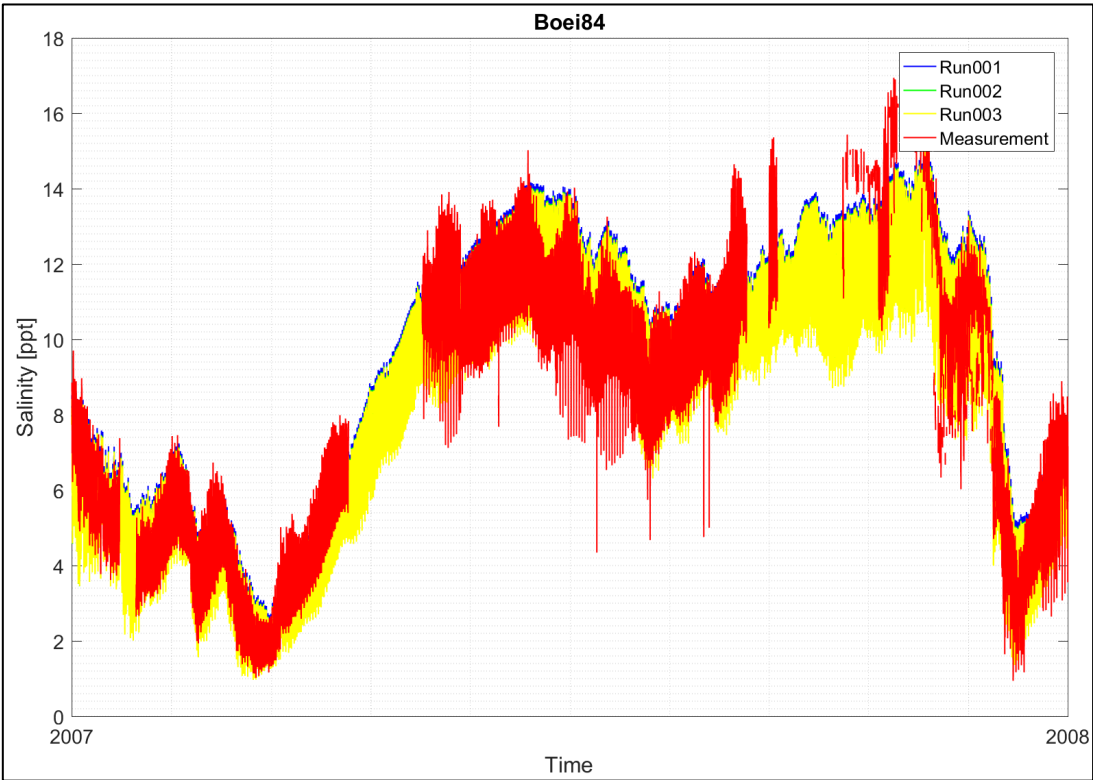


Figure 48 – Comparison of salinity between measurement and model runs at Oosterweel.

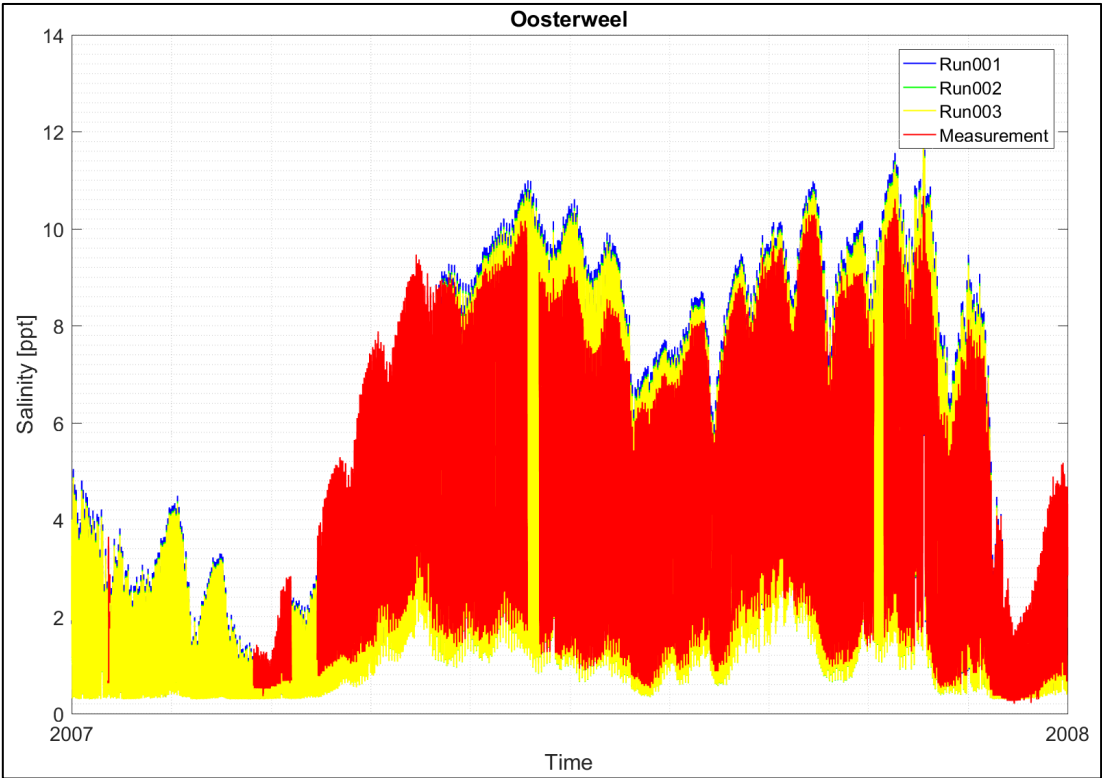


Table 25 – Statistic analysis of salinity between model and measurements

Nr	Measuring station	Bias [psu]			RMSE [psu]		
		Run001	Run002	Run003	Run001	Run002	Run003
1	Vlakte Van De Raan	0.7	0.7	0.7	1.3	1.4	1.4
2	Hoofdplaat	1.8	1.8	1.8	2.1	2.1	2.1
3	Baalhoek	0.7	0.6	0.6	1.5	1.5	1.5
4	Prosperpolder	0.5	0.4	0.4	1.0	1.0	1.0
5	Boei84	0.0	-0.1	-0.1	0.7	0.7	0.7
6	Oosterweel	0.1	0.0	-0.1	0.6	0.6	0.5

8.4 Discharge

The cross-sectional discharges predicted by the models are compared with measured data collected throughout the Scheldt during the past years (§4.3). In order to do so, the comparable tide analysis is applied in this study.

Comparable tide analysis is a method developed in-house to allow comparison of model results to measurements which are outside of the simulation period. The short term water level that occurred during a 13h measurement campaign (ADCP or Q) is compared with long term water level measurements. Those tidal cycles within the long term water level that have the best match with the tidal cycles in the short term water level are found and ranked. From this analysis, the period that contains the best similar tides to a set of 13h measurements (ADCP or Q) can be determined by calculating the RMSE or RMSE0 of all occurring tides.

For this study the comparable tide analysis searched the representative period from the entire year 2007. The resulted RMSE of each campaign is shown in Table 26. The averaged RMSE values of all the campaigns is 6.4 cm, which implies that the discharge comparison between model and measurement based on the comparable tidal analysis is reliable.

Figure 49 exemplifies the time series comparison of discharge at **R12 Wielingen 20020528**, which shows quite decent agreement between model and measurement. Figure 50 to Figure 52 show the error statistics of Bias, RMSE and RRMSE of the complete time series of discharges at all the locations. The relative RMSE suggests the maximum uncertainty between model and measurements is about 20%. Besides, the calibrated model from OpenDA (Run003) shows better results in the **Upper Sea Scheldt and Rupel**.

Table 26 – RMSE of the comparable tide analysis.

No.	Campaign Names	RMSE [cm]	No.	Campaign Names	RMSE [cm]
1	R12 Wielingen 20020528	7.4	22	R3 Overloop van Valkenisse 20070814	5.1
2	R12 Wielingen 20070619	6.4	23	R3 Zimmermangeul 20070815	5.8
3	R11 Wielingen 20060517	0.0	24	R1 Vaarwater boven Bath 20061025	8.2
4	R11 Wielingen 20000605	4.8	25	Liefkenshoek_20090527	6.6
5	R12 Deurloo 20000605	7.7	26	Liefkenshoek_20100430	8.3
6	R12 Deurloo 20020528	7.9	27	Liefkenshoek_20130625	9.2
7	R12 Deurloo 20070703	6.5	28	Oosterweel_20090529	8.2
8	R12 Oostgat 20000605	0.0	29	Oosterweel_20100429	9.9
9	R12 Oostgat 20020528	8.0	30	Oosterweel_20130627	7.1
10	R12 Oostgat 20070618	6.6	31	Kruikebe_20090526	8.7
11	R11 Sardijneul 20060516	0.0	32	Kruikebe_20100414	9.7
12	R11 Sardijneul 20000605	3.7	33	Kruikebe_20130530	8.3
13	R10 Vaarwater langs hoofdplaat 20020516	8.2	34	Driegoten_20090623	10.0
14	R10 Vaarwater langs hoofdplaat 20071011	6.1	35	Driegoten_20100415	7.2
15	R9 Vaarwater langs hoofdplaat 20060913	0.0	36	Driegoten_20130612	8.6
16	R7 Everingen 20080604	6.0	37	Boom_20090622	5.9
17	R7 Pas van Terneuzen 20080605	7.8	38	Boom_20100427	6.0
18	R6 Gat van Ossensisse 20041013	7.6	39	Schoonaarde_20090625	7.5
19	R6 Middelgat 20041013	7.4	40	Schoonaarde_20100414	5.6
20	R5 Schaar van Waarde 20051201	6.6	41	Schoonaarde_20130527	5.9
21	R5 Zuidergat 20051130	7.3	42	Terhagen_20130529	5.6

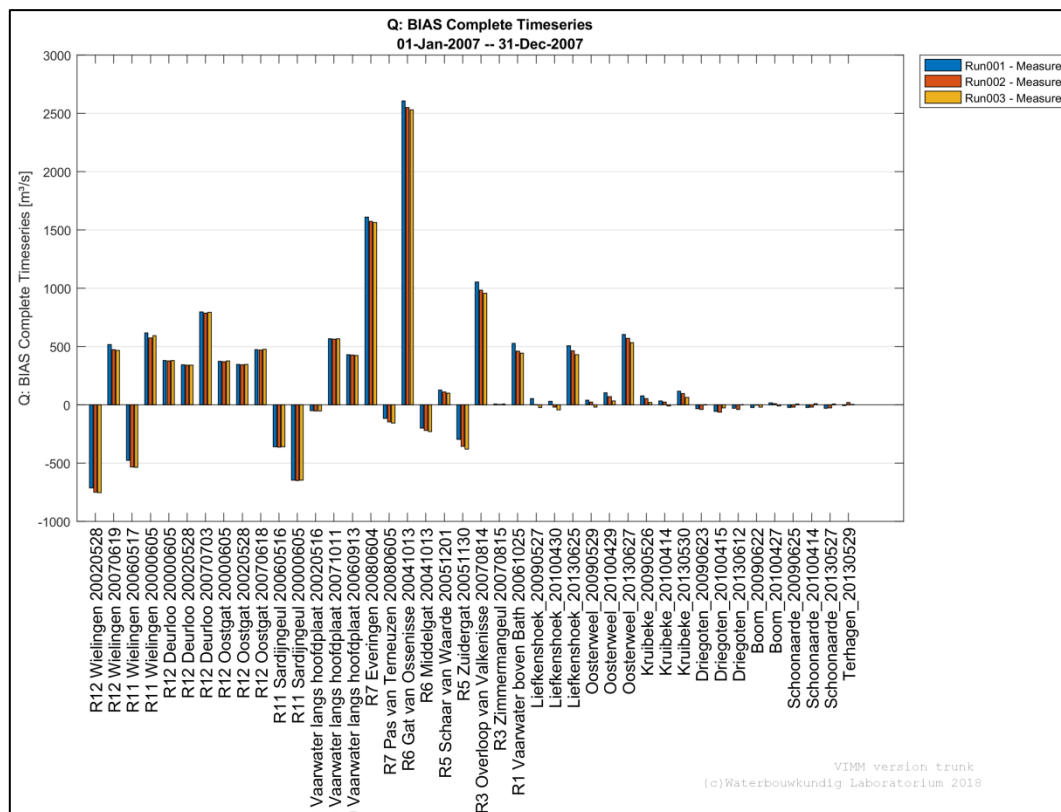
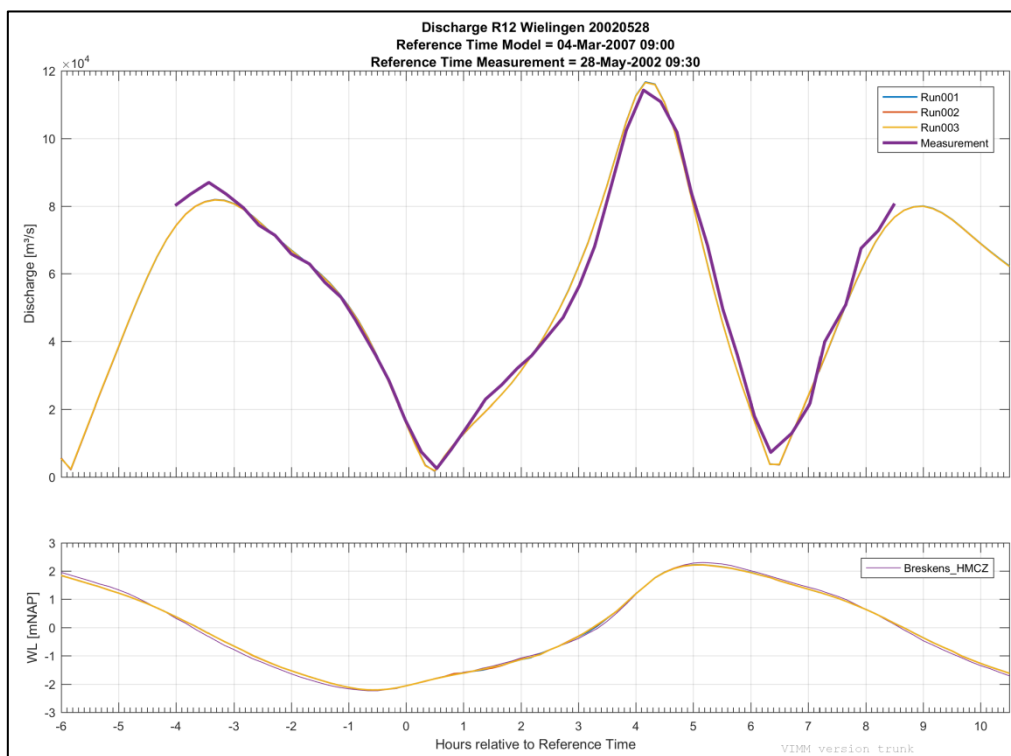


Figure 51 – RMSE of complete time series of discharges.

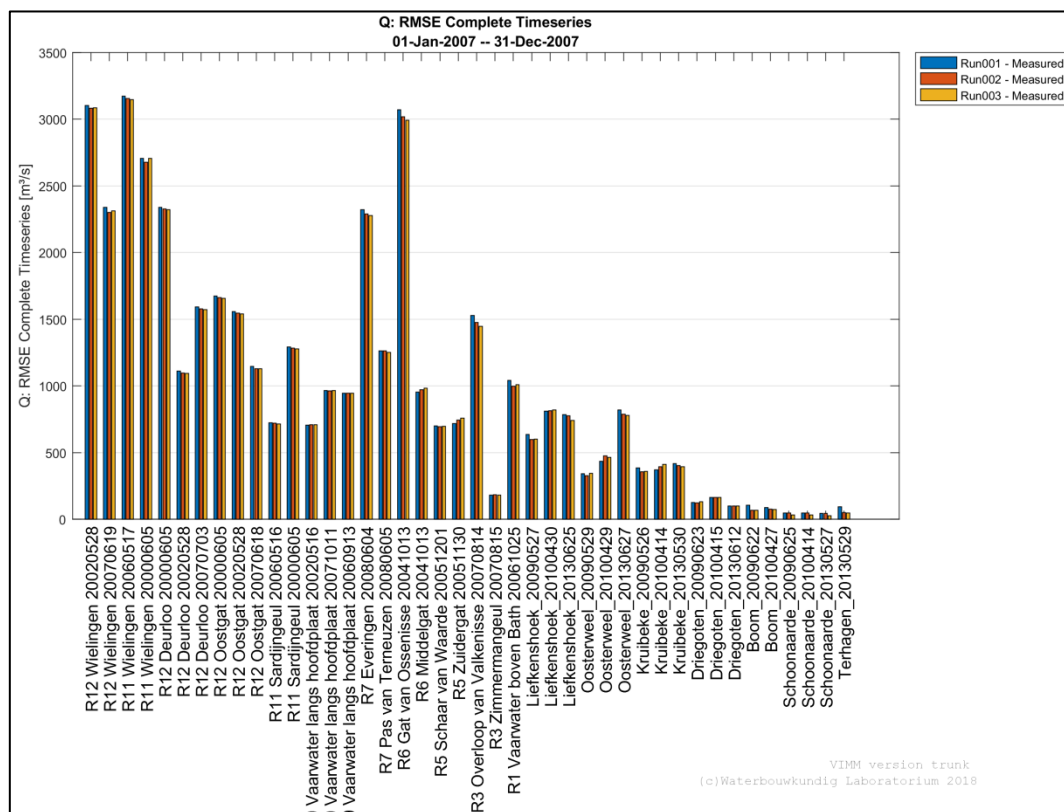
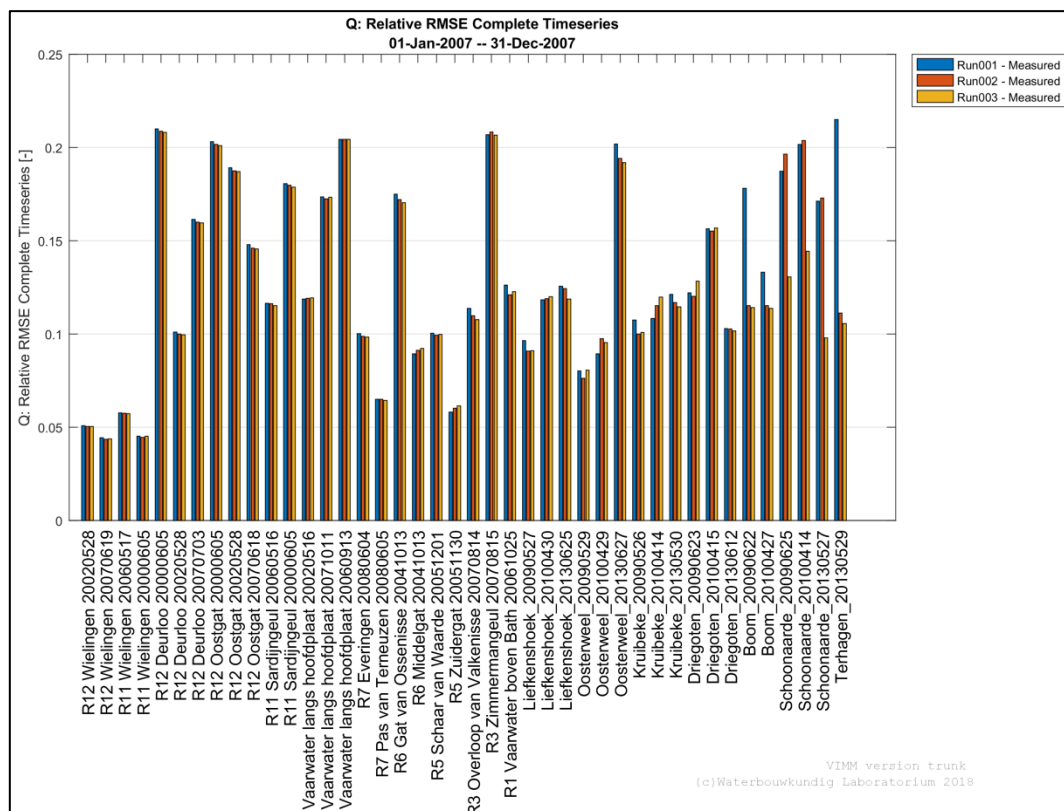


Figure 52 – Relative RMSE of complete time series of discharges.



9 Conclusions and Recommendations

In the summer of 2016 Deltares has finished the calibration and validation of the new WAQUA-Schelde_Nevla model (**waqua-schelde_nevla-j07_5-v4**) for the Dutch part of the River Scheldt. The continuation of the model calibration for the Flemish part was assigned to the Waterbouwkundig Laboratorium (Flanders Hydraulics Research or FHR).

This report details the update of the Baseline database, and the automatic calibration of the NEVLA model with OpenDA.

The main findings from this study are:

- The automatic calibration with OpenDA was successful, with the cost function reduced by 20%.
- The water level predictions downstream of **Bath** remain decent both before and after the OpenDA calibration. This was expected, because the roughness within those areas is not changed during the automatic calibration.
- The model quality in the Lower Sea Scheldt from **Zandvliet** until **Hemiksem** also did not change much through automatic calibration. This is consistent with the fact that OpenDA does not modify the bottom friction much in this area.
- The model quality in the area of Rupel (**Boom** and **Walem**) and Upper Sea Scheldt (**Temse** to **Melle**) is improved noticeably on both high and low water levels. However, the errors on low water level at **Dendermonde**, **StAmands** and **Schoonaarde** are still substantial.
- There are still room for model improvement for the tributaries Zenne, Dijle and Nete.
- The high and low water levels with OpenDA calibration are benchmarked against existing NEVLA2D model versions for hindcasting and forecasting. The manual calibrated NEVLA2D model for hindcasting has in general comparable quality to the calibrated model out of OpenDA. The manual calibrated NEVLA2D model for forecasting (VSSKS) typically performs worse on low water levels, especially in the Upper Sea Scheldt.
- Salinity is well reproduced by the model. The model changes performed in this study have limited impact on the salinity predictions.
- Cross-sectional discharge predicted by the models are compared with 42 measurements. The relative RMSE suggests the maximum error between model and measurements is about 20%. The model calibrated with OpenDA gives better predictions on discharges in the **Upper Sea Scheldt and Rupel**.

Some recommendations for future studies:

- The implementation of the barrier at Mechelen is not perfect due to the lack of operational data which introduces uncertainties to the water level predictions in the river Dijle.
- The tributaries Zenne, Dijle and Nete are all within the roughness polygon 467. Therefore the degrees of freedom for the model calibration is limited, which restrains the possibility to find *one* optimal value of Manning coefficient leading to satisfactory results at all the stations. Improvements can be foreseen if the roughness polygons 467 would be split into more smaller polygons.
- The cost function used in this study is based on comparison of complete time series of water levels only. This is one way of looking at the error signal, but there are other ways as well, e.g. looking at high/low water and tidal amplitude etc. Alternative elements of a cost function are presented in chapter 8. From the point view of operational forecasting for flood management, the high water levels could be given more weights. For future studies, this can be carried out by modifying the cost function. It is not immediately clear however how a cost function calculation performed on HW/LW in Matlab (with the VIMM toolbox) can be integrated in OpenDA.

- During the 1st phase of model calibration with OpenDA, the cost function could not be further reduced after 25 iterations. In the 2nd phase of model calibration (iterations 26 to 55), only line searches are done which do not further reduce the cost function, which indicates that the cost function is already close to minimal. The OpenDA calibration could not stop after 25 iterations because the stop criterion was set too strict in this study. For future studies, a more suitable setting for the different stop criteria should be considered.

10 References

- Adema, J** (2006). Evaluatie van hydraulische modellen voor operationele voorspellingen. Deelopdracht 3: Afregelen van Vlaamse rivieren in het Kustzuid model en vergelijking Kalman sturing. Rapport Alkyon A1401R3r2, in opdracht van WL Borgerhout (M.729-09).
- Chu, K.; Buitrago, S.; Depreiter, D.; Deschamps, M** (2016). Ondersteuning en verbetering operationeel voorspellingscluster VSSKS: Uitbreiding van het operationeel 2D Nevla model met GOG en GGG functionaliteit. Versie 1.0. WL Rapporten, 13_133_1. Waterbouwkundig Laboratorium & IMDC: Antwerpen, België.
- Deltares** (2015). Dataprotocol Baseline 5.
- Deltares** (2016). Handleiding Baseline 5 - Baseline User Manual.
- Groenenboom, J.; van der Kaaij, Th.; Plieger, R.** (2016). Schelde-estuarium, WAQUA model 5e generatie - Werkzaamheden 2016. Deltares Report. Delft, the Netherlands.
- LievenseCSO** (2015). Baseline Zuidwestelijke Delta – Achtergrondrapportage. Documentcode: 15M2006.RAP001. Netherlands.
- Maximova, T.; Ides, S.; Vanlede, J.; De Mulder, T.; Mostaert, F.** (2009a). Verbetering 2D randvoorwaardenmodel. Deelrapport 3: Kalibratie bovenlopen. WL Rapporten, 753_09. Flanders Hydraulics Research, Antwerp, Belgium.
- Maximova, T.; Ides, S.; De Mulder, T.; Mostaert, F.** (2009b). Verbetering randvoorwaardenmodel. Deelrapport 4: Extra aanpassingen Zeeschelde. WL Rapporten, 753_09. Flanders Hydraulics Research: Antwerp, Belgium
- OpenDA** (2016). OpenDA User Documentation. The OpenDA Association.
- Plieger, R.** (2015). Roosterschematisatie Zuidwestelijke Delta (Deel 2) - Westerschelde, Boven- en Benedenschelde. Deltares Report. Delft, the Netherlands.
- Ralston, M., and R. Jennrich.** (1978). DUD, a derivative-free algorithm for nonlinear least squares. *Technometrics*, 20, 7–14, doi:10.1080/00401706.1978.10489610.
- Rijkswaterstaat** (2015). User's Guide WAQPRE. The Netherlands.
- Vanlede, J.; Decrop, B.; De Clercq, B.; Ides, S.; De Mulder, T.; Mostaert, F.** (2008). Verbetering randvoorwaardenmodel - Deelrapport 1: gevoeligheidsanalyse. WL Rapporten, 753_09. Waterbouwkundig Laboratorium & IMDC: Antwerpen, België.
- Vanlede, J.; Delecluyse, K.; Primo, B.; Verheyen, B.; Leyssen, G.; Plancke, Y.; Verwaest, T.; Mostaert, F.** (2015). Verbetering randvoorwaardenmodel: Subreport 7 - Calibration of NEVLA 3D. Version 4.0. WL Rapporten, 00_018. Flanders Hydraulics Research & IMDC: Antwerp, Belgium.
- Velzen, E.H. et al.** (2003a), Stromingsweerstand vegetatie in Uiterwaarden, Deel 1 Handboek versie 1-2003, RIZA rapport 2003.028.
- Velzen, E.H. et. al.** (2003b), Stromingsweerstand vegetatie in Uiterwaarden, Deel2 Achtergronddocument versie 1-2003, RIZA rapport 2003.029.
- Vermeersch, S., Baeyens, R., De Marteleire, N., Gelaude, E., Pauwels, I., Pieters, S., Robberechts, K. & Coeck, J.** (2016). Evaluatie van de vismigratie in de Dijle ter hoogte van de Bovenstuw in Mechelen. Rapporten van het Instituut voor Natuur- en Bosonderzoek 2017 (14). Instituut voor Natuur- en Bosonderzoek, Brussel. DOI: doi.org/10.21436/inbor.12464189.

Appendix A Introduction of DUD

The DUD (Doesn't Use Derivative) algorithm (Ralston and Jennrich, 1978) is a derivative-free algorithm for nonlinear least squares. It can be seen as a Gauss-Newton method, in the sense that it transforms the nonlinear least square problem into the well-known linear square problem. DUD evaluates and optimizes uncertain model parameters by minimizing a cost function. The parameter values corresponding to the minimum value of the cost function are considered as the optimal parameter values for the given analysis.

For N calibration parameters, DUD requires $(N+1)$ set of parameters estimates. The affine function for the linearization is formed through all these $(N+1)$ guesses. Note that the affine function gives exact value at each of the $(N+1)$ points. The resulting least square problem is then solved along the affine function to get a new estimate, whose cost is smaller than those of all other previous estimates. If it does not produce a better estimate, the DUD will perform different steps, like searching in opposite direction and/or decreasing searching-step, until a better estimate is found. Afterwards, the estimate with the largest cost is replaced with the new one and the procedure is repeated for the new set of $(N+1)$ estimates. The procedure is stopped when one of the stopping criteria is fulfilled.

The general DUD implementation is given by the following steps:

- Start running first guess and modify each parameter;
- Linearize the model around these values and solve the linear problem;
- If this is an improvement, update linearization with new point;
- Or, do a line-search (only until there is improvement).

Suppose there is one uncertain model parameter $\mathbf{P} \in \mathbf{R}$ and a set of n observations $\mathbf{y} \in \mathbf{R}^n$. The cost function J is expressed as a sum of squares as

$$J(\mathbf{P}) = [\mathbf{y} - \mathbf{f}(\mathbf{P})]^T [\mathbf{y} - \mathbf{f}(\mathbf{P})]$$

\mathbf{f} is the model function. Note that calculating $J()$ involves doing one model run, and post-processing the results to calculate the cost function.

The DUD optimization starts with an unperturbed run (with initial guess $\mathbf{P1}$) and one sensitivity run ($\mathbf{P2}$). The corresponding function values $\mathbf{f}(\mathbf{P1})$ and $\mathbf{f}(\mathbf{P2})$ are stored in memory. The parameters are sorted according to their cost function $J(\mathbf{P})$ from high to low. Let's assume that in this case $\mathbf{P1}$ results in a higher cost function compared with $\mathbf{P2}$.

A linear approximation $\mathbf{L}(\alpha)$ is built of the function \mathbf{f} around $\mathbf{P2}$:

$$\mathbf{L}(\alpha) = \mathbf{f}(\mathbf{P2}) + \alpha \Delta \mathbf{F} \quad \text{where } \Delta \mathbf{F} = \mathbf{f}(\mathbf{P1}) - \mathbf{f}(\mathbf{P2})$$

In the cost function, the model evaluation $\mathbf{f}(\mathbf{P})$ is substituted by the linearized function $\mathbf{L}(\alpha)$. The linearized cost function $J(\alpha)$ becomes:

$$J(\alpha) = [\mathbf{y} - \mathbf{f}(\mathbf{P2}) - \alpha \Delta \mathbf{F}]^T [\mathbf{y} - \mathbf{f}(\mathbf{P2}) - \alpha \Delta \mathbf{F}]$$

We then solve for α that minimizes the linearized cost function $J(\alpha)$. After some algebra, this gives:

$$\alpha = (\Delta \mathbf{F}^T \Delta \mathbf{F})^{-1} \Delta \mathbf{F}^T [\mathbf{y} - \mathbf{f}(\mathbf{P2})]$$

The new parameter estimation of $\mathbf{P3}$ is then based on

- $\mathbf{P2}$,
- the difference between the two best estimates ($\Delta \mathbf{P} = \mathbf{P1} - \mathbf{P2}$),
- and the parameter α .

$$\mathbf{P3} = \mathbf{P2} + \alpha \Delta \mathbf{P}$$

If $\mathbf{J(P3)}$ is less than $\mathbf{J(P2)}$, then $\mathbf{P1}$ and $\mathbf{J(P1)}$ are tossed out from memory, $\mathbf{P2}$ is replaced by $\mathbf{P3}$, and the two estimates are again sorted according to their corresponding cost function ($\mathbf{P2}$ and $\mathbf{P3}$). This is called the **outer iteration**.

If $\mathbf{J(P3)}$ is not less than $\mathbf{J(P2)}$, then a **line search** is done in between $\mathbf{P2}$ and $\mathbf{P3}$:

$$\mathbf{P3} = \mathbf{P2} + \delta_i (\mathbf{P3} - \mathbf{P2})$$

The step size δ_i is calculated as:

$$\delta_i = \begin{cases} 1, & i = 0 \\ \beta \times (\eta)^i, & i > 1 \end{cases}$$

The line search stops until $\mathbf{P3}$ is reached for which $\mathbf{J(P3)}$ is less than $\mathbf{J(P2)}$, if that exists. This is called the **inner iteration**. The parameter $\beta = \pm 1$ determines whether the line search is continued in a positive (+) or negative (-) direction. In this study, negative search starts when $i > 3$ (**startIterationNegativeLook=3**). η is the **shorteningFactor** = 0.5 in this study. The procedure is stopped as soon as one of the stopping criteria is fulfilled (see §7.5). The best fit will be given by the value of \mathbf{P} with the lowest cost \mathbf{J} .

For a more detailed descriptions of the DUD algorithm, the reader is referred to OpenDA (2016).

Appendix B Definition of Statistics

Water levels

The **Bias** of water level represents the average deviation of the differences between model predicted water level and measurement.

The **RMSE** of water level is a measure of the spread of the predicted values level around the measurement. It corresponds to a sample standard deviation.

The **RMSE0** is the bias corrected root mean square error which describes the forecast errors not associated with the bias.

The mathematical expressions are listed below. y and x represent modelled and measured values respectively and n is the number of samples.

$$Bias = \bar{y} - \bar{x}$$

$$RMSE = \sqrt{\frac{\sum_{i=1}^n (y_i - x_i)^2}{n}}$$

$$RMSE0 = \sqrt{\frac{\sum_{i=1}^n ((y_i - x_i) - (\bar{y} - \bar{x}))^2}{n}}$$

Appendix C Sensitivity analysis of roughness

Figure 53 – M2 and M4 amplitude along the Scheldt between reference run and run with Manning increased by 0.002 in Zone 450.

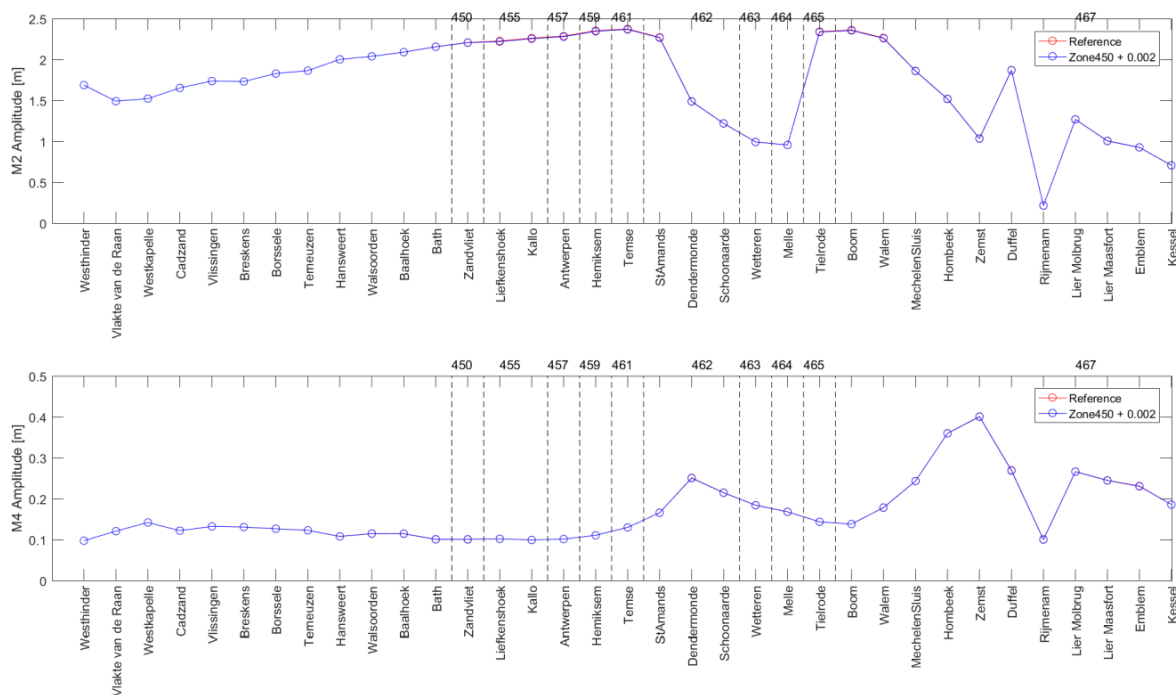


Figure 54 – M2 and M4 amplitude along the Scheldt between reference run and run with Manning increased by 0.002 in Zone 455.

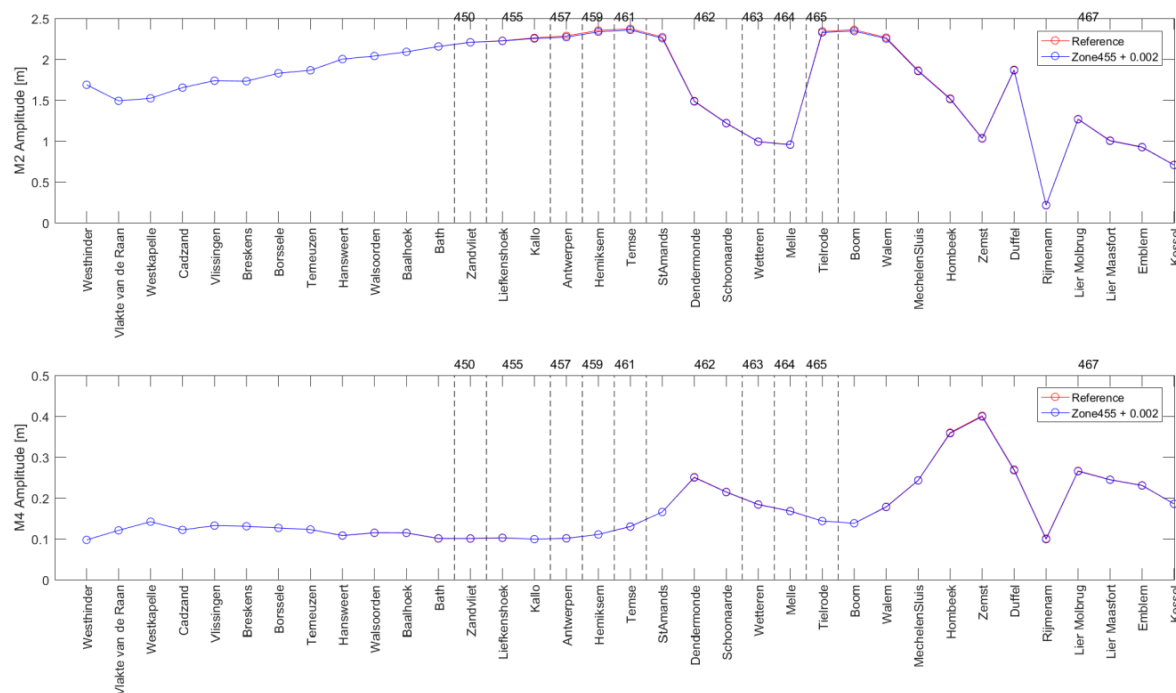


Figure 55 – M2 and M4 amplitude along the Scheldt between reference run and run with Manning increased by 0.002 in Zone 457.

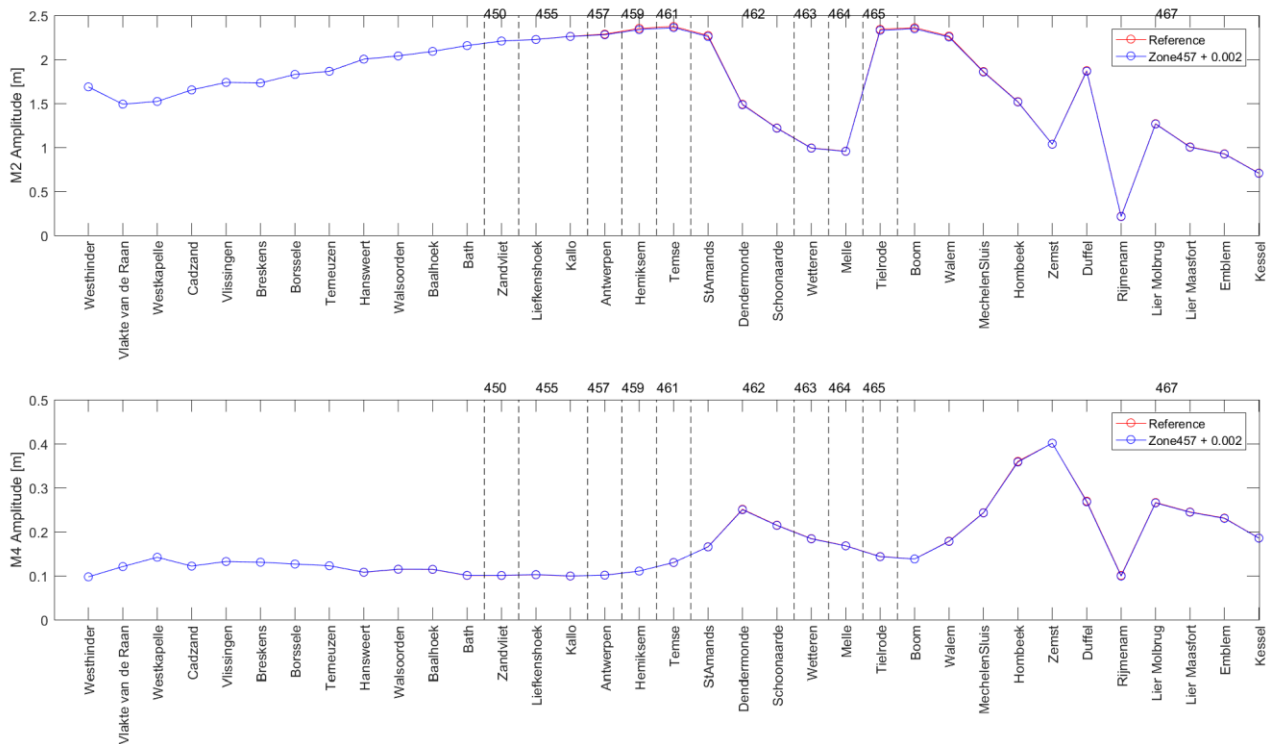


Figure 56 – M2 and M4 amplitude along the Scheldt between reference run and run with Manning increased by 0.002 in Zone 459.

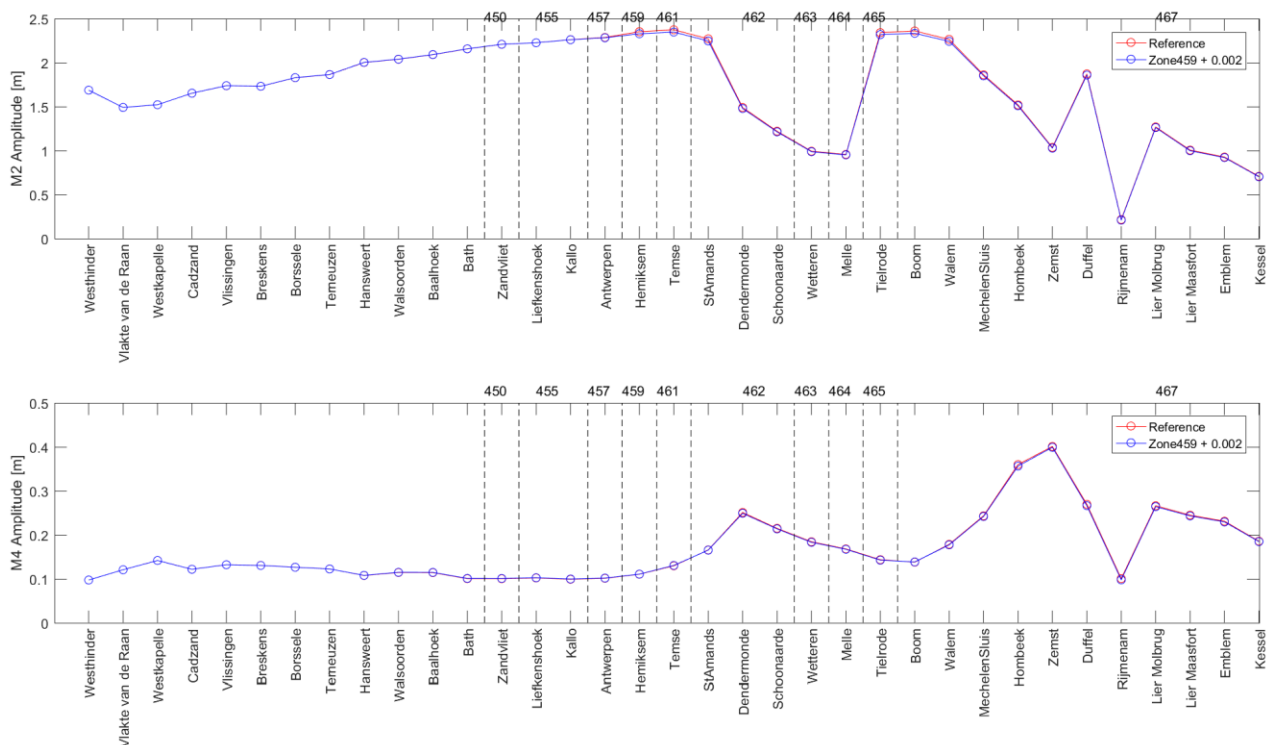


Figure 57 – M2 and M4 amplitude along the Scheldt between reference run and run with Manning increased by 0.002 in Zone 461.

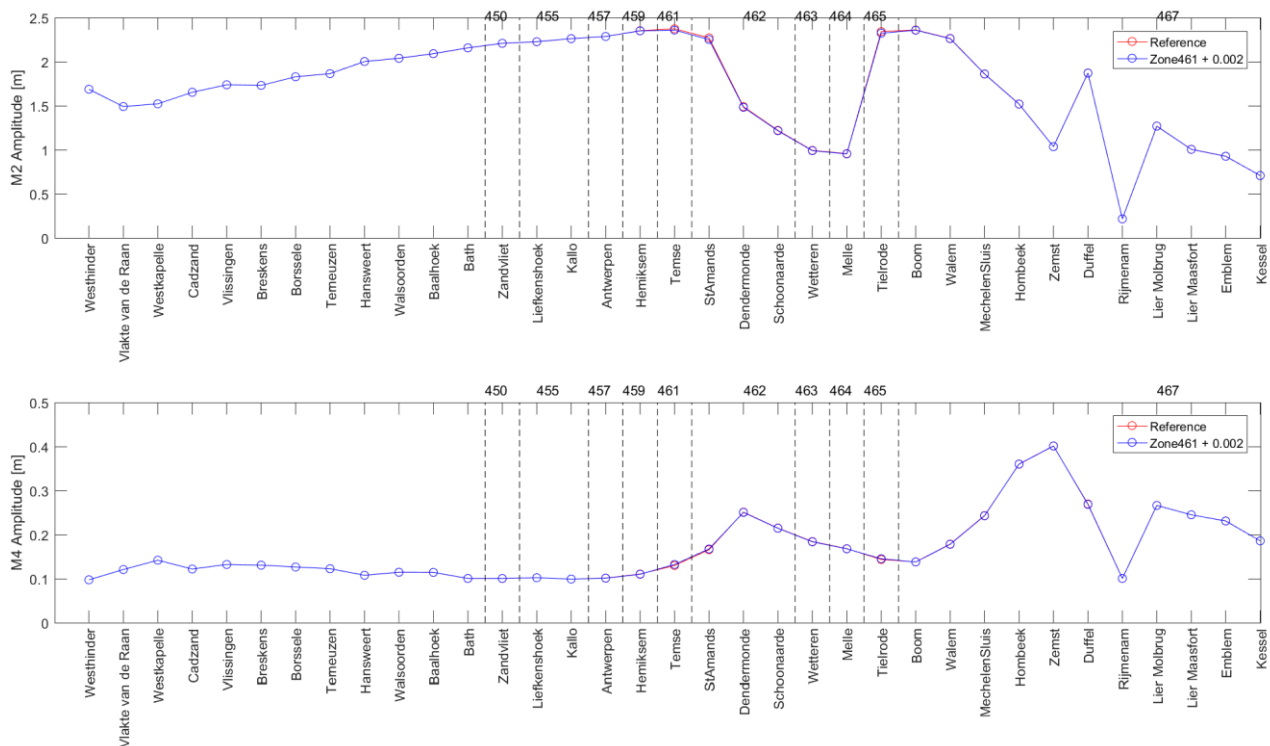


Figure 58 – M2 and M4 amplitude along the Scheldt between reference run and run with Manning increased by 0.002 in Zone 462.

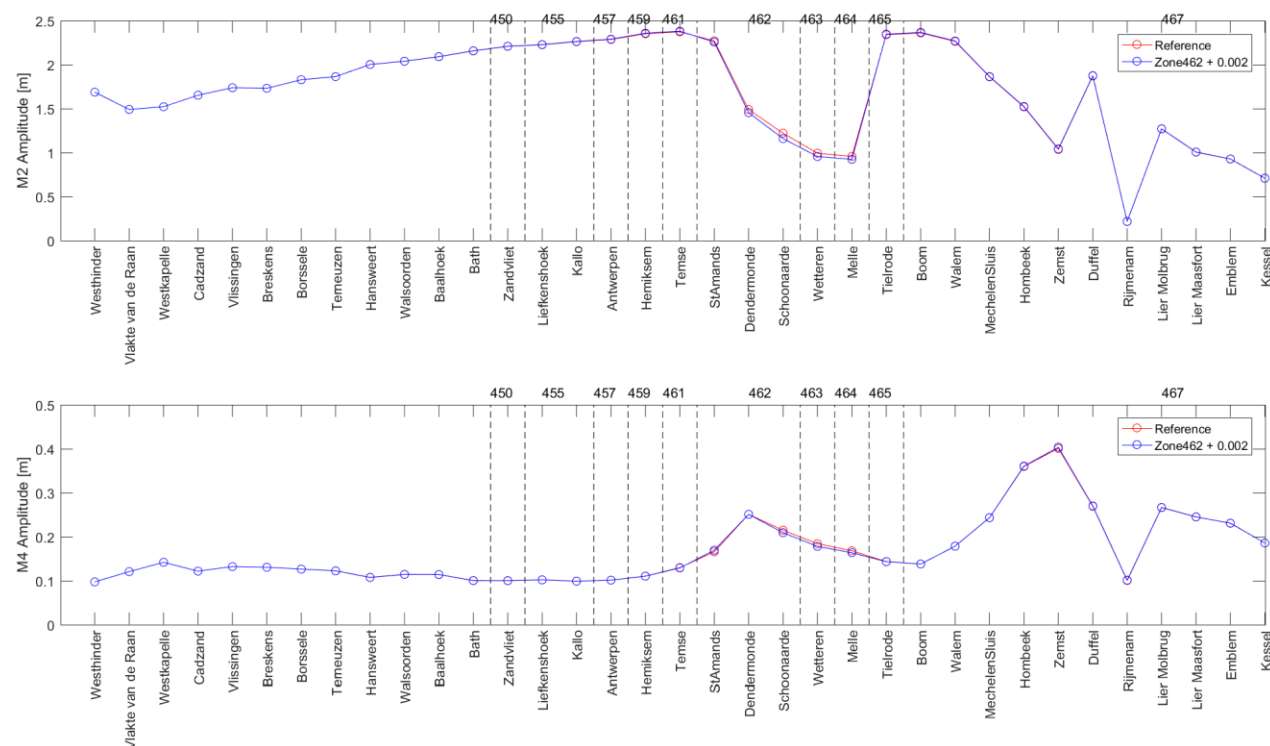


Figure 59 – M2 and M4 amplitude along the Scheldt between reference run and run with Manning increased by 0.002 in Zone 463.

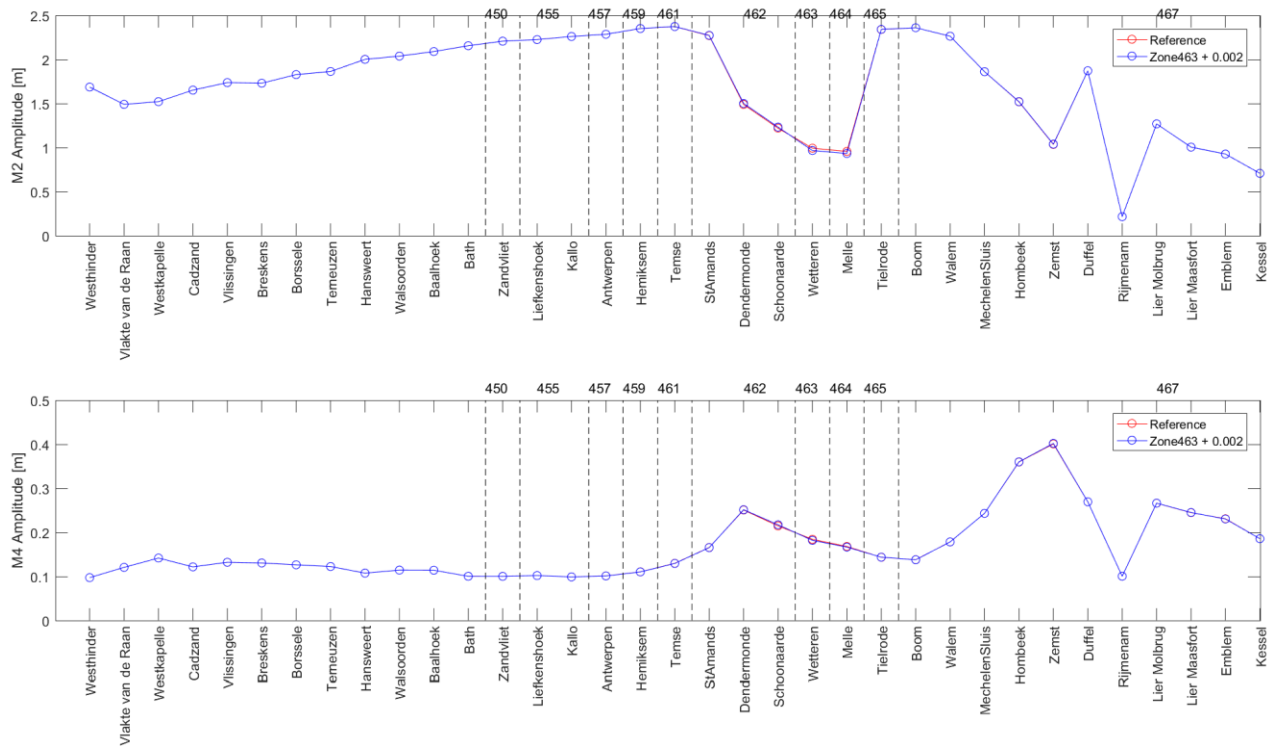


Figure 60 – M2 and M4 amplitude along the Scheldt between reference run and run with Manning increased by 0.002 in Zone 464.

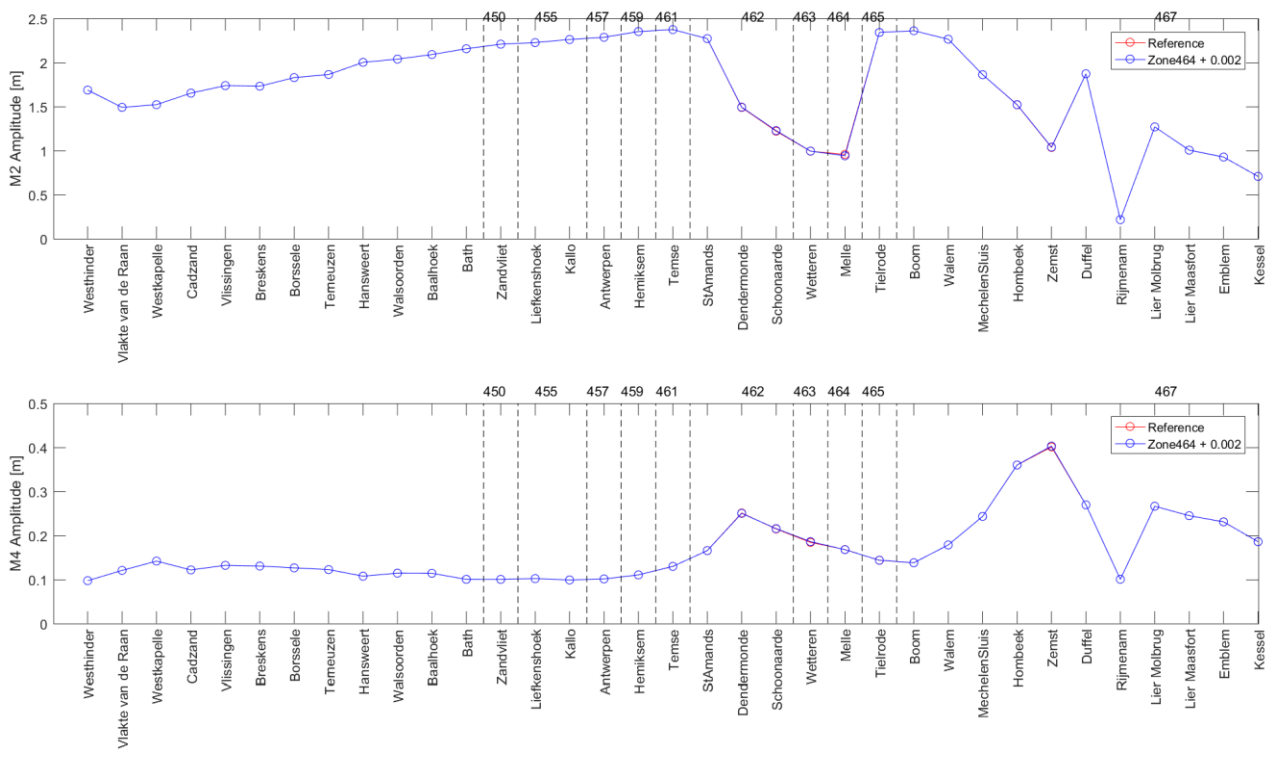


Figure 61 – M2 and M4 amplitude along the Scheldt between reference run and run with Manning increased by 0.002 in Zone 465.

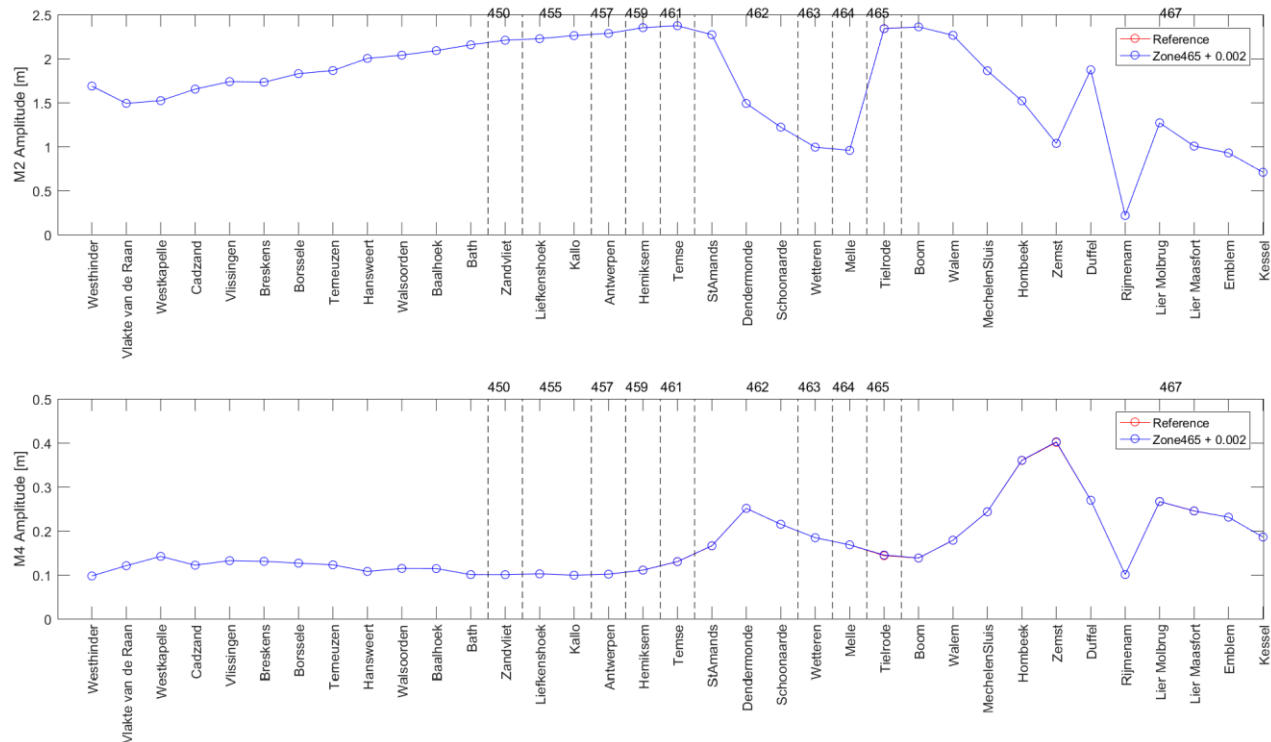
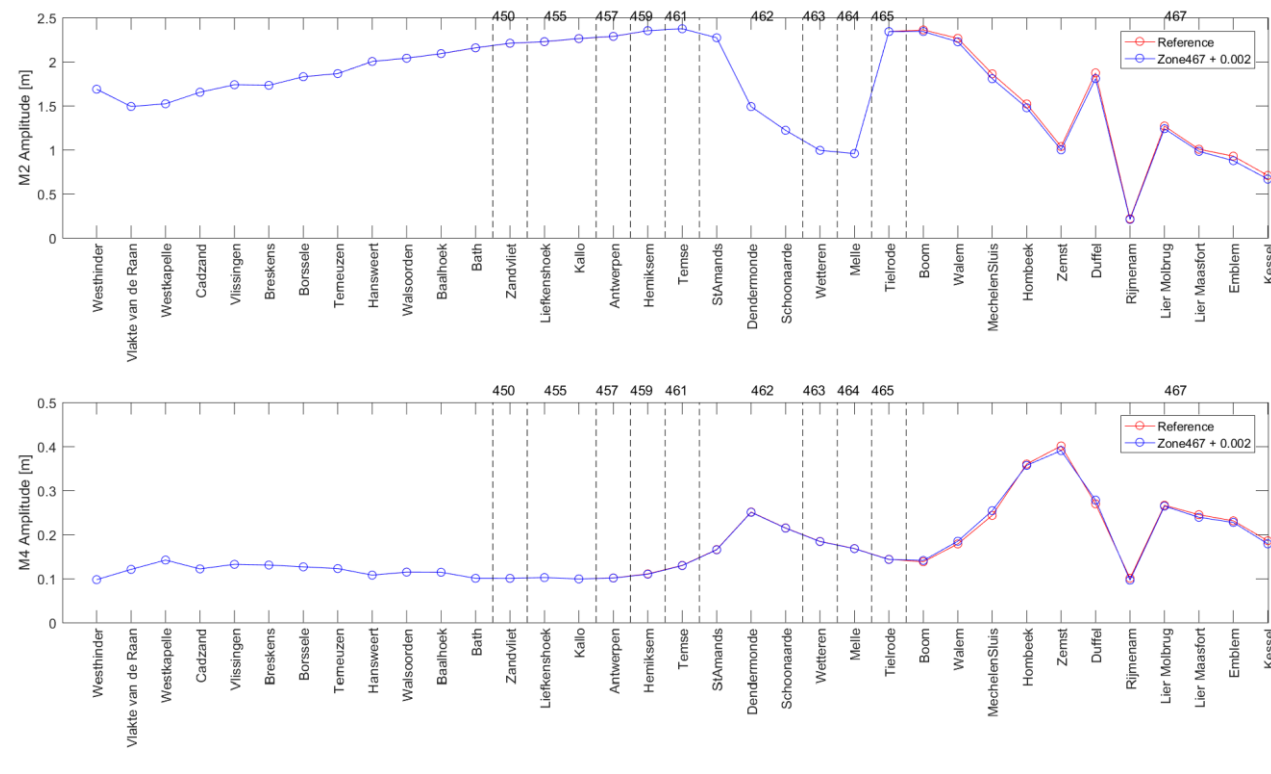


Figure 62 – M2 and M4 amplitude along the Scheldt between reference run and run with Manning increased by 0.002 in Zone 467.



Appendix D Definition of Vector Difference

The vector difference analysis combines the results from different tidal components regarding both amplitude and phase. In short vector difference is a unified variable with one value describing the model accuracy from harmonic point of view. The mathematical expression of vector difference is shown as below.

$$e_s = \sum_{i=1}^N \sqrt{[A_{c,i} \cos(\phi_{c,i}) - A_{m,i} \cos(\phi_{m,i})]^2 + [A_{c,i} \sin(\phi_{c,i}) - A_{m,i} \sin(\phi_{m,i})]^2}$$

where e_s is the vector difference calculated at a certain station. c and m represent the model computed and measured value. A and ϕ represent the tidal amplitude and phase. i represents the number of tidal components.

DEPARTMENT **MOBILITY & PUBLIC WORKS**
Flanders hydraulics Research

Berchemlei 115, 2140 Antwerp

T +32 (0)3 224 60 35

F +32 (0)3 224 60 36

waterbouwkundiglabo@vlaanderen.be

www.flandershydraulicsresearch.be